

2015

## Iron-Catalyzed Arylation of Heterocycles and Transition-Metal Free C-N Bond Formation

John Joseph Sirois  
*University of Rhode Island*, [john\\_sirois@my.uri.edu](mailto:john_sirois@my.uri.edu)

Follow this and additional works at: [https://digitalcommons.uri.edu/oa\\_diss](https://digitalcommons.uri.edu/oa_diss)

Terms of Use

All rights reserved under copyright.

---

### Recommended Citation

Sirois, John Joseph, "Iron-Catalyzed Arylation of Heterocycles and Transition-Metal Free C-N Bond Formation" (2015). *Open Access Dissertations*. Paper 369.  
[https://digitalcommons.uri.edu/oa\\_diss/369](https://digitalcommons.uri.edu/oa_diss/369)

This Dissertation is brought to you by the University of Rhode Island. It has been accepted for inclusion in Open Access Dissertations by an authorized administrator of DigitalCommons@URI. For more information, please contact [digitalcommons-group@uri.edu](mailto:digitalcommons-group@uri.edu). For permission to reuse copyrighted content, contact the author directly.

IRON-CATALYZED ARYLATION OF HETEROCYCLES

AND

TRANSITION-METAL FREE C-N BOND FORMATION

BY

JOHN JOSEPH SIROIS

A DISSERTATION SUBMITTED IN PARTIAL FULFILLMENT OF

THE REQUIREMENTS FOR THE DEGREE OF

DOCTOR OF PHILOSOPHY

IN

CHEMISTRY

UNIVERSITY OF RHODE ISLAND

2015

DOCTOR OF PHILOSOPHY IN CHEMISTRY DISSERTATION  
OF  
JOHN J. SIROIS

APPROVED:

Thesis Committee:

Major Professor: Brenton DeBoef

Mindy Levine

Navindra Seeram

Nasser H. Zawia

UNIVERSITY OF RHODE ISLAND  
2015

## ABSTRACT

The formation of carbon-carbon (C-C) and carbon-nitrogen (C-N) bonds is discussed and efforts towards expanding the known reactions of this type are the primary focus of this work. The iron-catalyzed arylation of aromatic heterocycles, such as pyridines, thiophenes and furans has been achieved. The use of an imine directing group allowed for the *ortho*-functionalization of these heterocycles with complete conversion in 15 minutes at 0 °C. Yields up to 88% were observed in the synthesis of 15 heterocyclic biaryls. C-N bond formation is achieved using aryl Grignard reagents and N-chloroamines at -78 °C.

## ACKNOWLEDGMENTS

I would like to thank my research advisor **Dr. Brenton DeBoef** for his guidance and support. He always kept me optimistic and motivated through the many ups and downs of academic research. The knowledge I gained from him is invaluable, and I am honored to have been a part of this research group.

The training I received from **Abhishek Kantak, Louis Marchetti, Ashley Porter, Marissa Simone, and Joseph Brown** was essential to developing the lab skills I used to complete this work.

I must thank **Riley Davis**, the first undergraduate student I trained, who helped me finally start the iron-catalysis project I had been procrastinating. I also want to thank the other excellent undergraduates I had the pleasure to train, **Joelle Bitar** and **Dylan Kritter**. I know each of these individuals will go on to have successful careers.

Most importantly I need to thank my family: My mother, **Peggy Boyle**, I never thought I would make it this far, and I couldn't have done it without you or **Terry Carbone**. To my father **Craig E. Sirois** and my siblings: **Heather, Craig, Michael, Joseph, Catherine**, my sister-in-law **Cheryl Tullis**, and my nephew **Christopher**; Thank you each for the never ending support and encouragement.

I need an entire chapter to thank all of my friends, so I won't try to list them here, but you know who you are. Thank you each for your indirect contribution to this work. I am grateful and humbled each day by the amazing people I share my life with.

## **PREFACE**

The following work is presented in manuscript format according to the guidelines presented by the University of Rhode Island Graduate School. The thesis will consist of two manuscripts.

## TABLE OF CONTENTS

ABSTRACT.....	ii
ACKNOWLEDGEMENTS.....	iii
PREFACE.....	iv
TABLE OF CONTENTS.....	v
LIST OF TABLES.....	vi
LIST OF SCHEMES.....	vii
LIST OF FIGURES.....	viii
CHAPTER 1: INTRODUCTION.....	1
REFERENCES.....	11
CHAPTER 2: MANUSCRIPT 1.....	14
REFERENCES.....	25
CHAPTER 3: MANUSCRIPT 2.....	29
REFERENCES.....	37
CHAPTER 4: EXPERIMENTAL SECTION MANUSCRIPT 1.....	38
REFERENCES.....	83
CHAPTER 5: EXPERIMENTAL SECTION MANUSCRIPT 2.....	85
REFERENCES.....	103
APPENDIX A: MAIN MECHANISM - MANUSCRIPT 1.....	104
APPENDIX B: MAIN MECHANISM - MANUSCRIPT 2.....	105

## LIST OF TABLES

<b>Table 2.1</b> Optimization of Pyridine Arylation.....	20
<b>Table 2.2.</b> Directing Group Optimization.....	22
<b>Table 2.3.</b> Substrate Scope.....	23
<b>Table 2.3.</b> (Continued) Substrate Scope.....	24
<b>Table 2.4.</b> Grignard Reagent Scope.....	25
<b>Table 3.1.</b> Optimization of Reaction Conditions.....	31
<b>Table 3.2.</b> Effect of Temperature on C-N Bond Formation.....	33
<b>Table 4.1.</b> Comparison of Reaction Vessel Sizes.....	42



## LIST OF SCHEMES

<b>Scheme 1.1.</b> Modern Cross-Coupling Reactions.....	2
<b>Scheme 1.2.</b> First Example of C–H Activation via Iron.....	4
<b>Scheme 1.3.</b> Scope of Grignard Arylation on 2-Phenylpyridine.....	5
<b>Scheme 1.4.</b> Directed C–H activation.....	6
<b>Scheme 1.5.</b> Gram Scale Reaction.....	7
<b>Scheme 1.6.</b> Carbon–Nitrogen Bond Formation via C–H activation.....	7
<b>Scheme 1.7.</b> Buchwald-Hartwig Reaction.....	8
<b>Scheme 1.8.</b> C–N Bond Formation via C–H Activation.....	9
<b>Scheme 1.9.</b> Metal-Catalyzed C–N Bond Formation.....	10
<b>Scheme 1.10.</b> Recent Examples of Copper-Catalyzed C–N Bond Formation.....	10
<b>Scheme 1.11.</b> Transition-Metal Free C–N Bond Formation.....	11
<b>Scheme 2.1.</b> Comparison of C–H Arylation Methods.....	19
<b>Scheme 3.1.</b> Initial Optimization Outline.....	31
<b>Scheme 3.2.</b> Reaction Scope.....	35

## LIST OF FIGURES

<b>Figure 4.1.</b> $^1\text{H}$ NMR of Compound 1.....	43
<b>Figure 4.2.</b> $^1\text{H}$ NMR of Compound 2.....	44
<b>Figure 4.3.</b> $^{13}\text{C}$ NMR of Compound 2.....	45
<b>Figure 4.4.</b> $^1\text{H}$ NMR of Compound 3.....	46
<b>Figure 4.5.</b> $^{13}\text{C}$ NMR of Compound 3.....	47
<b>Figure 4.6.</b> $^1\text{H}$ NMR of Compound 4.....	48
<b>Figure 4.7.</b> $^1\text{H}$ NMR of Compound 5.....	49
<b>Figure 4.8.</b> $^1\text{H}$ NMR of Compound 6.....	50
<b>Figure 4.9.</b> $^{13}\text{C}$ NMR of Compound 6.....	51
<b>Figure 4.10.</b> $^1\text{H}$ NMR of Compound 7.....	52
<b>Figure 4.11.</b> $^{13}\text{C}$ NMR of Compound 7.....	53
<b>Figure 4.12.</b> $^1\text{H}$ NMR of Compound 8.....	54
<b>Figure 4.13.</b> $^{13}\text{C}$ NMR of Compound 8.....	55
<b>Figure 4.14.</b> $^1\text{H}$ NMR of Compound 9.....	56
<b>Figure 4.15.</b> $^1\text{H}$ NMR of Compound 11.....	57
<b>Figure 4.16.</b> $^1\text{H}$ NMR of Compound 12.....	58
<b>Figure 4.17.</b> $^1\text{H}$ NMR of Compound 13.....	59
<b>Figure 4.18.</b> $^1\text{H}$ NMR of Compound 14.....	60
<b>Figure 4.19.</b> $^1\text{H}$ NMR of Compound 15.....	61
<b>Figure 4.20.</b> $^1\text{H}$ NMR of Compound 17.....	62
<b>Figure 4.21.</b> $^1\text{H}$ NMR of Compound 18.....	63
<b>Figure 4.22.</b> $^{13}\text{C}$ NMR of Compound 18.....	64

<b>Figure 4.23.</b> $^1\text{H}$ NMR of Compound 19.....	65
<b>Figure 4.24.</b> $^{13}\text{C}$ NMR of Compound 19.....	66
<b>Figure 4.25.</b> $^1\text{H}$ NMR of Compound 20.....	67
<b>Figure 4.26.</b> $^{13}\text{C}$ NMR of Compound 20.....	68
<b>Figure 4.27.</b> $^1\text{H}$ NMR of Compound 21.....	69
<b>Figure 4.28.</b> $^1\text{H}$ NMR of Compound 22.....	70
<b>Figure 4.29.</b> $^{13}\text{C}$ NMR of Compound 22.....	71
<b>Figure 4.30.</b> $^1\text{H}$ NMR of Compound 23.....	72
<b>Figure 4.31.</b> $^1\text{H}$ NMR of Compound 24.....	73
<b>Figure 4.32.</b> $^{13}\text{C}$ NMR of Compound 24.....	74
<b>Figure 4.33.</b> $^1\text{H}$ NMR of Compound 25.....	75
<b>Figure 4.34.</b> $^{13}\text{C}$ NMR of Compound 25.....	76
<b>Figure 4.35.</b> $^1\text{H}$ NMR of Compound 26.....	77
<b>Figure 4.36.</b> $^{13}\text{C}$ NMR of Compound 26.....	78
<b>Figure 4.37.</b> $^1\text{H}$ NMR of Compound 27.....	79
<b>Figure 4.38.</b> $^1\text{H}$ NMR of Compound 28.....	80
<b>Figure 4.39.</b> $^{13}\text{C}$ NMR of Compound 28.....	81
<b>Figure 4.40.</b> $^{13}\text{C}$ NMR of Compound 29.....	82
<b>Figure 5.1.</b> $^1\text{H}$ NMR of 4-chloromorpholine.....	86
<b>Figure 5.2.</b> $^{13}\text{C}$ NMR of 4-chloromorpholine.....	87
<b>Figure 5.3.</b> $^1\text{H}$ NMR of 4-chloropiperidine.....	88
<b>Figure 5.4.</b> $^{13}\text{C}$ NMR of 4-chloropiperidine.....	89
<b>Figure 5.5.</b> $^1\text{H}$ NMR of 1,4-dichloropiperazine.....	90

<b>Figure 5.6.</b> $^1\text{H}$ NMR of 4-phenylmorpholine.....	91
<b>Figure 5.7.</b> $^{13}\text{C}$ NMR of 4-phenylmorpholine.....	92
<b>Figure 5.8.</b> $^1\text{H}$ NMR of 4-(4-methylphenyl)-morpholine.....	93
<b>Figure 5.9.</b> $^{13}\text{C}$ NMR of 4-(4-methylphenyl)-morpholine.....	94
<b>Figure 5.10.</b> $^1\text{H}$ NMR of 4-(4-methoxyphenyl)-morpholine.....	95
<b>Figure 5.11.</b> $^{13}\text{C}$ NMR of 4-(4-methoxyphenyl)-morpholine.....	96
<b>Figure 5.12.</b> $^1\text{H}$ NMR of 4-(4-methylphenyl)-piperidine.....	97
<b>Figure 5.13.</b> $^{13}\text{C}$ NMR of 4-(4-methylphenyl)-piperidine.....	98
<b>Figure 5.14.</b> $^1\text{H}$ NMR of 4-(4-methoxyphenyl)-piperidine.....	99
<b>Figure 5.15.</b> $^{13}\text{C}$ NMR of 4-(4-methoxyphenyl)-piperidine.....	100
<b>Figure 5.16.</b> $^1\text{H}$ NMR of 1,4-diphenylpiperazine.....	101
<b>Figure 5.17.</b> $^{13}\text{C}$ NMR of 1,4-diphenylpiperazine.....	102

## CHAPTER 1: INTRODUCTION

Sustainable chemistry might seem like a contradictory term; however this is the only way we can continue to provide the ability to generate the compounds we need as a society on a large scale without damaging our environment, diminishing our resources, or compromising the health of future generations. Consequently, green chemistry is a growing field that has quickly generated a lot of interest. The applications of these practices to synthetic chemistry are highly desirable.

Many physical transformations exist for the modern synthetic chemist. In particular, the formation of new carbon-carbon (C-C) bonds is quite literally the backbone of organic chemistry. Developing and understanding these C-C forming reactions has always been at the forefront of chemical synthesis. Some traditional methods to create these bonds include Grignard reagents<sup>1</sup>, organocuprates<sup>2</sup>, organolithium reagents<sup>3</sup>, and Wittig type reactions.<sup>4</sup>

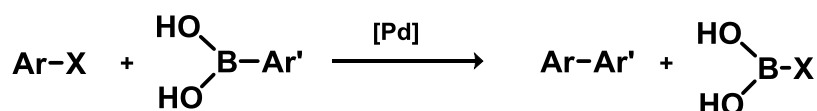
More recently over the past few decades several metal-catalyzed cross-coupling methods have been developed<sup>5</sup>; including the Suzuki-Miyaura, Stille, Heck, Negishi, Kumada, and Sonogashira coupling reactions (Scheme 1.1). These reactions have shown great promise for expanding the organic chemists' tool box and providing robust methods to obtain a variety of products.

One major downfall of these methods is the need to pre-functionalize the starting compounds in order to obtain both the substituted halides and organometallic reagents required for each reaction to occur. The generation of hazardous waste has always been a concern to the environmentally conscious chemist. These extra steps inherently generate more waste, result in a lower atom economy, and consume more

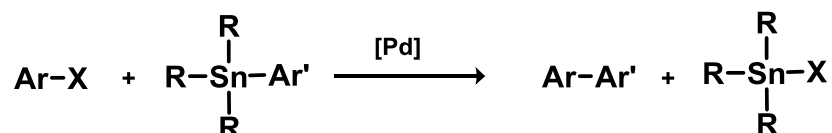
resources than would be necessary if the product could be synthesized in a more direct way.

**Scheme 1.1.** Modern Cross-Coupling Reactions

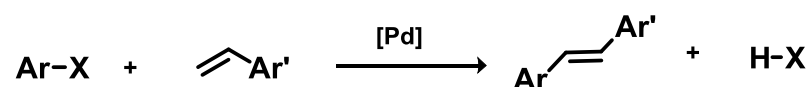
**Suzuki-Miyaura**



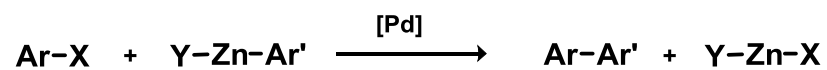
**Stille**



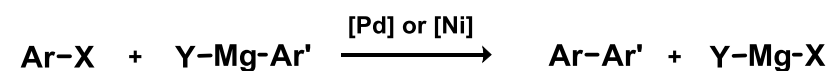
**Heck**



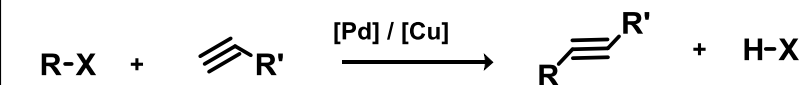
**Negishi**



**Kumada**



**Sonogashira**



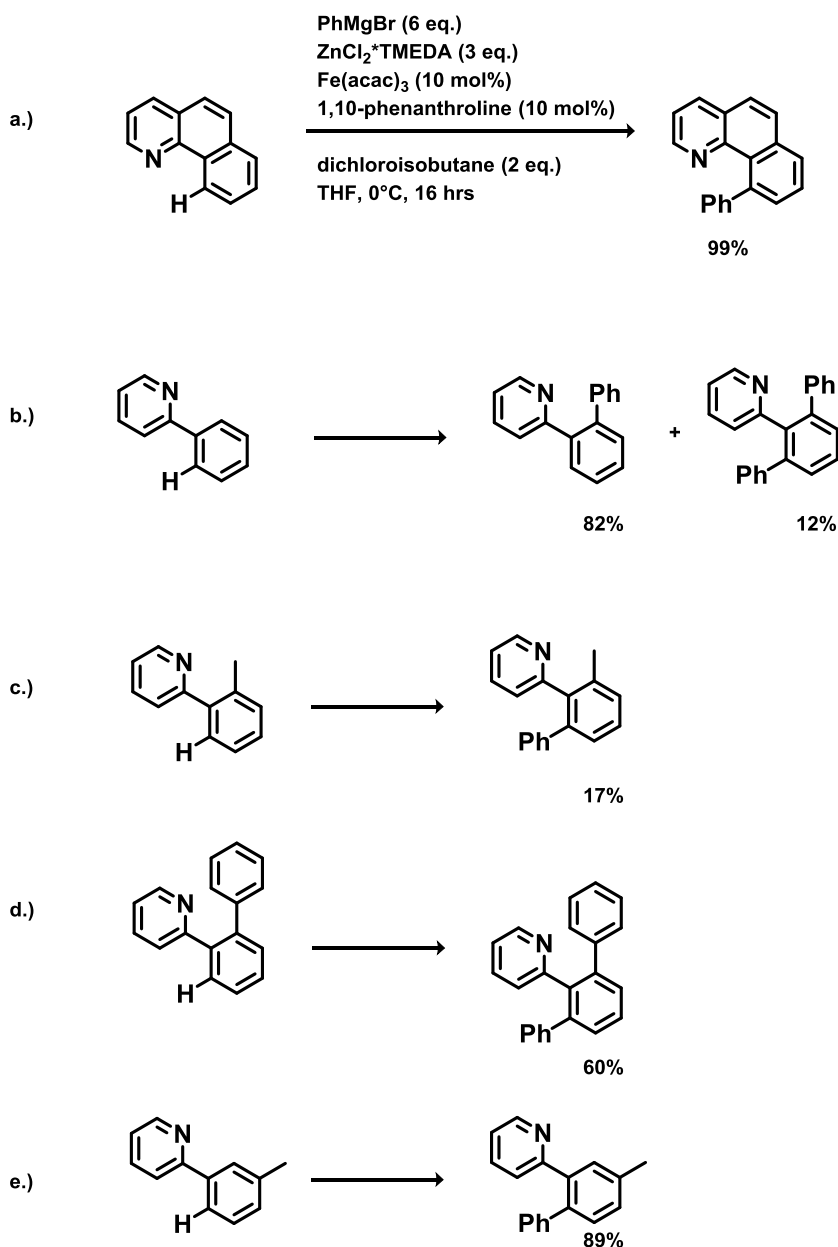
This is the driving concept behind carbon-hydrogen (C–H) bond activation. A C–H bond can be directly substituted to form C–C and C–heteroatom bonds without prior functionalization at the reacting carbons or heterocyclic centers. Although sometimes directing groups (such as imines, carbonyls, or carboxylic acids) are required<sup>6</sup>, usually these can still be used for further substitution, or in some cases easily removed.

The activation of C–H bonds provides one excellent remedy to the aforementioned environmental problem; but additional efforts can be made to increase the overall “greenness” of a reaction. The first and easiest alternative is to use “green solvents” such as water, 2-methyltetrahydrofuran, or cyclohexane instead of more undesirable solvents like dichloromethane, benzene, and hexanes. The real challenge lies in variations of the reagents themselves and their role in the reaction mechanism (catalytic vs. stoichiometric). The majority of research in the field of C–H activation has focused on catalysts with relatively easy to understand mechanisms like palladium. More recently work has revolved around the use of cheap, non-toxic transition-metal catalysts to promote these same desired reactions through “green” methodology.

Our primary interest was to work exclusively with iron catalysts to develop novel methods for C–C and C–N bond formation through the C–H activation pathway in particular. We chose to work with iron due to its low toxicity and availability. There was also precedent set by Nakamura that demonstrated the ability of iron to activate

the C–H bond.<sup>7</sup> Nakamura's pioneering work involved the nucleophilic displacement of a hydrogen atom *ortho*- to a nitrogen-containing directing group (Scheme 1.2)

**Scheme 1.2.** First Example of C–H Activation via Iron



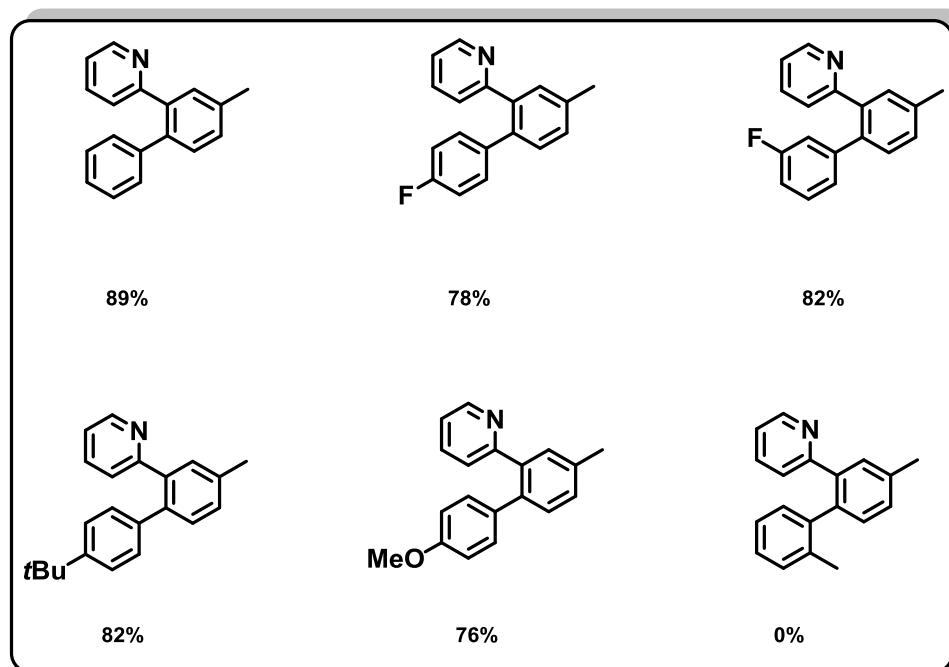
The reaction in Scheme 1.2a shows a hindered system that is sterically fixed for the C–H activation of only one carbon in  $\alpha$ -benzoquinoline. The reaction of



various substituted substrates gives insight to the limitations of this system. When these reaction conditions are applied to a substrate with two equivalent hydrogens, like in the case of 2-phenyl pyridine, then a mixture of products is obtained (Scheme 1.2b). Increasing steric hindrance at the *ortho*- position on the phenyl ring decreases the product yield (Scheme 1.2c and 1.2d). Interestingly, when a methyl substituent is added to the 3-position on the phenyl group the mono-arylated product is formed exclusively (Scheme 1.2e). These results can be attributed to steric hindrance.

Scheme 1.3 shows that Grignard reagents bearing both electron donating and electron withdrawing substituents are readily coupled with this methylated 2-phenylpyridine in good yields over 36 hours. The exception to these is the *ortho*-tolyl Grignard reagent which afforded no product, reinforcing the important role of steric restraints on this catalytic system.

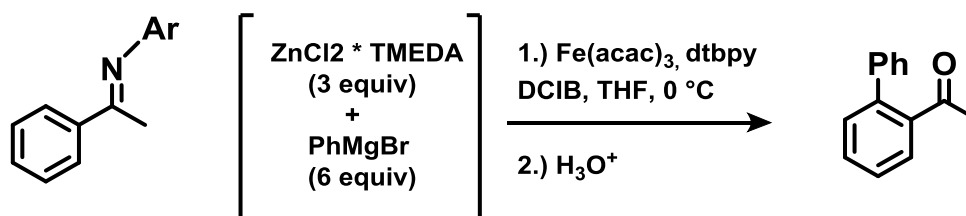
**Scheme 1.3.** Scope of Grignard arylation on 2-phenylpyridine



These initial findings showed that iron could be used for C–H activation and provide arylated products under mild conditions, although long reaction times and large equivalents of Grignard reagents are necessary. The scope of the reaction shows the tolerance of electronic effects on the Grignard reagent and the influence of the steric environment around the hydrogen leaving group. Both electron donating, *t*-butyl and methoxy substituents, and electron withdrawing fluorine substituents on the Grignard reagent are tolerated. These are key concepts that must be considered when attempting to develop more iron-catalyzed reactions.

The ability to use an imine as a directing group instead of the pyridine ring allows for subsequent hydrolysis, and yields the product with the carbonyl suitable for further functionalization<sup>8</sup> (Scheme 1.4).

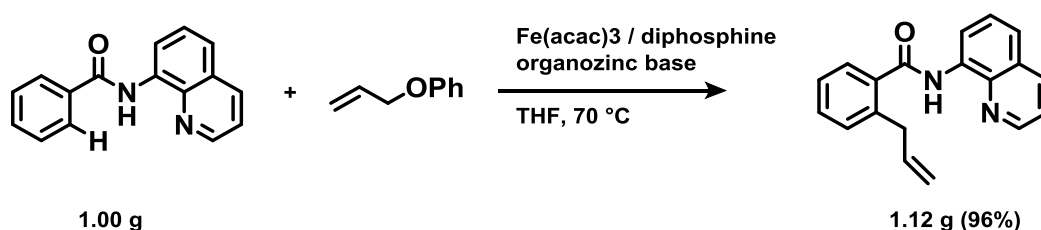
**Scheme 1.4.** Directed C–H activation



However, the use of an organozinc reagent to generate the active transmetalating complex is still necessary. This system is not limited to aromatic hydrogens, and has been shown to effectively arylate  $sp^2$ -hybridized olefins<sup>9</sup> and  $sp^3$ -hybridized carbons.<sup>10</sup> Carbon–nitrogen (C–N) bond formation is possible if primary amines are converted into an organozinc species.<sup>11</sup> The Grignard reagent can also be generated in situ, with excellent yields.<sup>12</sup> Eventually it was discovered that the

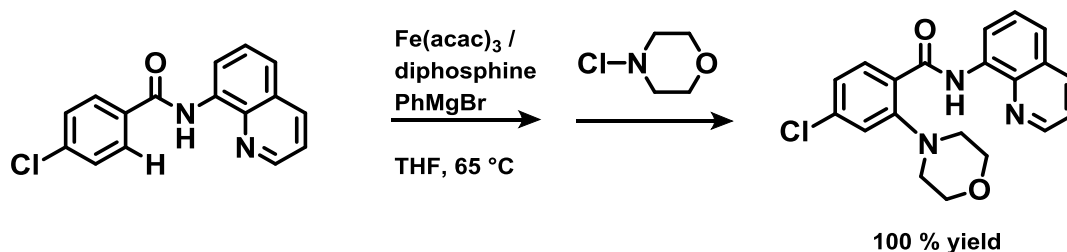
reaction can proceed without the use of organozinc reagents<sup>13</sup> and it has also been shown that oxygen can be used as an oxidant.<sup>14</sup> The decrease in metals required results in a higher atom economy; and the use of oxygen is considered environmentally friendly. Further manipulation of the directing group allows for an increase in the product scope of these reactions up to a gram scale<sup>15, 16</sup> (Scheme 1.5).

**Scheme 1.5.** Gram Scale Reaction



Another example of C–N bond formation is possible using this quinoline directing group.<sup>17</sup> The incorporation of deuterium was demonstrated, which suggests the oxidative addition of the iron species into the original C–H bond of interest (Scheme 1.6).

**Scheme 1.6.** Carbon–Nitrogen Bond Formation via C–H activation

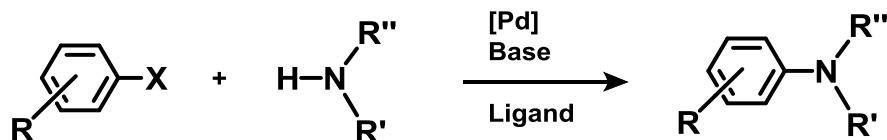


The variations of this initial system have been significantly manipulated and expanded to allow for substantial coupling reactions to occur predictably and reliably.<sup>18</sup> The result is a process that affords aryl-aryl, alkenyl-alkenyl, alkenyl-aryl, and (hetero)aryl-aryl coupling. A final testament to the future of iron-catalysis and its abilities is the iron-catalyzed Suzuki-Miyaura coupling of alkyl halides with aryl boronic esters.<sup>19</sup>

Using this scaffold, we applied similar conditions and continued to employ the imine directing group to successfully perform C–H activations resulting in the substitution of a variety of heterocycles using an iron catalyst. The focus on heterocycles is imperative and highly desirable because almost all biologically active compounds and pharmaceuticals produced on an industrial scale contain some type of heteroatom with aromatic substituents. The scope and limitations of this reaction are discussed further in Manuscript 1.

New C–N bond formation reactions are in high demand due to the prevalence of these bonds in almost all pharmaceutical products. These bonds are traditionally formed through Buchwald-Hartwig type reactions<sup>20, 21</sup> (Scheme 1.7).

**Scheme 1.7.** Buchwald-Hartwig Reaction

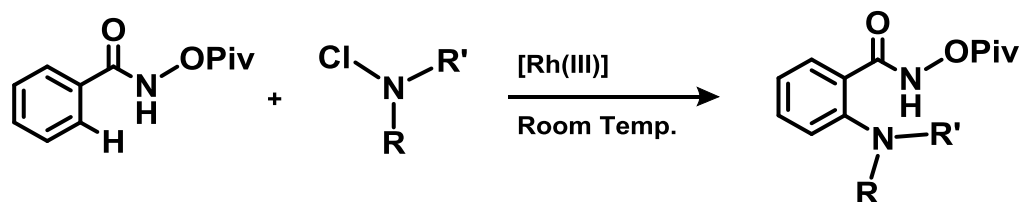


As previously mentioned, the goal of the work presented herein is to eliminate the dependence on expensive metals, especially palladium catalysts. Variants of the

Buchwald-Hartwig reaction are still being investigated, and palladium still plays a dominant role in these reactions.<sup>22</sup> Fortunately, we are not alone in trying to move away from this reagent. Recent work by several groups shows a promising future for C–N bond formation using less toxic transition metals such as copper and cobalt.

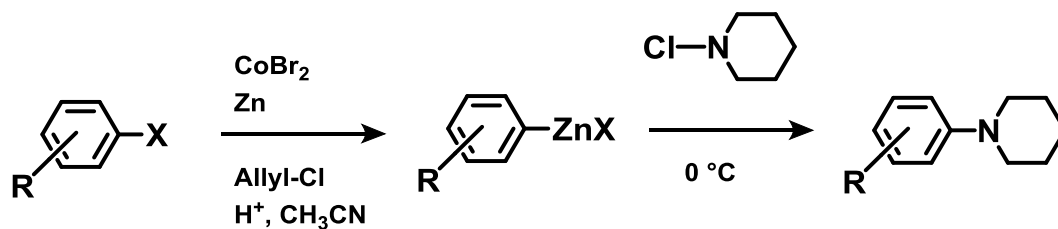
The most common methods for C–N bond formation through C–H activation pathways are only accessible through an intramolecular pathway performed with palladium or copper catalysts.<sup>23, 24</sup> An alternative method to these types of reactions was proposed by Glorius and coworkers which described a C–H activation mechanism using an N-pivaloyloxy amide directing group with chloroamines<sup>25</sup> (Scheme 1.8).

**Scheme 1.8.** C–N Bond Formation via C–H Activation

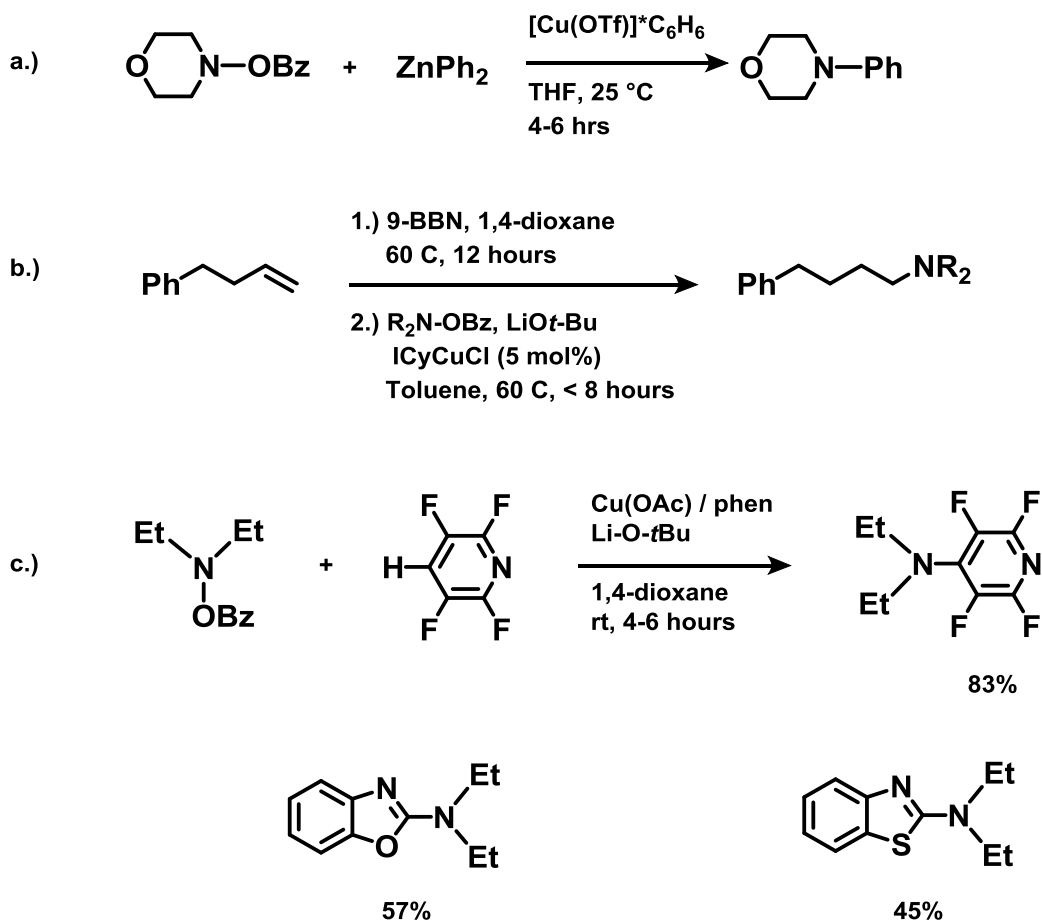


When C–H bond activation is not possible, the use of prefunctionalized compounds is often necessary to obtain the desired products required. N-chloroamines are commonly used in association with aryl organometallic reagents. In some cases stoichiometric zinc is used with catalytic amounts of cobalt or copper.<sup>26</sup> Generation of an aryl-zinc species through cobalt-catalyzed arylation has been shown to produce the desired aryl-amine product in high yields with good functional group tolerance. (Scheme 1.9)

**Scheme 1.9.** Metal-Catalyzed C–N Bond Formation



**Scheme 1.10.** Recent Examples of Copper-Catalyzed C–N Bond Formation

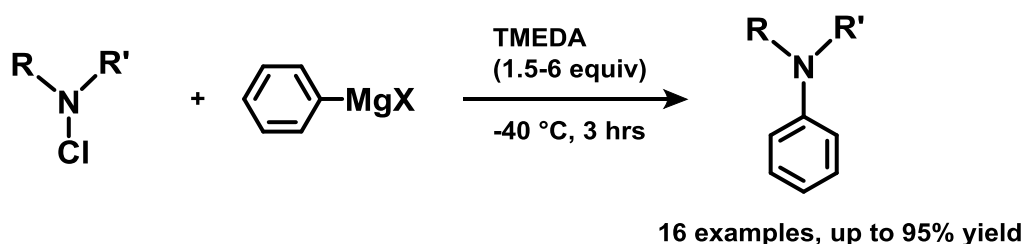


The weakness of the nitrogen-oxygen bond has been exploited using *O*-acyl hydroxylamine derivatives as leaving groups in the copper-catalyzed electrophilic

amination of diorganozinc reagents to form substituted amines<sup>27</sup> (Scheme 1.10a). Alkyl-alkyl bond formation is achieved using copper catalysts with these functionalized amines through a hydroamination mechanism<sup>28</sup> (Scheme 1.10b) and direct amination is possible on highly electron deficient arenes and azoles<sup>29</sup> (Scheme 1.10c).

One of the more interesting amination reactions is a transition-metal free electrophilic amination using aryl-Grignard reagents and N-chloroamines. This is achieved using TMEDA as an additive although high equivalents are needed to drive the reaction to completion<sup>30</sup> (Scheme 1.11).

**Scheme 1.11.** Transition-Metal Free C–N Bond Formation



Our attempts to repeat and expand on the above method began with experiments using iron-catalysts. Preliminary studies showed that the reaction could proceed at room temperature, resulting in low yields, without any catalyst using N-chloroamines and Grignard reagents. We found that the reaction seemed to work much better at 0 °C in the presence of several iron salts. High throughput screening of additives and both dinitrogen and diphosphine ligands at 0 °C resulted in a moderate increase in yield. We maintained this catalytic system and decided to lower the temperature to prevent unwanted side products. We were initially delighted to

discover that a decrease in temperature to  $-78\text{ }^{\circ}\text{C}$  resulted in an excellent 88% yield in just 5 minutes.

Interestingly, when the reaction was held at  $-78\text{ }^{\circ}\text{C}$ , and the iron was removed for the control reaction, in the presence of dinitrogen ligands we still produced the product in comparably high yields. Our next reaction involved eliminating the ligands. Surprisingly, this provided the desired product in quantitative yield (99%). We had discovered that the reaction proceeds smoothly and quickly at this specific temperature. While initially dismayed at the lack of a need for the iron-catalyst, we quickly realized the benefits of a transition-metal and ligand free, temperature controlled amination reaction. Thus we explored the scope and limitations of this reaction, and this is discussed further in Manuscript 2.



## REFERENCES

- 1.) Maruyama, K.; Katagiri, T., *J. Phys. Org. Chem.* **1989**, 2, 205-213
- 2.) Gilman, H.; Jones, R. G.; Woods, L. A., *J. Org. Chem.* **1952**, 17(12), 1630–1634),
- 3.) Wu, G.; Huang, M., *Chem. Rev.* **2006**, 106, 2596-2616
- 4.) Hoffman, R.W., *Angew. Chem. Int. Ed.* **2001**, 40(8).1411-1416
- 5.) Seechurn, C.; Kitching, M.; Colacot, T.; Snieckus, V., *Angew. Chem. Int. Ed.* **2012**, 51, 5062-5085
- 6.) Bruckl, T.; Baxter, R.D.; Ishihara, Y.; Baran, P.S., *Acc. Chem. Res.* **2012**, 45(6), 826–839
- 7.) Norinder, J.; Matsumoto, A.; Yoshikai, N.; Nakamura, E., *J. Am. Chem. Soc.* **2008**, 130 (18), 5858–5859
- 8.) Yoshikai, N.; Matsumoto, A.; Norinder, J.; Nakamura, E., *Angew. Chem. Int. Ed.* **2009**, 48, 2925-2928
- 9.) Ilies, L.; Asako, S.; Nakamura, E.; *J. Am. Chem. Soc.* **2011**, 133, 7672-7675
- 10.) Shang, R.; Ilies, L.; Matsumoto, A.; Nakamura, E.; *J. Am. Chem. Soc.* **2013**, 135, 6030-6032
- 11.) Nakamura, Y.; Ilies, L.; Nakamura, E. *Org. Lett.* **2011**, 13, 5998-6001
- 12.) Ilies, L.; Kobayashi, M.; Matsumoto, A.; Yoshikai, N.; Nakamura, E., *Adv. Synth. Catal.* **2012**, 354, 593-596
- 13.) Yoshikai, N.; Asako, S.; Yamakawa, T.; Ilies, L.; Nakamura, E. *Chem. Asian J.* **2011**, 6, 3059-3065
- 14.) Yoshikai, N.; Matsumoto, A.; Norinder, J.; Nakamura, E. *Synlett.* **2010**, 313-316
- 15.) Asako, S.; Ilies, L.; Nakamura, E. *J. Am. Chem. Soc.* **2013**, 135, 17755-17757

- 16.) Asako, S.; Norinder, J.; Ilies, L.; Yoshikai, N.; Nakamura, E., *Adv. Synth. Catal.* **2014**, *356*, 1481-1485
- 17.) Matsubara, T.; Asako, S.; Ilies, L.; Nakamura, E. *J. Am. Chem. Soc.* **2014**, *136*, 646-649
- 18.) Shang, R.; Ilies, L.; Asako, S.; Nakamura, E., *J. Am. Chem. Soc.* **2014**, *136*, 14349-14352
- 19.) Hatekeyama, T.; Hashimoto, T.; Kondo, Y.; Fujiwara, Y.; Seike, H.; Takaya, H.; Tamada, Y.; Ono, T.; Nakamura, M., *J. Am. Chem. Soc.* **2010**, *132*, 10674–10676
- 20.) Guram, A.; Buchwald, S., *J. Am. Chem. Soc.* **1994**, *116*, 7901-7902
- 21.) Paul, F.; Patt, J.; Hartwig, J., *J. Am. Chem. Soc.* **1994**, *116*, 5969-5970
- 22.) Ehrentraut, A.; Zapf, A.; Beller M., *J. Molec. Cat. A*: **2002**, (182-183), 515-523
- 23.) Tsang, W. C. P.; Zheng, N.; Buchwald, S. L., *J. Am. Chem. Soc.* **2005**, *127*, 14560-14561.
- 24.) Brasche, G.; Buchwald, S. L., *Angew. Chem., Int. Ed.* **2008**, *47*, 1932.
- 25.) Gromhann, C.; Wang, H.; Glorius, F., *Org. Lett.* **2012**, *14*(2), 656-659
- 26.) Qian, X.; Yu, Z.; Auffrant, A.; Gosmini, C., *Chem. Eur. J.*, **2013**, *19*, 6225 – 6229
- 27.) Berman, A.; Johnson, J. S., *J. Am. Chem. Soc.* **2004**, *126*, 5680-568
- 28.) Rucker, R.; Whittaker, A.M.; Dang, H.; Lalic, G., *J. Am. Chem. Soc.* **2012**, *134*, 6571–6574
- 29.) Matsuda, N.; Hirano, K.; Satoh, T.; Miura, M., *Org. Lett.* **2011**, *13*(11), 2860-2863

30.) Hatakeyama, T.; Yoshimoto, Y.; Ghorai, S.K.; Nakamura, M., *Org. Lett.* **2010**,  
12(7), 1516-1519

## CHAPTER 2: MANUSCRIPT 1

Manuscript 1 entitled, “Iron-Catalyzed Arylation of Heterocycles via Direct C-H Activation” was published in Organic Letters in January 2014.

There is an increasing need in both the fine chemical and pharmaceutical industries for the development of new methods that easily provide substituted heterocycles. One of the methods that have been extensively explored for this function is the direct conversion of carbon–hydrogen (C–H) bonds into carbon–carbon (C–C) bonds.<sup>1</sup> This process is considered a “green” synthetic pathway because it eliminates the prefunctionalization steps required in modern coupling reactions and, therefore, directly reduces time, expenses, and hazardous waste. In fact, the ACS Green Chemistry Roundtable described C–H functionalizations of heterocycles as the most desirable new reactions that could benefit the pharmaceutical industry.<sup>2,3</sup>

For decades, precious metals, namely palladium, have been the primary catalysts used for both traditional coupling and C–H arylation reactions.<sup>4</sup> Iron catalysts, which are readily available, cheap, and nontoxic, have been relatively unexplored for coupling reactions. However, new methods are emerging that suggest an important role for this transition metal in modern organic synthesis.<sup>5</sup> Notably, Nakamura has recently developed an iron-catalyzed C–H arylation reaction.<sup>6</sup> Comparison of the metallic catalyst used in two similar methods for the direct C–H arylation of 2-phenylpyridine shows that the iron-catalyzed reaction proceeds at lower temperatures and is higher yielding and the catalyst is 22 times cheaper (Scheme 2.1).<sup>4b,6b,7</sup> Though the utility of iron-catalyzed C–H arylation reactions is apparent, the scope of these potentially transformative reactions has yet to be expanded to include the arylation of highly desired heterocycles, and the mechanism is still not fully

understood. Herein, we describe the ability to perform directed C–H arylations of heterocyclic substrates using cheap and nontoxic iron catalysts.

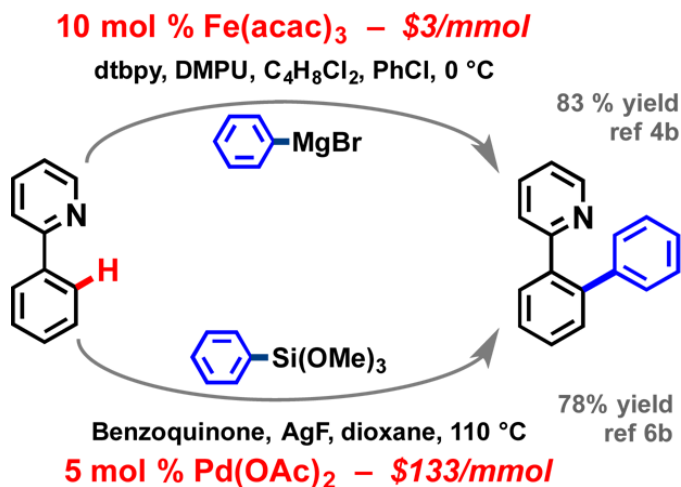
Our initial studies commenced with the pyridine substrate shown in Table 2.1. Nakamura's conditions that were previously shown in Scheme 2.1 were not optimal, producing only a 67% yield (entry 3). Also in contrast to Nakamura's work, the monoarylated product was exclusively obtained; the diarylated product was never observed for any of the reactions presented herein. Extended reaction times led to deterioration of the reaction's yield, possibly as a consequence of reduction of the imine; on a few occasions, the corresponding amine was isolated as a minor product.

Careful control of reaction conditions allowed for complete conversion in 15 min. Notable difficulty arose with regards to the drop rate of the Grignard reagent and the stir rate of the reaction.<sup>6b</sup> It appears that the size of the reaction vessel can also dramatically alter yield. Dropwise Grignard addition into small, narrow vials provided almost no reaction, with exclusive homocoupling of the Grignard reagent resulting in biphenyl formation. This is likely caused by a combination of small surface area for substrate reactivity and inadequate stir rates. Larger flasks (e.g., 35–50 mL round-bottom flasks for a 0.55mmol reaction), providing more surface area, and high stir rates proved to be the best choice (see Supporting Information for details.)

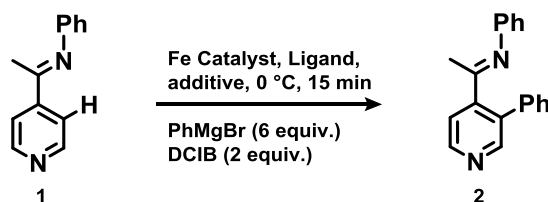
The reactions were very clean; the only compounds that could be observed by GCMS were the starting materials, the biaryl product and biphenyl, arising from homocoupling of the Grignard reagent. To minimize the aerobic iron-catalyzed homocoupling, an inert atmosphere and excess Grignard reagent were required.<sup>8</sup>

Additionally, we employed additives such as DMPU<sup>9</sup> or KF<sup>10</sup> which have been previously shown to minimize Grignard homocoupling.

**Scheme 2.1.** Comparison of C–H Arylation Methods



The best conversion was achieved with a catalyst/ligand ratio of 1:2 (Table 2.1, entry 2). As shown by Nakamura, 4,4'-di-tertbutyl bipyridine (dtbpy) appeared to be the optimal ligand (entries 2, 5, and 6). Interestingly, the use of FeF<sub>3</sub>·3H<sub>2</sub>O showed 18% product formation, with no biphenyl present (entry 9); but the optimal catalyst was Fe(acac)<sub>3</sub> (entries 7 and 8), so this was used for subsequent experiments. We ultimately chose to perform the reactions in the presence of the KF additive (entry 7) due to a slight suppression of the biphenyl byproduct.

**Table 2.1** Optimization of Pyridine Arylation

Entry	Catalyst (loading)	Ligand <sup>a</sup> (loading)	Additive	% Conversion <sup>b</sup>
1	Fe(acac) <sub>3</sub> (20 mol %)	dtbpy (20 mol %)	DMPU	73
2	Fe(acac) <sub>3</sub> (10 mol %)	dtbpy (20 mol %)	DMPU	90
3	Fe(acac) <sub>3</sub> (10 mol %)	dtbpy (10 mol %)	DMPU	67
4	Fe(acac) <sub>3</sub> (5 mol %)	dtbpy (20 mol %)	DMPU	58
5	Fe(acac) <sub>3</sub> (10 mol %)	bpy (20 mol %)	DMPU	15
6	Fe(acac) <sub>3</sub> (10 mol %)	bphen (20 mol %)	DMPU	37
7	Fe(acac) <sub>3</sub> (10 mol %)	dtbpy (20 mol %)	KF	100
8	Fe(acac) <sub>3</sub> (10 mol %)	dtbpy (20 mol %)	none	100
9	FeF <sub>3</sub> ·3H <sub>2</sub> O (10 mol %)	dtbpy (20 mol %)	KF	18
10	FeF <sub>3</sub> ·3H <sub>2</sub> O (10 mol %)	dtbpy (20 mol %)	KF	76
11	Fe(acac) <sub>2</sub> (10 mol %)	dtbpy (20 mol %)	KF	7

<sup>a</sup>dtbpy = 4,4'-di-*tert*-butyl-2,2'-dipyridyl, bpy = 2,2'-bipyridine, bathophenanthroline. <sup>b</sup>All reactions were performed on a 0.55 mmol substrate scale. Percent conversion based on GC analysis of product:starting material ratio.

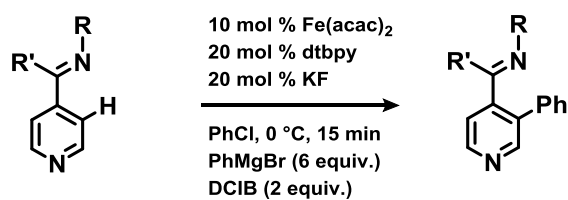


Interestingly, an iron(II) catalyst was ineffective (entry 11). Future research efforts in our laboratory will be directed toward identifying the catalytic intermediates in this reaction, including the oxidation state of the iron in this process. Further screening of solvents and oxidants showed that our original choices, chlorobenzene and 1,2-dichloro-2-methylpropane, were optimal.

When our optimized conditions were applied to the nonheterocyclic substrate derived from acetophenone, diarylated products were observed, as previously shown by Nakamura (not shown).<sup>6</sup>

A screen of directing groups was performed (Table 2.2). Use of the paramethoxyphenyl (PMP) directing group showed promising conversion (entry 3), but complete conversion was achieved using aniline derivatives (entry 1). Comparison of the imines derived from heterocyclic aldehydes and ketones (entries 1 and 4) showed drastic steric requirements for reaction conversion. Oxime ethers and alkyl imines completely inhibited the reaction (entries 2 and 5), possibly by strong coordination to the iron catalyst.

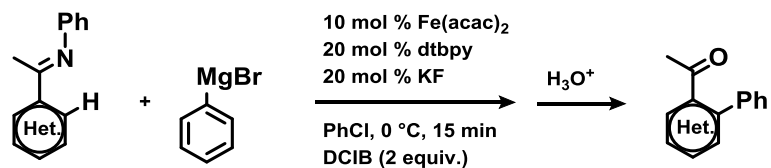
Our optimized reaction conditions were then applied to a variety of heterocyclic substrates (Table 2.3). In most cases, the imine group could be easily hydrolyzed to the ketone.<sup>11</sup> Several nitrogen-containing heterocyclic biaryls could only be isolated as imines (entries 1 and 3) because the hydrolysis of these compounds proved more difficult than expected, presumably due to protonation of the heterocycle's basic nitrogen. For reactions that did not reach complete conversion, the isolated yields were reduced considerably due to difficult chromatographic separations.

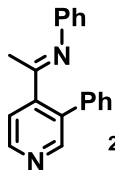
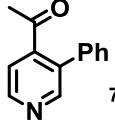
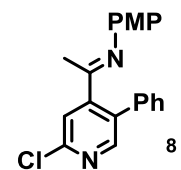
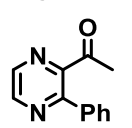
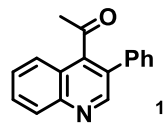
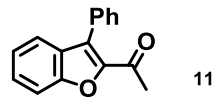
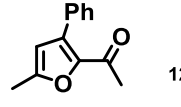
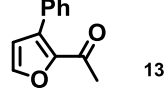
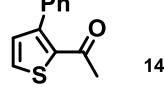
**Table 2.2.** Directing Group Optimization

Entry	Substrate	% Conversion <sup>a</sup>	Isolated % Yield <sup>b</sup>
1	 1	>99	88
2	 3	0	-
3	 4	39	38
4	 5	0	-
5	 7	0	-

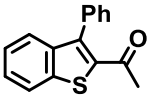
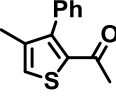
<sup>a</sup>All reactions were performed on a 0.55 mmol substrate scale. Conversion was calculated by subtracting  $A_{\text{starting material}} / A_{\text{product}}$  from 100%, where  $A_{\text{starting material}}$  and  $A_{\text{product}}$  were calculated using the areas of the corresponding peaks in the gas chromatogram. <sup>b</sup>Isolated yields obtained after flash chromatography.

**Table 2.3:** Substrate Scope



Entry	Product	% Conversion <sup>a</sup>	Isolated % Yield <sup>b</sup>
1	 2	>99	88 <sup>c</sup>
2	 7	>99	34
3	 8	>99	67
4	 9	100	25
5	 10	0	-
6	 11	90	52
7	 12	100	66
8	 13	100	15
9	 14	100	82

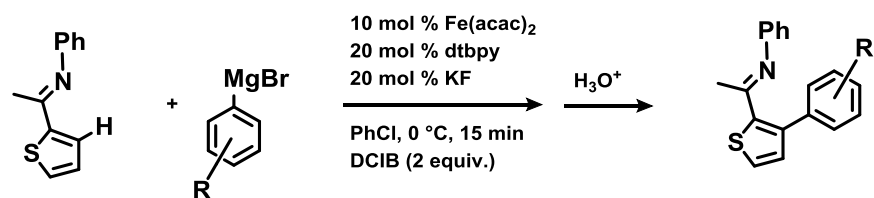
**Table 2.3.** (Continued) Substrate Scope

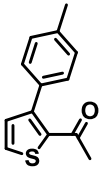
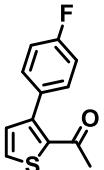
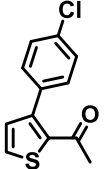
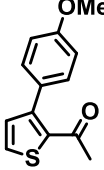
Entry	Product	% Conversion <sup>a</sup>	Isolated % Yield <sup>b</sup>
10	 15	50	45 (91 <sup>d</sup> )
11	 16	0	-

<sup>a</sup>All reactions were performed on a 0.55 mmol substrate scale. Conversion was calculated by subtracting  $A_{\text{starting material}} / A_{\text{product}}$  from 100%, where  $A_{\text{starting material}}$  and  $A_{\text{product}}$  were calculated using the areas of the corresponding peaks in the gas chromatogram. <sup>b</sup>Isolated yields obtained after flash chromatography. <sup>c</sup>Trace starting material detected by <sup>1</sup>H NMR but not GC. <sup>d</sup>Based on recovered starting material

The yields of the arylations were sterically dependent, and opposing trends were observed for pyridines, thiophenes, and furans. Comparison of sulfur-containing compounds shows that benzothiophene was less reactive than thiophene (entries 10 and 9), and 3-methyl thiophene (entry 11) was completely nonreactive, indicating a decrease in reactivity with increasing steric hindrance.

Analysis of the oxygen-containing heterocycles shows that conversions and yields increased with steric constraints (entries 6–8). Azole substrates appear to be more robust (entries 1–4). Notably, chlorinated pyridines can be readily substituted, allowing for subsequent functionalization (entry 3). A quinoline substrate was nonreactive (entry 5); however, this could be attributed to the aldehyde-derived directing group described in Table 2.2, entry 4.

**Table 2.4.** Grignard Reagent Scope

Entry	Product	% Conversion <sup>a</sup>	Isolated % Yield <sup>b</sup>
1	 18	100	70
2	 19	50	32
3	 20	95	71
4	 21	75	63

<sup>a</sup>All reactions were performed on a 0.55 mmol substrate scale. Conversion was calculated by subtracting  $A_{\text{starting material}} / A_{\text{product}}$  from 100%, where  $A_{\text{starting material}}$  and  $A_{\text{product}}$  were calculated using the areas of the corresponding peaks in the gas chromatogram. <sup>b</sup>Isolated yields obtained after flash chromatography.

As the thiophene substrate provided the highest yields, it was used to generate a brief Grignard scope (Table 2.4). Halogen substituted aromatic Grignard reagents reduced the conversion and decreased the overall yield (entries 2 and 3). Electron

donating groups also appeared to slightly decrease the yield (entries 1 and 4). Methyl and cyclohexyl Grignard reagents afforded no reaction. The elucidation of the seemingly contradictory electronic and steric trends for this reaction will be the subject of future studies.

In summary, we have shown that iron-catalyzed arylation via C–H bond activation can be successfully carried out on a variety of N-, S-, and O-containing heterocycles at 0 °C, over 15 min. Future work will involve insight into the reaction mechanism to provide further understanding and reaction control.

## REFERENCES

- 1.) The field has been reviewed extensively. For examples, see: (a) Dyker, G.  
Handbook of C–H transformations: applications in organic synthesis; Wiley-VCH:  
**2005**. (b) Godula, K.; Sames, D., *Science*, **2006**, *312*, 67. (c) Alberico, D.; Scott,  
M. E.; Lautens, M. *Chem. Rev.*, **2007**, *107*, 174. (d) Bellina, F.; Rossi, R.,  
*Tetrahedron*, **2009**, *65*, 10269. (e) Chen, X.; Engle, K. M.; Wang, D.; Yu, J.,  
*Angew. Chem., Int. Ed.*, **2009**, *48*, 5094. (f) Joucla, L.; Djakovitch, L. *Adv. Synth.*  
*Catal.*, **2009**, *351*, 673. (g) White, C. M., *Synlett* **2012**, *23*, 2746.
  
- 2.) For a review of C–H arylation of heterocycles, see: Kantak, A.; DeBoef, B.  
Intermolecular Coupling via C(sp<sup>2</sup>)–H Activation. In *Science of Synthesis*;  
George Thieme Verlag KG: New York, 2013; pp 585–641.
  
- 3.) Constable, D. J. C.; Dunn, P. J.; Hayler, J. D.; Humphrey, G. R.; Leazer, J. L., Jr.;  
Linderman, R. J.; Lorenz, K.; Manley, J.; Pearlman, B. A.; Wells, A.; Zaks, A.;  
Zhang, T. Y., *Green Chem.*, **2007**, *9*, 411.
  
- 4.) (a) *Modern Arylation Methods*; Ackermann, L.; Wiley-VCH: Weinheim, **2009**. (b)  
Yu, W.-Y.; Sit, W. N.; Zhou, Z.; Chan, A. S.-C., *Org. Lett.*, **2009**, *11*, 3174. (c)  
Chu, J.-H.; Tsai, S.; Wu, M., *Synthesis*, **2009**, *22*, 3757. (d) Li, W.; Jiang, X.; Sun,  
P., *J. Org. Chem.*, **2011**, *76* (20), 8543. (e) Kirchberg, S.; Volger, T.; Studer, A.,  
*Synlett*, **2008**, *18*, 2841.
  
- 5.) For examples, see: (a) Wen, J.; Zhang, Ji.; Chen, S.-Y.; Li, J.; Yu, X.-Q., *Angew.*  
*Chem.*, **2008**, *47*, 8897. (b) Tran, L. D.; Daugulis, O., *Org. Lett.*, **2010**, *12*, 4277.  
(c) Chen, M. S.; White, C. M., *Science*, **2007**, *318*, 783. (d) Correa, A.; Bolm, C.,

- Angew. Chem.*, **2007**, *119*, 9018. (e) Bart, S. C.; Lobkovsky, E.; Chirki, P. J., *J. Am. Chem. Soc.*, **2004**, *126*, 13794.
- 6.) (a) Norinder, J.; Matsumoto, A.; Yoshikai, N.; Nakamura, E., *J. Am. Chem. Soc.*, **2008**, *130*, 5858. (b) Yshikai, N.; Sobi, A.; Yamakawa, T.; Ilies, L.; Nakamura, E., *Chem. Asian J.*, **2011**, *6*, 3059.
- 7.) Prices compared for 25 g bottles from Sigma-Aldrich Co.: [www.sigmaaldrich.com](http://www.sigmaaldrich.com), Accessed Dec. 16, 2013.
- 8.) Cahiez, G.; Moyeux, A.; Buendia, J.; Duplais, C., *J. Am. Chem. Soc.*, **2007**, *129*, 13788.
- 9.) Ilies, L.; Matsubara, T.; Nakamura, E., *Org. Lett.*, **2012**, *14*, 5570.
- 10.) Agrawal, T.; Cook, S. P., *Org. Lett.*, **2013**, *15*, 96.
- 11.) Anderson, L. L.; Arnold, J.; Bergman, R. G., *Org. Lett.*, **2004**, *6*, 2519.



### CHAPTER 3: MANUSCRIPT 2

Manuscript 2 entitled, “Transition-Metal Free Carbon-Nitrogen Bond Formation Mediated by Low Temperatures” will be submitted to Tetrahedron Letters for publication in May 2015.

The formation of C-N bonds is essential for the synthesis of highly desirable pharmaceutical and biologically active targets. Current methods rely on transition metals such as palladium<sup>1</sup> and rhodium.<sup>2</sup> More recently the focus has shifted towards reagents that are more environmentally friendly and affordable catalysts like cobalt,<sup>3</sup> copper,<sup>4,5,6</sup> and nickel.<sup>7,8,9</sup> Recent advances have discovered transition metal free methods that also result in C-N bond formation.<sup>10</sup> We report herein a fast and easy method for the formation of C-N bonds resulting in arylated tertiary amines.

Considering our recent work involving iron and Grignard reagents to directly form carbon-carbon (C-C) bonds on various heterocycles,<sup>11</sup> and the success of other transition metals accomplishing reactions of this type, we envisioned that iron-catalyzed reactions could play a role in these mechanisms as well.

Bolm and Correa have already demonstrated that iron can efficiently form C<sub>sp2</sub>-N bonds from aryl iodides and nucleophilic nitrogen sources.<sup>12</sup> Our initial optimization focused on the coupling of N-chloroamines with phenylmagnesium bromide in an effort to form similar C<sub>sp2</sub>-N bonds in an Umpolung fashion. The variables investigated included the screening of iron catalysts, nitrogen and phosphine ligands, several additives, and a range of temperatures.

**Scheme 3.1.** Initial Optimization Outline

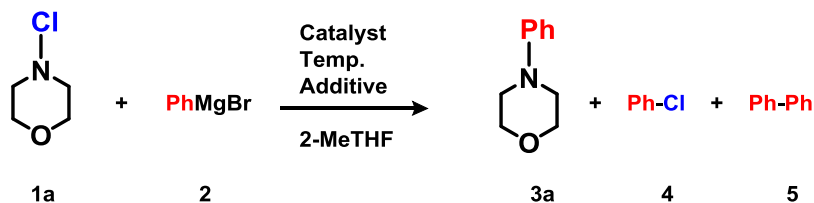


**Table 3.1.** Optimization of Reaction Conditions<sup>a</sup>

Entry	Catalyst (10 mol %)	Temp. (°C)	Additive	Isolated Yields
1	FeCl <sub>2</sub>	0	None	36 <sup>b</sup>
2	Fe(SO <sub>4</sub> ) <sub>3</sub> *H <sub>2</sub> O	0	None	62 <sup>b</sup>
3	Fe(C <sub>2</sub> O <sub>4</sub> ) <sub>2</sub> *2H <sub>2</sub> O	0	None	40 <sup>b</sup>
4	FeF <sub>3</sub> *3H <sub>2</sub> O	0	None	46 <sup>b</sup>
5	Fe(NO <sub>3</sub> ) <sub>3</sub> *9H <sub>2</sub> O	0	None	19 <sup>b</sup>
6	Fe(acac) <sub>3</sub>	0	None	46 <sup>b</sup>
7	None	0	None	49 <sup>b</sup>
<b>8</b>	<b>Fe(acac)<sub>2</sub></b>	<b>0</b>	<b>None</b>	<b>88<sup>b</sup></b>
9	Fe(acac) <sub>2</sub>	0	None	47
10	Fe(acac) <sub>2</sub>	0	LiCl	58
11	Fe(acac) <sub>2</sub>	0	MgBr <sub>2</sub>	0
12	Fe(acac) <sub>2</sub>	-40	None	79
13	Fe(acac) <sub>2</sub>	-78	None	49 <sup>c</sup>
14	Fe(acac) <sub>2</sub>	-78	None	75
15	Fe(acac) <sub>2</sub>	-78	None	74 <sup>d</sup>
16	Fe(acac) <sub>2</sub>	-78	dtbpy	77
17	Fe(acac) <sub>2</sub>	-78	bpy	75
18	Fe(acac) <sub>2</sub>	-78	phen	84
19	Fe(acac) <sub>2</sub>	-78	binap	81
20	Fe(acac) <sub>2</sub>	-78	dppbz	74
21	None	-78	phen	80
<b>22</b>	<b>None</b>	<b>-78</b>	<b>None</b>	<b>99</b>

a.) reactions performed on a 1.00 mmol scale in 2.00 mL of 2-MeTHF using 1.5 eq. of Grignard reagent b.) yields determined by GC-MS using dodecane as an internal standard. c.) 1.0 eq. Grignard reagent used. d.) 2.0 Grignard reagents used.

Our initial efforts to use iron catalysts appeared successful. Several iron salts were shown to produce the expected product in reasonable yields (entries 1-8). However attempts to isolate this product significantly decreased the yield (entry 9).

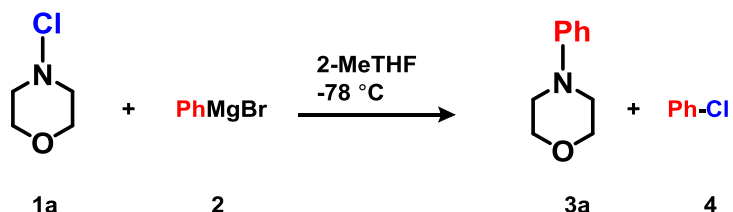
Inorganic salts have been shown to promote the presumed transmetallation step.<sup>13</sup> In our case these were detrimental to the yield (entries 10 and 11), and in the case of  $\text{MgBr}_2$  completely shut off the reaction. Contrary to other's reports throughout the process we detected chlorobenzene as a dominant byproduct as well as small amounts of biphenyl. In an attempt to minimize these side reactions we lowered the temperature and varied the equivalents of Grignard reagent used (entries 12-14). We found that with 1.5 equivalents of Grignard reagent at  $-78\text{ }^\circ\text{C}$  the reaction afforded a 75% yield. With these optimized conditions we attempted to investigate the substrate scope. Unfortunately the  $\text{Fe}(\text{acac})_2$  catalyzed reactions performed on other substrates showed a significant decrease in yield (Figure 1: 3b and 3g), and other metals,  $\text{CoBr}_2$  and  $\text{Cu}(\text{OTf})_2$ , were detrimental (3b and 3c).

Not satisfied with these results, we screened several ligands hoping to increase our yield further (entries 16-20). Introducing dinitrogen ligands had a small beneficial effect on the reaction (entries 16-20). However we were aware that these reactants could successfully couple in the presence of these dinitrogen bases without any catalyst,<sup>10</sup> although those reactions were performed at  $-40\text{ }^\circ\text{C}$  and required several hours for completion. Removing the iron as a control afforded the product in near-equal yields (entry 21). This was discouraging; but we quickly realized that the ligand itself was also not necessary for the reaction to occur (entry 22). This has been

demonstrated previously by Knochel<sup>14</sup> at -45 °C, however he suggested limitations to the reaction scope and that this was only applicable to benzylic N-chloroamines.

Transition metal free reactions were performed at several temperatures (Table 3.2). The decrease in temperature showed a steady increase in product formation, as well as a decrease in overall byproducts.

**Table 3.2.** Effect of Temperature on C-N Bond Formation

			
1a	2	3a	4
Temperature (°C)	Yield 3a	Yield 4	3a : 4
22	48	55	0.9
0	59	30	2.0
-21	77	35	2.2
-41	86	36	2.4
-78	87	29	3.0

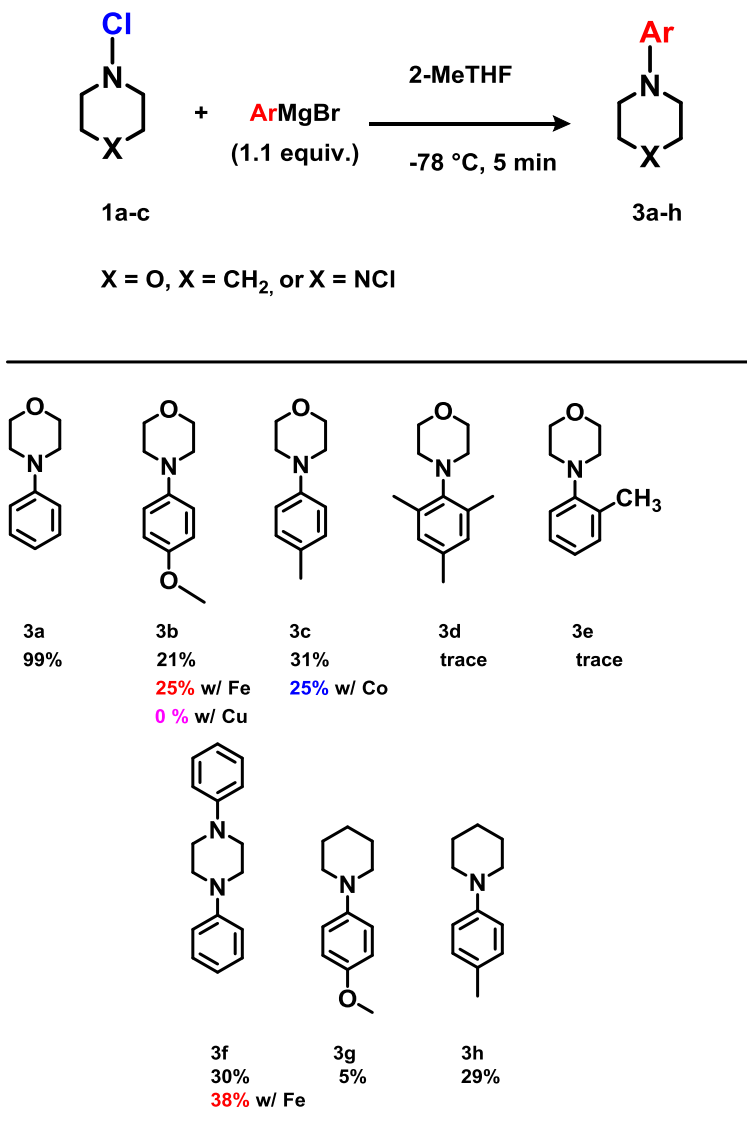
The results of our extensive optimization showed that N-chloroamines and aryl Grignard reagents readily couple between -40 and -78 °C with no need for additives or catalysts. The coupling does occur at room temperature. However the resulting biphenyl, from the homo-coupled Grignard reagent, as well as chlorobenzene from

chlorinated Grignard reagent are present in high amounts. Prolonged reaction times had no immediate affect and eventually resulted in product decomposition.

2-methyl tetrahydrofuran (2-MeTHF) was used as the primary solvent. Since the yields achieved from our reactions are comparable to that performed in THF. We chose this as it originates from a renewable source. Unfortunately, further attempts to expand the reaction to other amines beyond morpholine, and a variety of substituted Grignard reagents, still resulted in low yields (Scheme 3.2).

Only the original N-phenylmorpholine product (1a) showed high yields. The mesitylmorpholine (3d) and o-methylmorpholine (3e) reactions showed only trace amounts of products detected by NMR spectroscopy. The diarylated product (3f) was also respectable since the reaction must have occurred twice.

**Scheme 3.2.** Reaction Scope



Despite these poor results, we are still comfortable with these established baseline yields for directly reacting N-chloroamines with aryl Grignard reagents. The reactions run smoothly and are complete upon the drop-wise addition of the Grignard reagent (<5 minutes). We hope that this work serves as a cautionary example to be considered when testing for presumed catalytic activity in future systems. Future work will investigate the mechanism governing these reactions. Further efforts to use other

organometallic reagents, like organolithium or organozinc species, will be performed as well as expansion of this reaction to include alkyl Grignards and amines.



## REFERENCES

- 1.) Ehrentraut, A.; Zapf, A.; Beller, M. *Journal of Molecular Catalysis*. **2002**, *182–183*, 515–523
- 2.) Grohmann, C.; Wang, H.; and Glorius, F., *Org. Lett.* **2012**, *14* (2), 656-659
- 3.) Qian, X.; Yu, Z.; Auffrant, A.; Gosmini, C., *Chem. Eur. J.*, **2013**, *19*, 6225 – 6229
- 4.) Berman, A.; Johnson, J. S., *J. Am. Chem. Soc.*, **2004**, *126*, 5680-5681
- 5.) Rucker, R.; Whittaker, A.M.; Dang, H.; Lalic, G., *J. Am. Chem. Soc.* **2012**, *134*, 6571–6574
- 6.) Matsuda, N.; Hirano, K.; Satoh, T.; Miura, M., *Org. Lett.* **2011**, *13*(11), 2011, 2860-2863
- 7.) Desmarets, C.; Schneider, R.; Fort, Y., *J. Org. Chem.* **2002**, *67*, 3029-3036
- 8.) Brenner, E.; Schneider, R.; Fort, Y., *Tetrahedron* **1999**, *55*, 12829-12842
- 9.) Barker, T.; Jarvo, E.; *J. Am. Chem. Soc.* **2009**, *131*, 15598-15599
- 10.) Hatakeyama, T.; Yoshimoto, Y.; Ghorai, S.K.; Nakamura, M., *Org. Lett.* **2010**, *12*(7), 1516-1519
- 11.) Sirois, J.J.; Davis, R.; DeBoef, B., *Org. Lett.* 2014, *16*, 868–871
- 12.) Correa, A.; Bolm, C., *Angew. Chem. Int. Ed.* **2007**, *46*, 8862 –8865
- 13.) Hatakeyama, T.; Hashimoto, T.; Kondo, Y.; Fujiwara, Y.; Seike, H.; Takaya, H.; Tamada, Y.; Ono, T.; Nakamura, M., *J. Am. Chem. Soc.* **2010**, *132*, 10674-10676
- 14.) Sinha, P.; Knochel, P., *Synlett*. **2006**, *19*, 3304–3308

## CHAPTER 4: EXPERIMENTAL SECTION MANUSCRIPT 1

### **Instrumentation:**

GC/MS analysis was carried out on an Agilent Technologies 6890 GC system fixed with a 5973 mass selective detector. GC/MS Conditions: J & W Scientific DB-1, capillary 25.0m x 200 $\mu$ m x 0.33 $\mu$ m, 1.3 mL/min, 40 °C, hold 0.50 min, 12 °C/min to 320 °C, hold 6.0 min. NMR spectra were acquired with a Bruker Avance 300 MHz spectrometer.

### **General Synthesis of Imines**

To an oven dried 50 mL RBF with stir bar was added 5 g of 3 Å molecular sieves and 12.00 mL of toluene. The system was sealed with a rubber septum and flushed with N<sub>2</sub>. The amine (2.5 mmol) and heterocyclic ketone (2.3 mmol) were added successively via syringe. The reaction was stirred at 100 °C for 4 hrs, then cooled to room temp. The mixture was filtered through Celite, and the filtrate was concentrated *in vacuo*. The crude residue was purified by column chromatography (9:1 Hexanes:EtOAc).

### **Representative Procedure for Arylation of N-Heterocyclic Imines:**

To an oven dried 35 mL RBF with stir bar was added the imine ( 0.55 mmol), dtbpy (0.0303 g, 0.11 mmol) KF (0.0064 g, 0.11 mmol), 2.00 mL of chlorobenzene, and 0.55 mL of 0.10 M Fe(acac)<sub>3</sub> in THF. The solution was stirred at room temperature for 5 minutes while being flushed with N<sub>2</sub> and evacuated 3x. The RBF was degassed by sonication for 15 minutes, and then transferred to an ice/H<sub>2</sub>O bath for 15 minutes under N<sub>2</sub>. The 1,2-dichloroisobutane (0.13 mL, 1.10 mmol) was added and the system was again purged with N<sub>2</sub> / evacuated 3x. Then 1.0 M PhMgBr (3.30 mL,

3.30 mmol) was added dropwise over 15 minutes. The reaction was then removed from ice and warmed to room temperature. The solution was diluted with EtOAc and extracted 3x with 25 mL DI H<sub>2</sub>O to remove iron. The organic layer was dried over MgSO<sub>4</sub>, filtered, and concentrated *in vacuo*. The crude residue was purified by column chromatography.

**Representative Procedure for Arylation and *in situ* Hydrolysis of N-Heterocyclic Imines:**

To an oven dried 35 mL RBF with stir bar was added the imine ( 0.55 mmol), dtbpy (0.0303 g, 0.11 mmol) KF (0.0064 g, 0.11 mmol), 2.00 mL of chlorobenzene, and 0.55 mL of 0.10 M Fe(acac)<sub>3</sub> in THF. The solution was stirred at room temperature for 5 minutes while being flushed with N<sub>2</sub> and evacuated 3x. The RBF was degassed by sonication for 15 minutes, and then transferred to an ice/H<sub>2</sub>O bath for 15 minutes under N<sub>2</sub>. The 1,2-dichloroisobutane (0.13 mL, 1.10 mmol) was added and the system was again purged with N<sub>2</sub> / evacuated 3x. Then 1.0 M PhMgBr (3.30 mL, 3.30 mmol) was added dropwise over 15 minutes. The reaction was then removed from ice and warmed to room temperature. The reaction was then removed from ice and warmed to room temperature. 10 mL of EtOAc, 10 mL of H<sub>2</sub>O and 3.00 mL of 6.00 M HCl were added successively. The reaction was stirred at 45 °C overnight. The mixture was extracted 3x with EtOAc. The organic layer was dried over MgSO<sub>4</sub>, filtered, and concentrated *in vacuo*. The crude residue was purified by column chromatography.

**Representative Procedure for Arylation and *in situ* Hydrolysis of S- and O-Heterocyclic Imines:**

To an oven dried 35 mL RBF with stir bar was added the imine (0.55 mmol), dtbpy (0.0303 g, 0.11 mmol) KF (0.0064 g, 1.10 mmol), 2.00 mL of chlorobenzene, and 0.55 mL of 0.10 M Fe(acac)<sub>3</sub> in THF. The solution was stirred at room temperature for 5 minutes while being flushed with N<sub>2</sub> and evacuated 3x. The RBF was degassed by sonication for 15 minutes, and then transferred to an ice/H<sub>2</sub>O bath for 15 minutes under N<sub>2</sub>. The 1,2-dichloroisobutane (0.13 mL, 1.10 mmol) was added, and the system was again purged with N<sub>2</sub> / evacuated 3x. Then 1.0 M PhMgBr (3.30 mL, 3.30 mmol) was added dropwise over 15 minutes. The reaction was then removed from ice and warmed to room temperature. 10 mL of EtOAc, 10 mL of H<sub>2</sub>O and 3.00 mL of 3.00 M HCl were added successively. The reaction was stirred at room temperature overnight. The mixture was extracted 3x with EtOAc. The organic layer was dried over MgSO<sub>4</sub>, filtered, and concentrated *in vacuo*. The crude residue was purified by column chromatography.

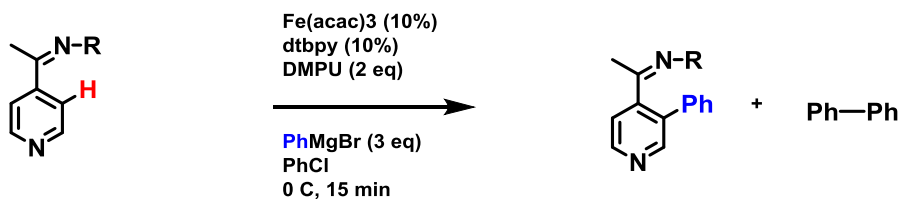
**Representative Procedure of Arylation and *in situ* Hydrolysis of Thiophene Imines:**

To an oven dried 35 mL RBF with stir bar was added the imine (0.55 mmol), dtbpy (0.0303 g, 0.11 mmol) KF (0.0064 g, 0.11 mmol), 2.00 mL of chlorobenzene, and 0.55 mL of 0.10 M Fe(acac)<sub>3</sub> in THF. The solution was stirred at room temperature for 5 minutes while being flushed with N<sub>2</sub> and evacuated 3x. The RBF was degassed by sonication for 15 minutes, and then transferred to an ice/H<sub>2</sub>O bath for 15 minutes under N<sub>2</sub>. The 1,2-dichloroisobutane (0.13 mL, 1.10 mmol) was added,

and the system was again purged with N<sub>2</sub> / evacuated 3x. The Grignard reagent (1.0 M) was added dropwise over 15 minutes. The reaction was then removed from ice and warmed to room temperature. 10mL of EtOAc, 10 mL of H<sub>2</sub>O and 3.00 mL of 3.00 M HCl were added successively. The reaction was stirred at room temperature overnight. The mixture was extracted 3x with EtOAc. The organic layer was dried over MgSO<sub>4</sub>, filtered, and concentrated *in vacuo*. The crude residue was purified by column chromatography.

#### **Reaction Vessel Size Comparison:**

Analysis of various reaction vessel sizes was performed using gas chromatography. The percent composition of each compound at the end of the 15 minute reaction was obtained, and a ratio of the biphenyl byproduct to the desired arylated product is shown. Narrow reaction vessels such as vials and Schlenk tubes showed a large biphenyl:product ratio. Wide, round bottom flasks showed significant product formation with comparative efficiency relative to vials and Schlenk tubes; 35 mL RBF's were shown to be the best.

**Table 4.1.** Comparison of Reaction Vessel Sizes

Vessel	% Ph-Ph	% Starting Material	% Product	Ph-Ph : Product
11 mL vial	66.4	27.5	6.1	10.9
11 mL vial	67.2	30.7	2.1	32.0
25 mL Schlenk Tube	74.5	19.5	6.0	12.4
25 mL RBF	70.6	18.3	11.1	6.4
35 mL RBF	40.3	0.0	59.6	0.7
50 mL RBF	54.7	9.5	35.8	1.5
50 mL RBF	50.5	25.2	24.3	2.1
100 mL RBF	71.2	5.7	23.1	3.1

**Characterization of Compounds:**

Known compounds were obtained by the procedures above and characterized via NMR spectroscopy; A  $^1\text{H}$  spectrum was provided for each compound and the relevant reference was cited. All novel compounds obtained have been characterized with  $^1\text{H}$  NMR,  $^{13}\text{C}$  NMR, and Mass Spectroscopy.

Characterization of (1)<sup>1</sup>

**<sup>1</sup>H NMR (300 MHz, CDCl<sub>3</sub>):**  $\delta$  8.74 (d,  $J$ =6.45 Hz, 2H), (dd,  $J$ =6.20, 1.62 Hz, 2H),  
7.38 (t,  $J$ =7.95 Hz, 2H), 7.13 (t,  $J$ =7.95 Hz, 1H), 6.79 (d,  $J$ =7.50 Hz, 2H), 2.24 (s, 3H)

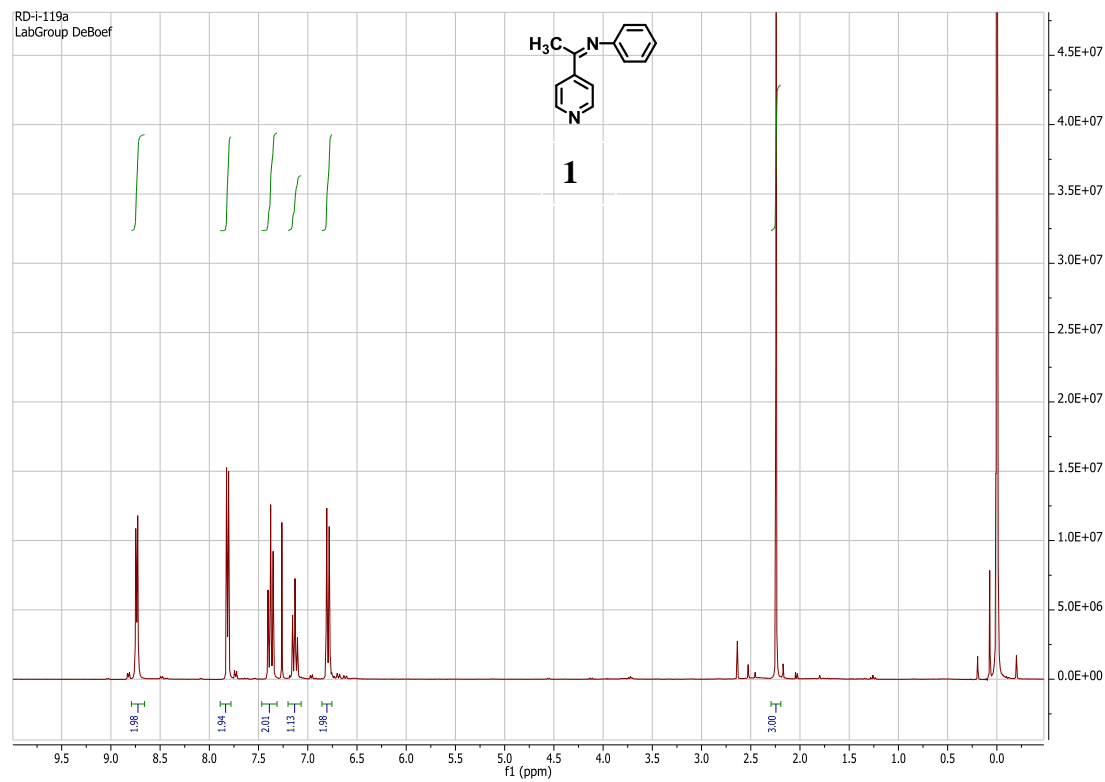


**Figure 4.1.** <sup>1</sup>H NMR of Compound 1

### Characterization of (2)

**$^1\text{H}$  NMR (300 MHz,  $\text{CDCl}_3$ ):**  $\delta$  8.69 (d,  $J=6.72$  Hz, 2H) 7.49 (m, 6H), 7.34 (t,  $J=7.27$  Hz, 2H), 7.10 (t,  $J=6.72$  Hz, 1H), 6.75 (t,  $J=7.77$  Hz, 2H), 1.69 (s, 3H)

**$^{13}\text{C}$  NMR (75 MHz,  $\text{CDCl}_3$ ):**  $\delta$  169.12, 150.62, 150.29, 149.00, 137.46, 129.13, 129.09, 128.80, 128.72, 128.47, 128.27, 123.95, 120.61, 119.02, 20.69

**LRMS EI ( $m/z$ ):**  $[M]^+$  calc'd for 272.13, observed 272.10 ( $m/z$ )

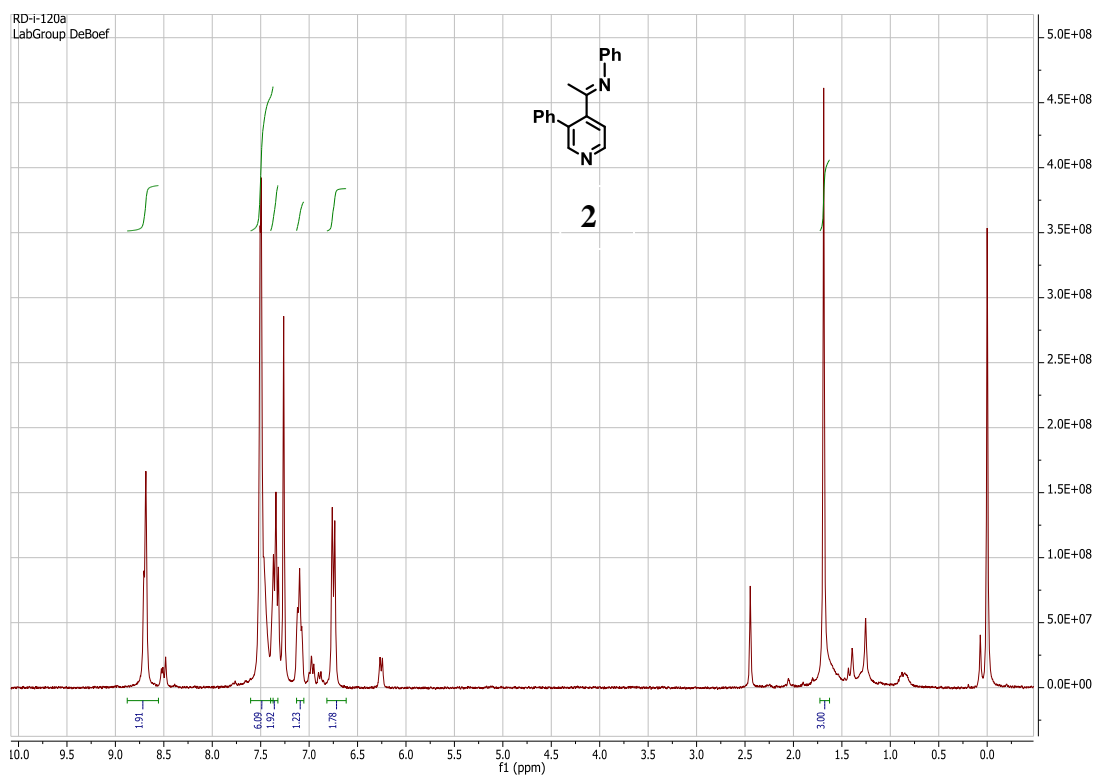


**Figure 4.2.**  $^1\text{H}$  NMR of Compound 2



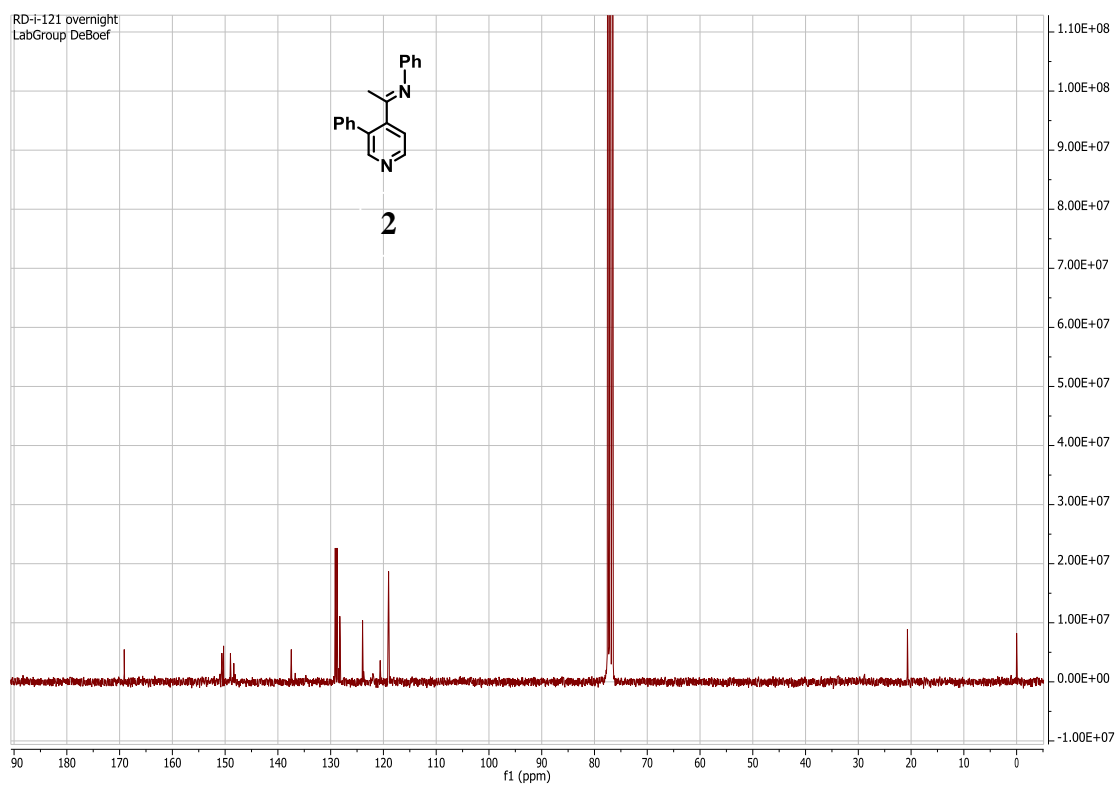


**Figure 4.3.**  $^{13}\text{C}$  NMR of Compound 2

Characterization of (3)

**$^1\text{H}$  NMR (300 MHz,  $\text{CDCl}_3$ ):**  $\delta$  8.8 (d,  $J=6.88$  Hz, 2H), 8.19 (d,  $J=6.88$  Hz, 2H), 4.15 (s, 3H), 2.30 (s, 3H)

**$^{13}\text{C}$  NMR (75 MHz,  $\text{CDCl}_3$ ):**  $\delta$  152.67, 149.66, 140.78, 122.78, 63.66, 11.45

**LRMS EI ( $m/z$ ):**  $[M]^+$  calc'd for 150.08, observed 150.05 ( $m/z$ )

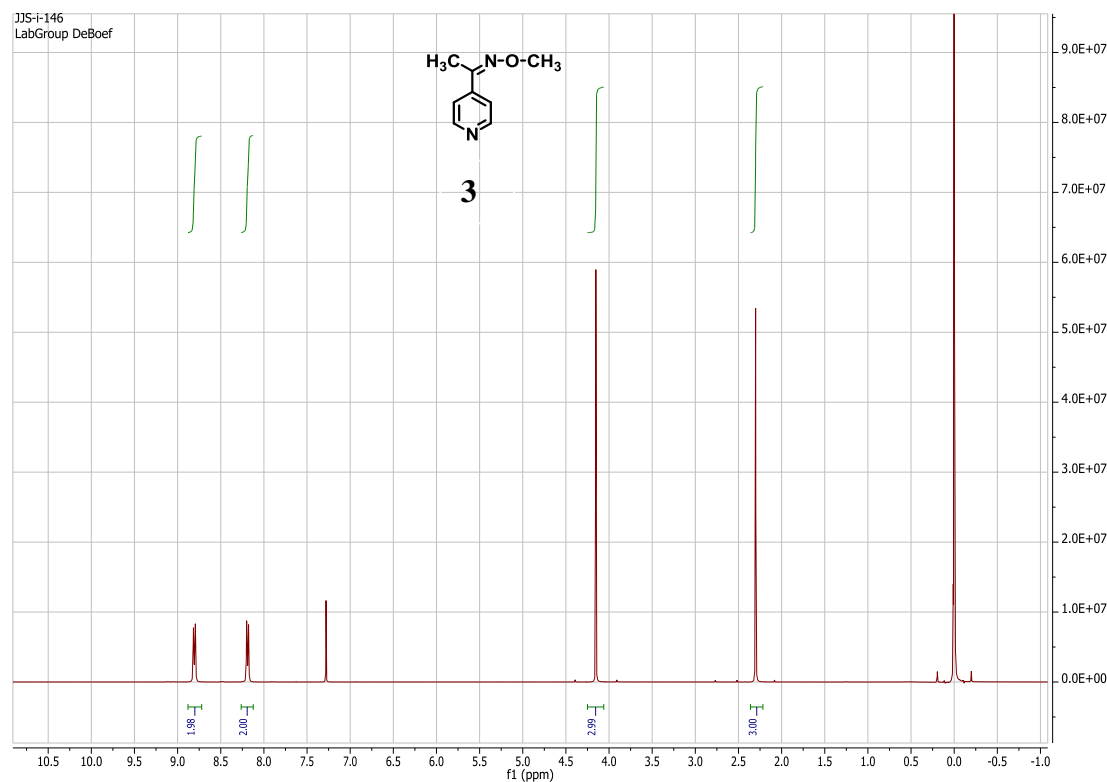


**Figure 4.4.**  $^1\text{H}$  NMR of Compound 3

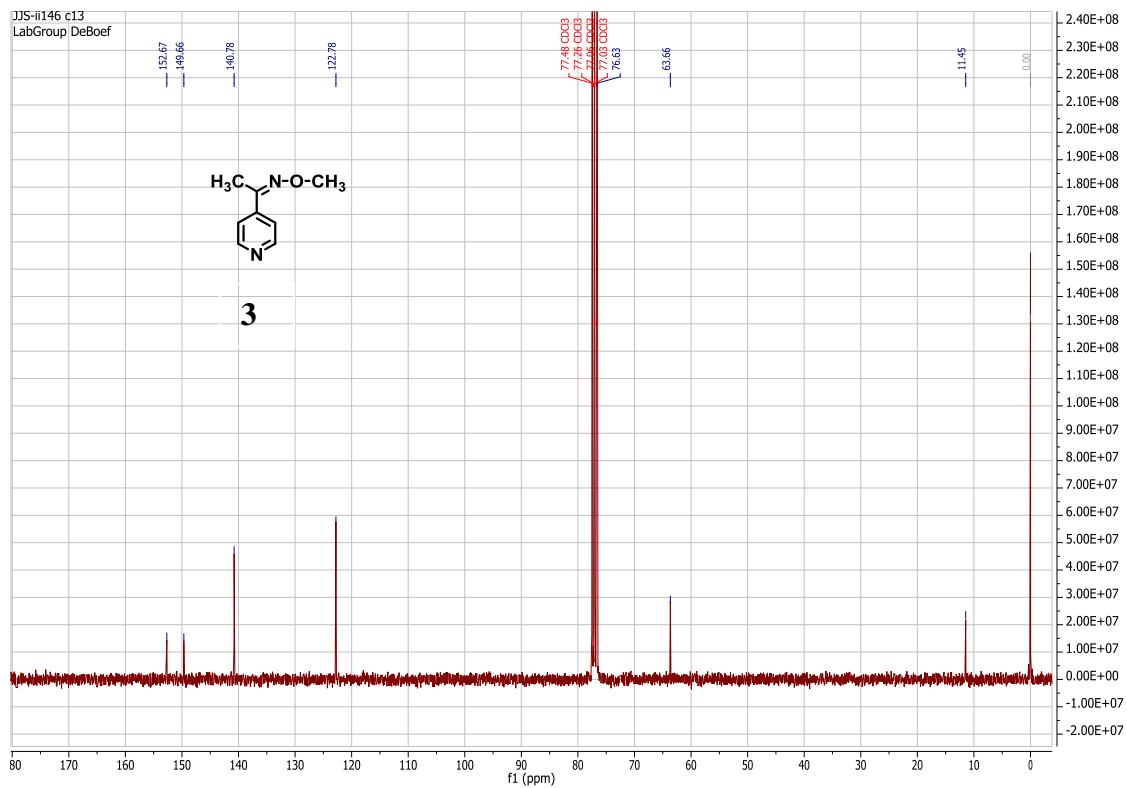


**Figure 4.5.**  $^{13}\text{C}$ NMR of Compound 3

## Characterization (**4**)<sup>2</sup>

**<sup>1</sup>H NMR (300 MHz, CDCl<sub>3</sub>):**  $\delta$  8.72 (d,  $J=6.26$  Hz, 2H), 7.80 (d,  $J=6.26$  Hz, 2H), 6.93 (d,  $J=8.90$  Hz, 2H), 6.77 (d,  $J=8.71$  Hz, 2H), 3.83 (s, 3H), 2.27 (s, 3H)

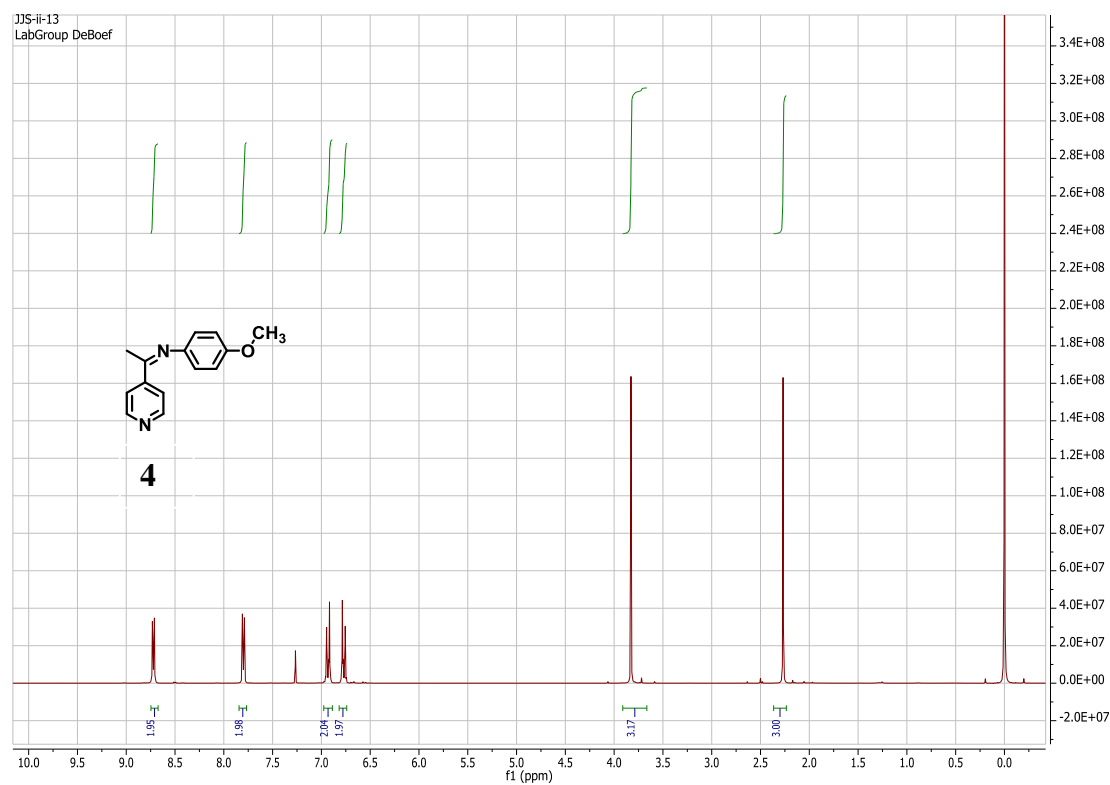


**Figure 4.6.** <sup>1</sup>H NMR of Compound 4

Characterization of (5)<sup>3</sup>

**<sup>1</sup>H NMR (300 MHz, CDCl<sub>3</sub>):**  $\delta$  8.76 (d,  $J=6.11$  Hz, 2H), 8.46 (s, 1H), 7.75 (d,  $J=6.19$  Hz, 2H), 7.43 (t,  $J=7.20$  Hz, 2H), 7.32-7.22 (m, 3H)

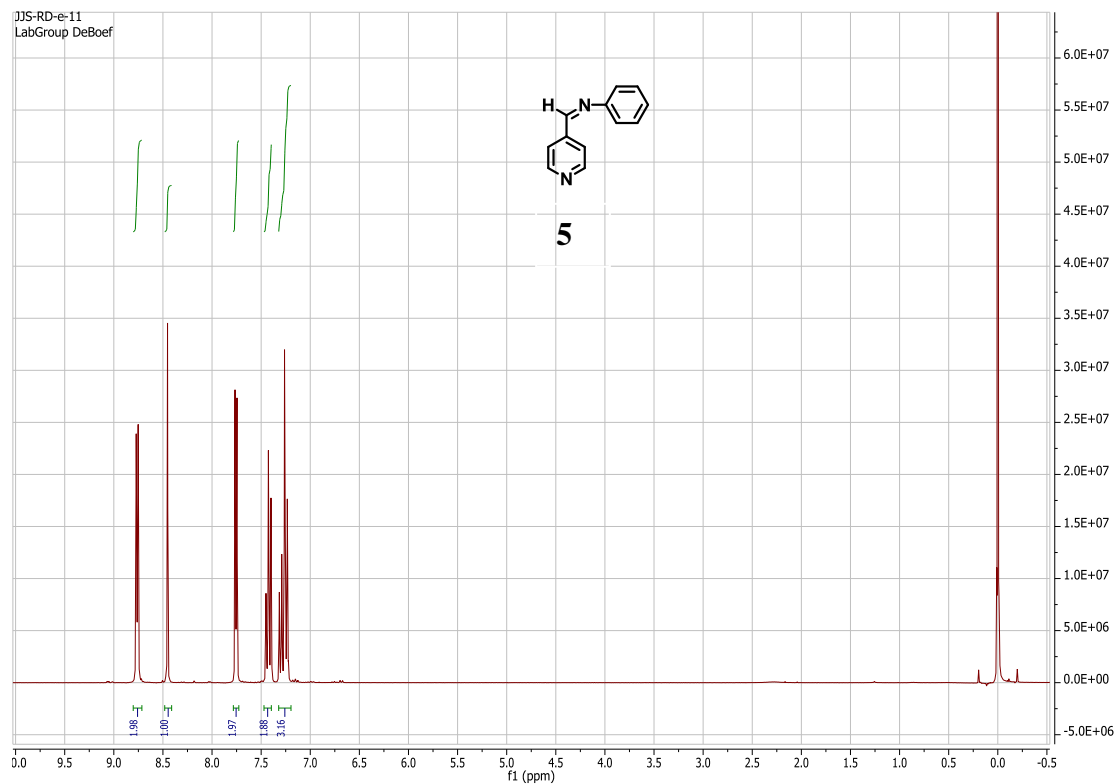


**Figure 4.7.** <sup>1</sup>H NMR of Compound 5

Characterization of (6)

**$^1\text{H}$  NMR (300 MHz,  $\text{CDCl}_3$ ):**  $\delta$  8.66 (d,  $J=6.08$  Hz, 2H), 7.72 (d,  $J=6.12$  Hz, 2H),

7.46-7.30 (m, 5H), 4.76 (s, 2H), 2.34 (s, 3H)

**$^{13}\text{C}$  NMR (75 MHz,  $\text{CDCl}_3$ ):**  $\delta$  164.08, 150.14, 147.61, 139.84, 128.51, 127.69,

126.83, 120.91, 56.02, 15.53

**LRMS EI ( $m/z$ ):**  $[M]^+$  calc'd for 210.12, observed 210.10 ( $m/z$ )

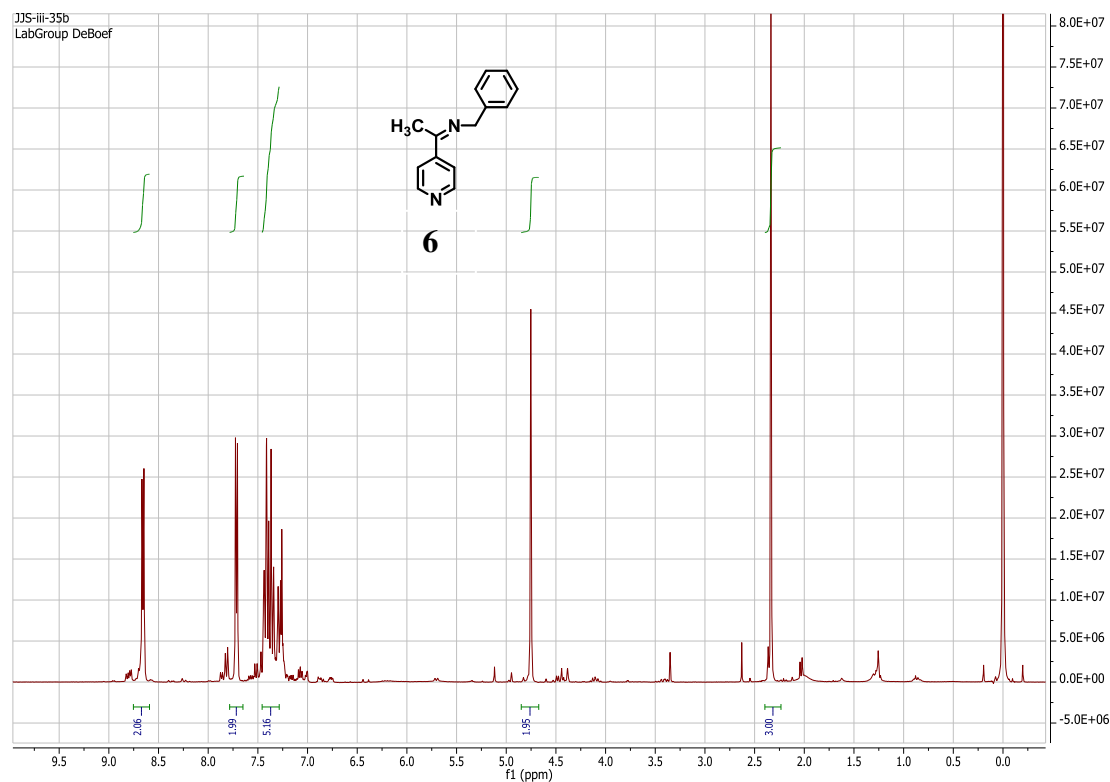


**Figure 4.8.**  $^1\text{H}$  NMR of Compound 6

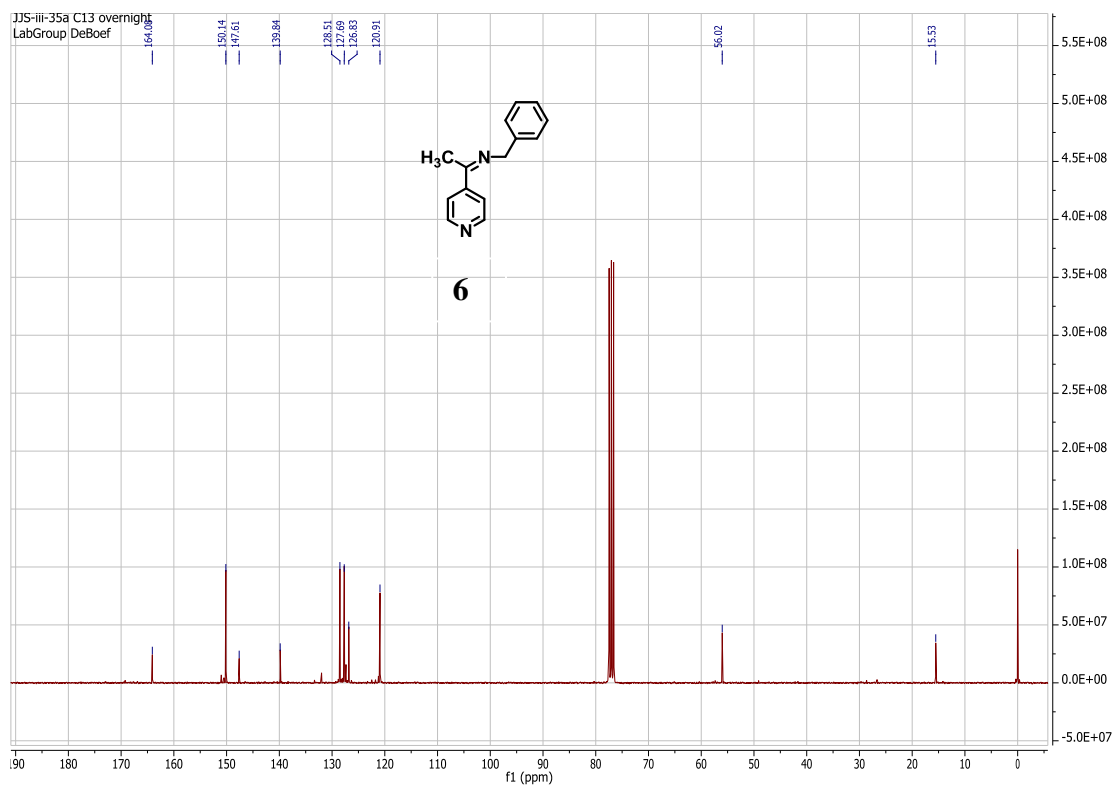


**Figure 4.9.**  $^{13}\text{C}$  NMR of Compound 6

Characterization of (7)

**$^1\text{H}$  NMR (300 MHz,  $\text{CDCl}_3$ ):**  $\delta$  8.71 (s, 2H), 7.41 (m, 6H), 2.05 (s, 3H)

**$^{13}\text{C}$  NMR (75 MHz,  $\text{CDCl}_3$ ):**  $\delta$  203.23, 150.96, 149.20, 145.80, 136.69, 134.10, 129.05, 128.95, 128.69, 120.59, 30.13

**LRMS EI ( $m/z$ ):**  $[M^+]$  calc'd for 197.08, observed 197.00 ( $m/z$ )

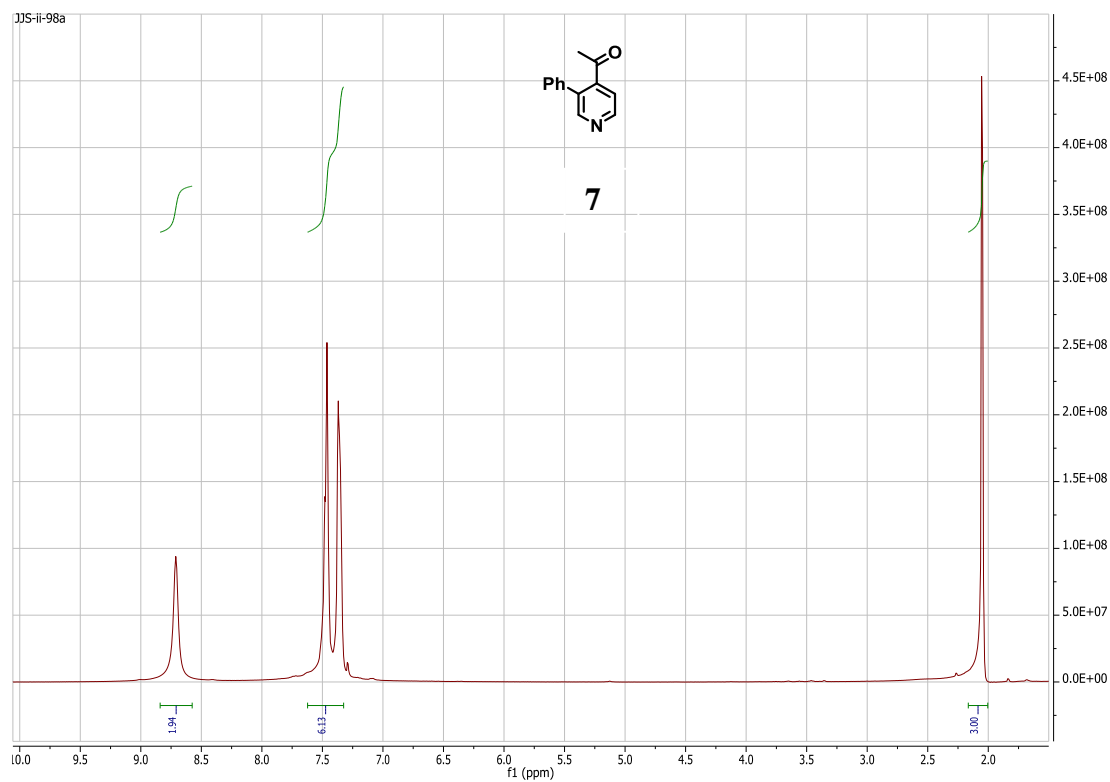


**Figure 4.10.**  $^1\text{H}$  NMR of Compound 7



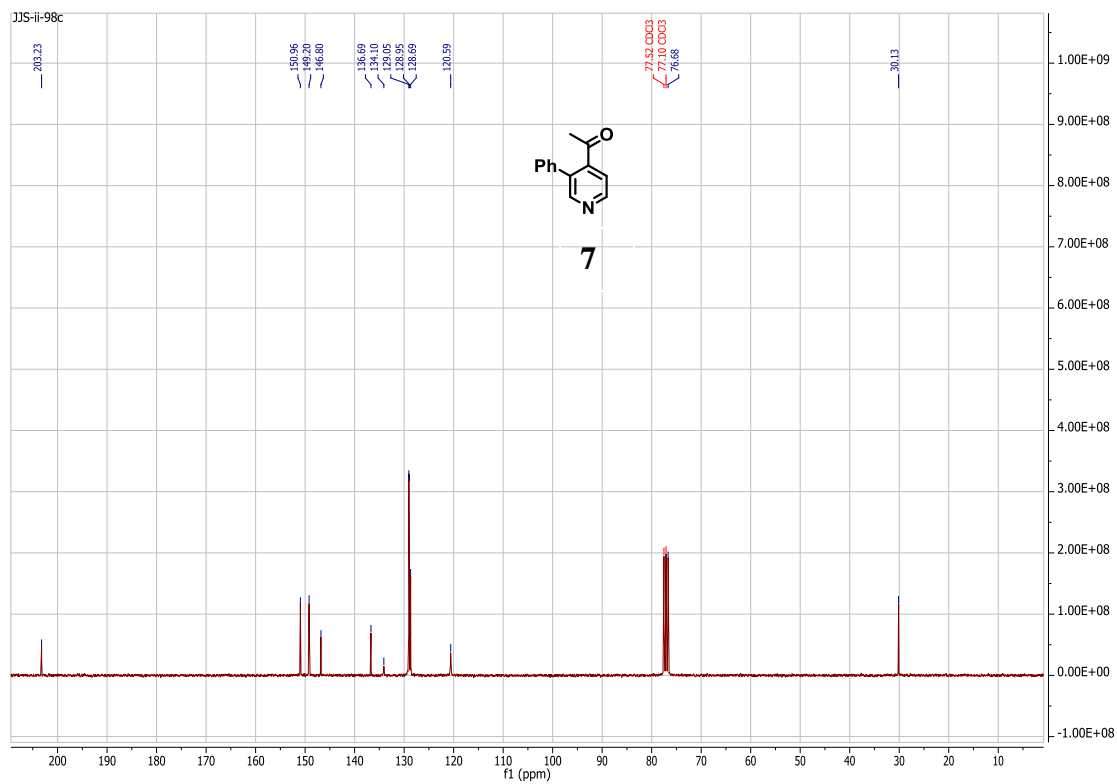


**Figure 4.11.**  $^{13}\text{C}$  NMR of Compound 7

Characterization of (8)

**$^1\text{H}$  NMR (300 MHz,  $\text{CDCl}_3$ ):**  $\delta$  8.44 (s, 1H), 7.54 (s, 1H), 7.48 (m, 5H), 7.35 (t,  $J=7.94$  Hz, 2H), 7.10 (t,  $J=7.98$  Hz, 1H), 6.74 (d,  $J=7.95$  Hz, 2H), 1.66 (s, 3H)

**$^{13}\text{C}$  NMR (75 MHz,  $\text{CDCl}_3$ ):**  $\delta$  167.89, 151.12, 150.78, 150.39, 149.85, 136.22, 133.83, 129.14, 129.00, 128.93, 128.60, 124.20, 122.60, 118.95, 20.48

**LRMS EI (m/z):**  $[\text{M}^+]$  calc'd for 306.09, observed 306.10 (m/z)

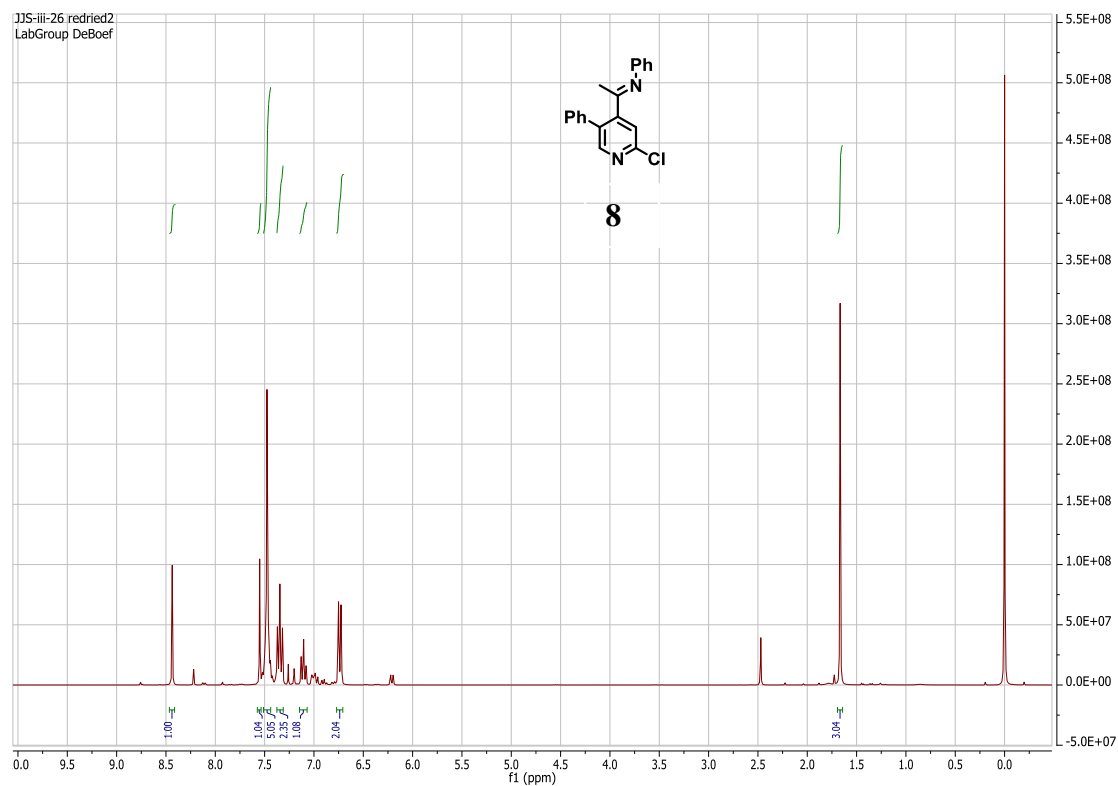


**Figure 4.12.**  $^1\text{H}$  NMR of Compound 8

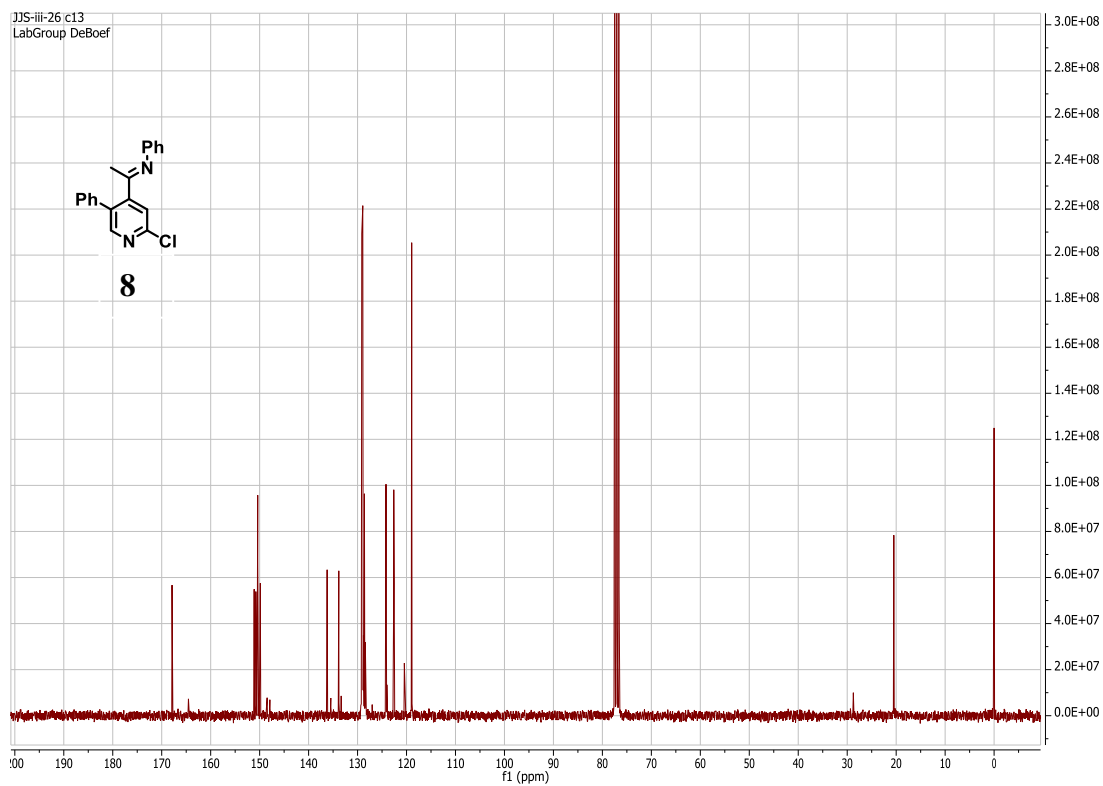


**Figure 4.13.**  $^{13}\text{C}$  NMR of Compound 8

Characterization of (9)<sup>4</sup>

**<sup>1</sup>H NMR (300 MHz, CDCl<sub>3</sub>):** δ 9.27 (s, 1H), 9.07 (s, 1H), 8.10 (dd, *J*=7.66 Hz, 4.23, 2H), 7.60-7.50 (m, 3H), 2.75 (s, 3H)

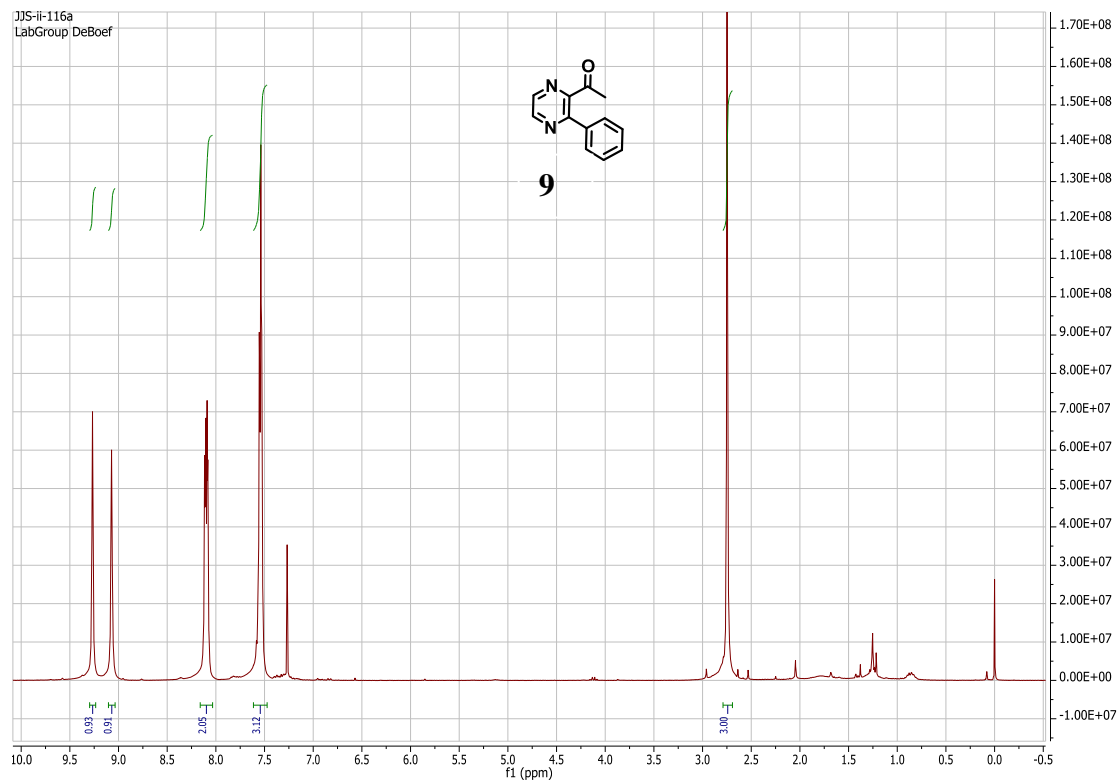


**Figure 4.14.** <sup>1</sup>H NMR of Compound 9

Characterization of (11)<sup>5</sup>

<sup>1</sup>H NMR (300 MHz, CDCl<sub>3</sub>): δ 7.63-7.44 (m, 8H), 7.31 (t, *J*=7.0 Hz, 1H), 2.48 (s, 3H)

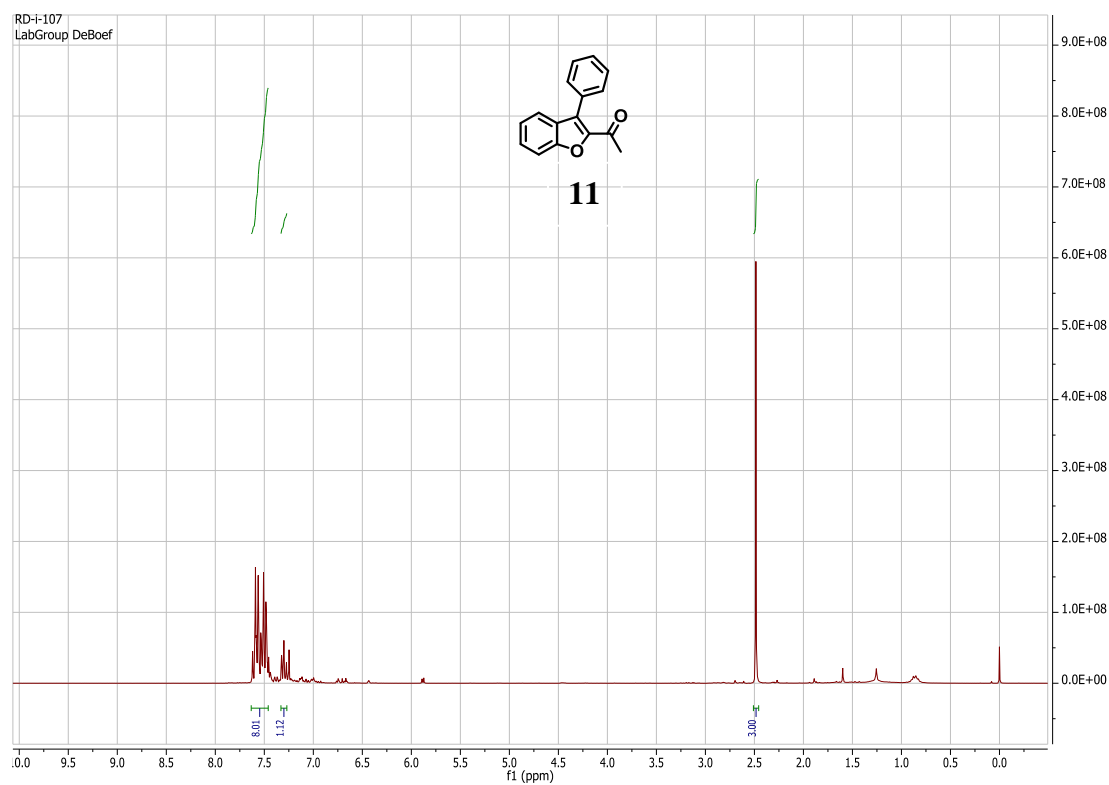


**Figure 4.15.** <sup>1</sup>H NMR of Compound 11

Characterization of (12)<sup>6</sup>

<sup>1</sup>H NMR (300 MHz, CDCl<sub>3</sub>): δ 7.59 (dd, *J* = 8.05, 1.80 Hz, 2H), 7.43-7.31 (m, 3H), 2.41 (s, 3H), 2.38 (s, 3H)

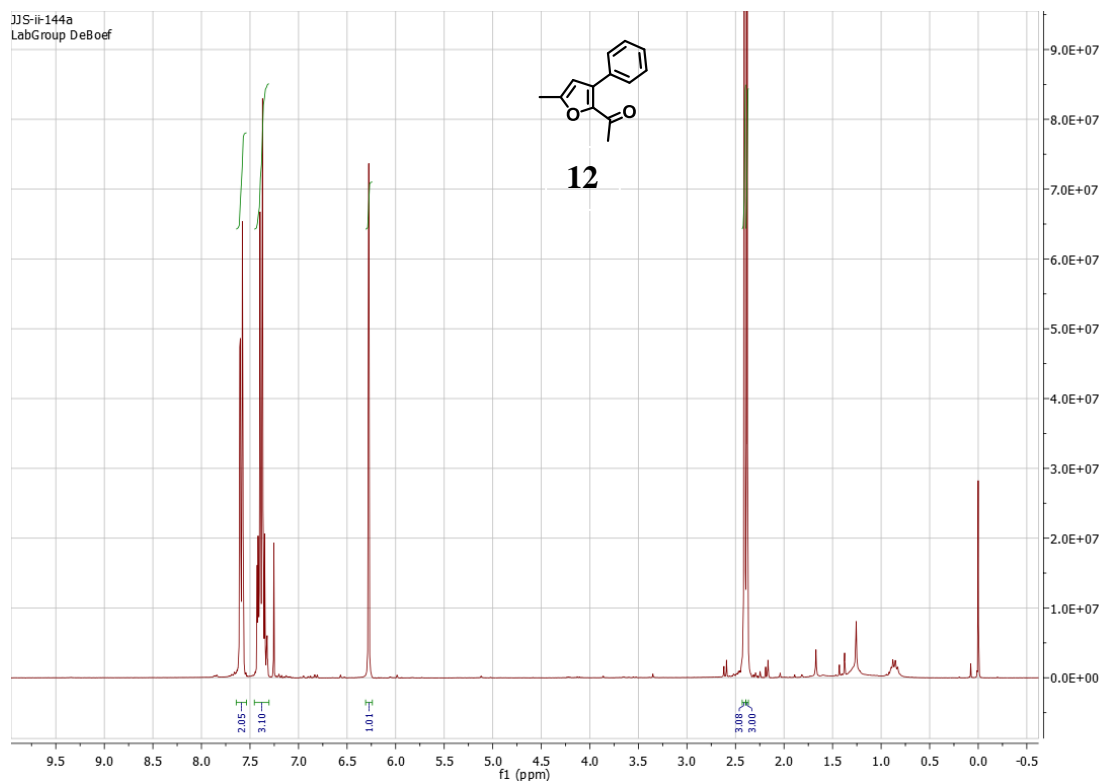


**Figure 4.16.** <sup>1</sup>H NMR of Compound 12

Characterization of (13)<sup>7</sup>

<sup>1</sup>H NMR (300 MHz, CDCl<sub>3</sub>): δ 7.62 (dd, *J*=8.17, 1.87 Hz, 2H), 7.54 (d, *J*=1.57 Hz, 1H), 7.45-7.36 (m, 3H), 6.65 (d, *J*=1.61 Hz, 1H), 2.46 (s, 3H)

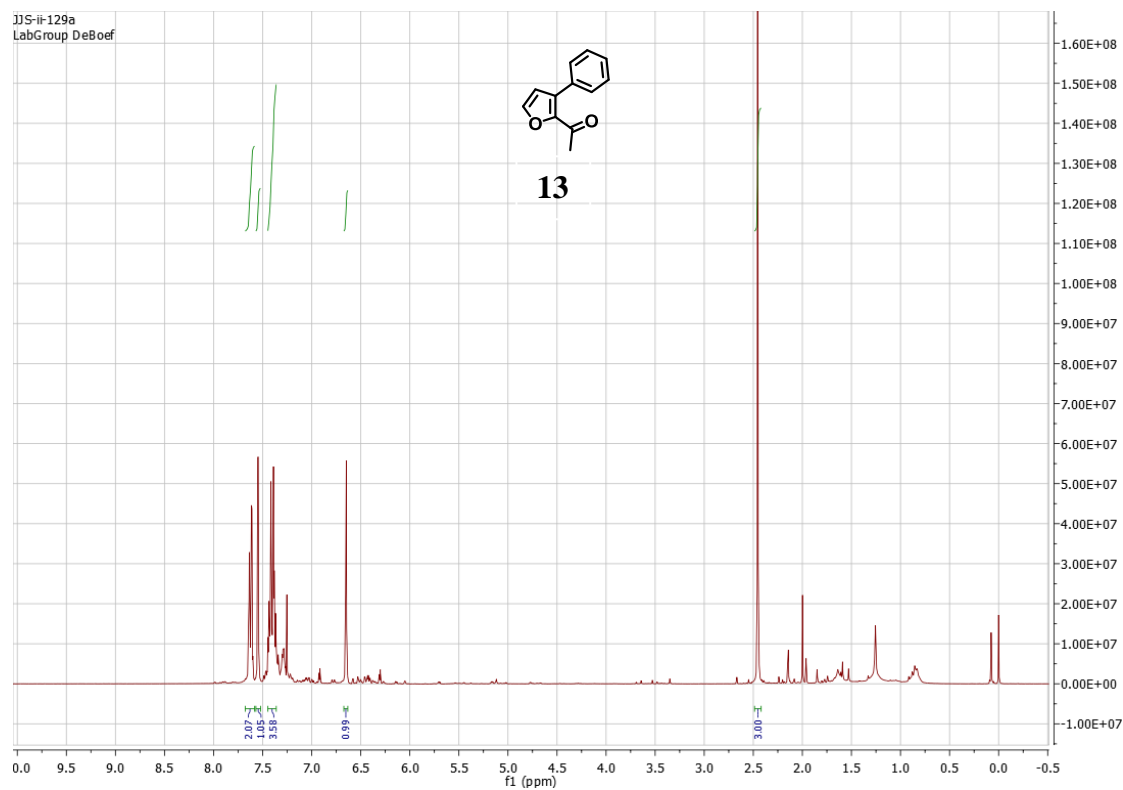


**Figure 4.17.** <sup>1</sup>H NMR of Compound 13

Characterization of (14)<sup>8</sup>

**<sup>1</sup>H NMR (300 MHz, CDCl<sub>3</sub>):**  $\delta$  7.53 (d,  $J=5.04$  Hz, 1H), 7.46-7.32 (m, 5H), 7.03 (d,  $J=5.08$  Hz, 1H), 2.13 (s, 3H)

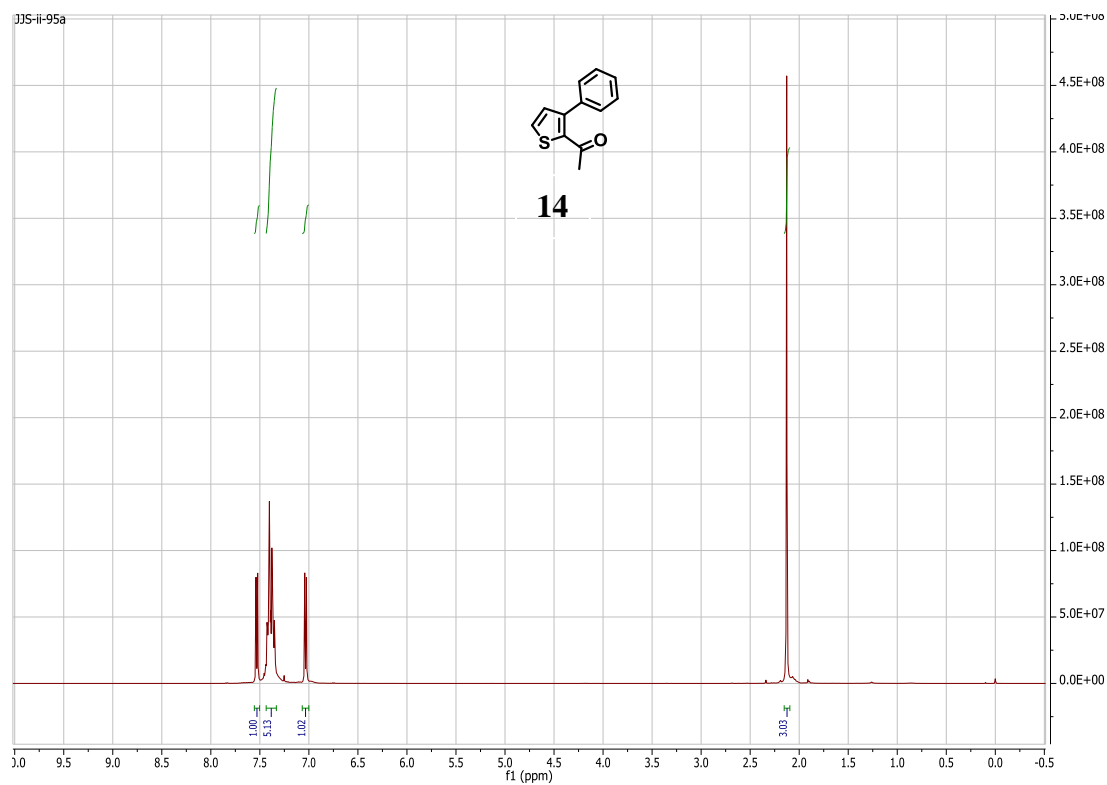


**Figure 4.18.** <sup>1</sup>H NMR of Compound 14



Characterization of (15)<sup>9</sup>

**<sup>1</sup>H NMR (300 MHz, CDCl<sub>3</sub>):**  $\delta$  7.87 (d,  $J=8.62$  Hz, 1H), 7.54-7.30 (m, 8H), 2.09 (s, 3H)

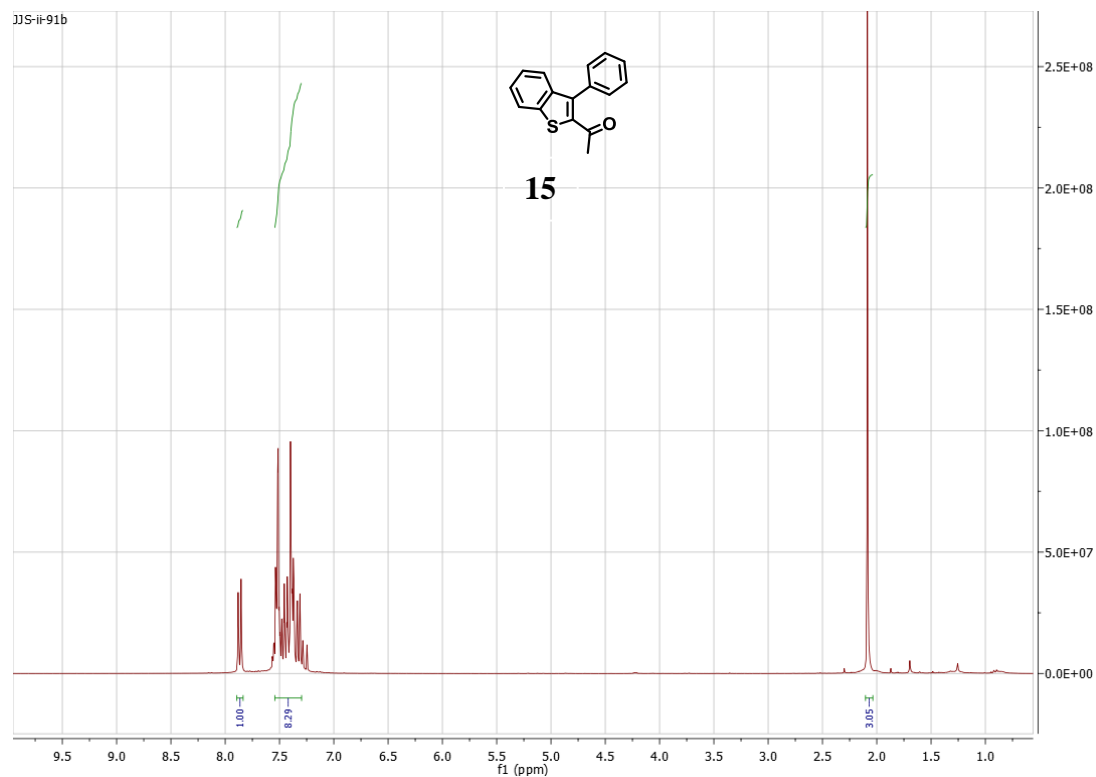


**Figure 4.19.** <sup>1</sup>H NMR of Compound 15

Characterization of (17)<sup>10</sup>

**<sup>1</sup>H NMR (300 MHz, CDCl<sub>3</sub>):**  $\delta$  7.47 (t,  $J=5.13$  Hz, 2H), 7.34 (t,  $J=8.14$  Hz, 2H), 7.09 (t,  $J=5.45$  Hz, 2H), 6.82 (d,  $J=8.14$  Hz, 2H), 2.24 (s, 3H)

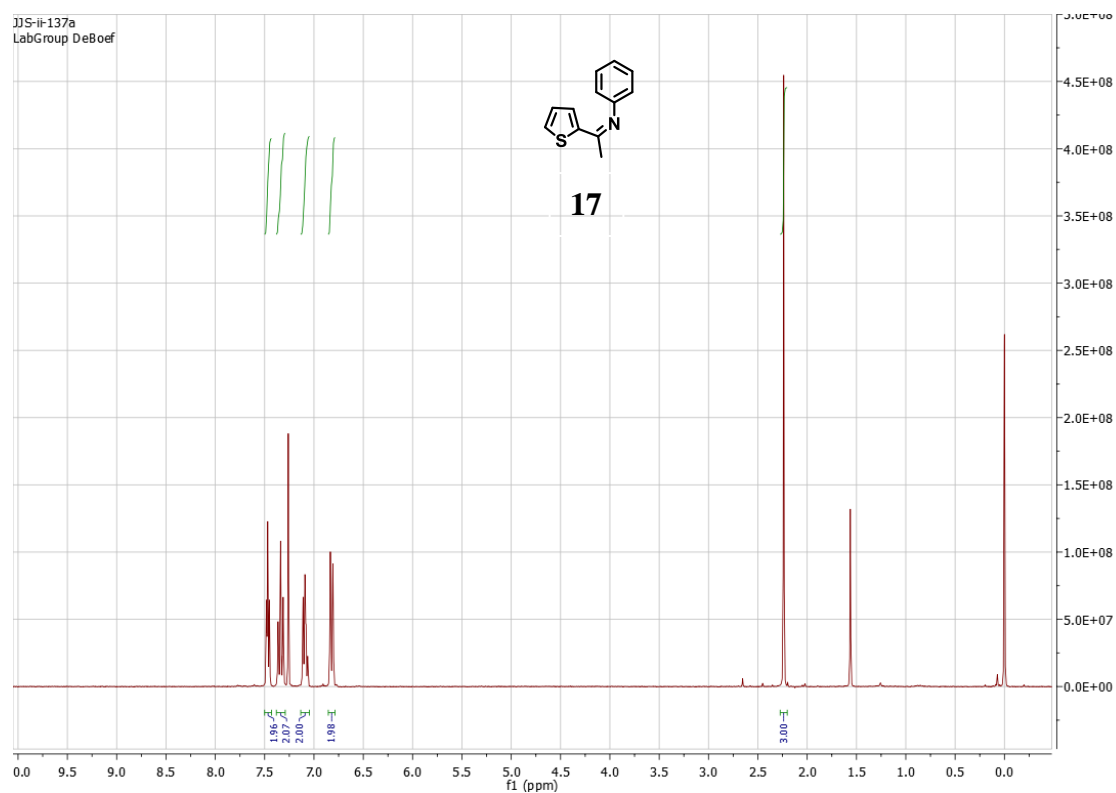


**Figure 4.20.** <sup>1</sup>H NMR of Compound 17

Characterization of (18)

**$^1\text{H}$  NMR (300 MHz,  $(\text{CD}_3)_2\text{CO}$ ):**  $\delta$  7.53 (d,  $J=5.0$  Hz, 1 H), 7.27(d,  $J=8.5$  Hz, 2 H),

7.23(d,  $J=8.4$  Hz, 2 H), 7.03 (d,  $J=5.0$  Hz, 1 H), 2.41 (s, 3 H), 2.15 (s, 3 H)

**$^{13}\text{C}$  NMR (75 MHz,  $(\text{CD}_3)_2\text{CO}$ ):**  $\delta$  191.81, 147.50, 140.59, 138.89, 134.55, 132.94,

132.09, 129.89, 128.79 29.36. 21.25

**IR:** 3017,2914, 2359, 2342, 1650, 1498, 1398  $\text{cm}^{-1}$

**LRMS EI ( $m/z$ ):**  $[\text{M}^+]$  calc'd for 216.06, observed: 216.10 ( $m/z$ )

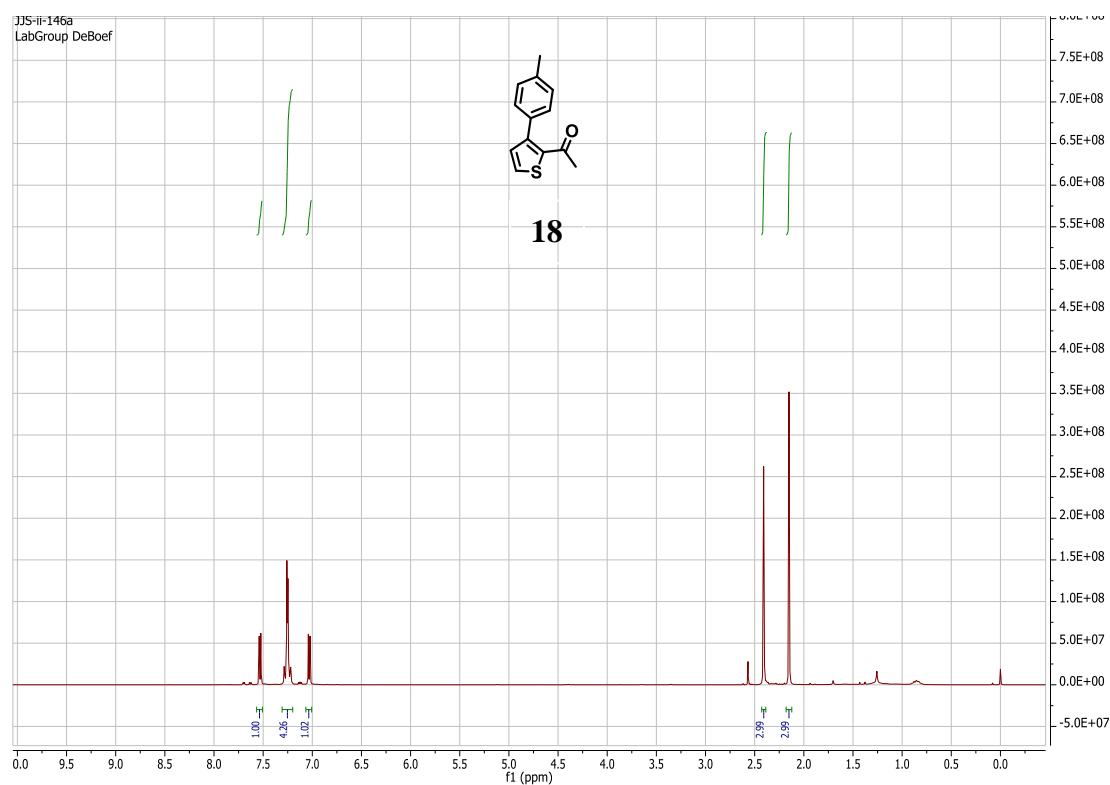


**Figure 4.21.**  $^1\text{H}$  NMR of Compound 18

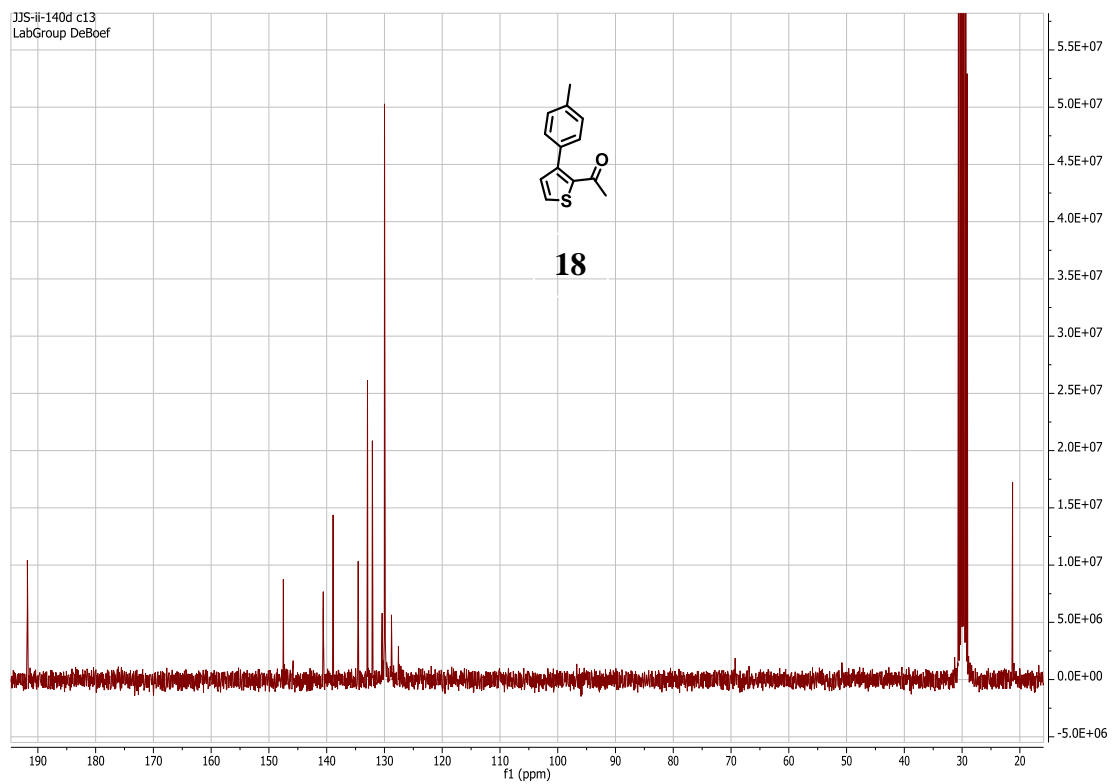


**Figure 4.22.**  $^{13}\text{C}$  NMR of Compound 18

Characterization of (19)

**<sup>1</sup>H NMR (300 MHz, CDCl<sub>3</sub>):** δ 7.56 (d, *J*=12.0 Hz, 1 H), 7.34-7.40 (m, 2 H), 7.09-7.17 (m, 2 H) 7.04 (d, *J*=12.0 Hz, 1 H), 2.18-2.21 (s, 3 H)

**<sup>13</sup>C NMR (75 MHz, CDCl<sub>3</sub>):** δ 191.70, 162.76 (d, *J*<sub>C-F</sub> = 246), 145.65, 139.53, 132.02, 130.94 (*J*<sub>C-F</sub> = 4.9), 130.80, 128.59, 115.40 (*J*<sub>C-F</sub> = 21.3), 29.37

**IR:** 3099, 3074, 3026, 2919, 2858, 1673, 1648, 1614, 1531, 1498 cm<sup>-1</sup>

**LRMS EI (*m/z*):** [M<sup>+</sup>] calc'd for C<sub>12</sub>H<sub>9</sub>FOS 220.04, observed 220.10 (*m/z*)

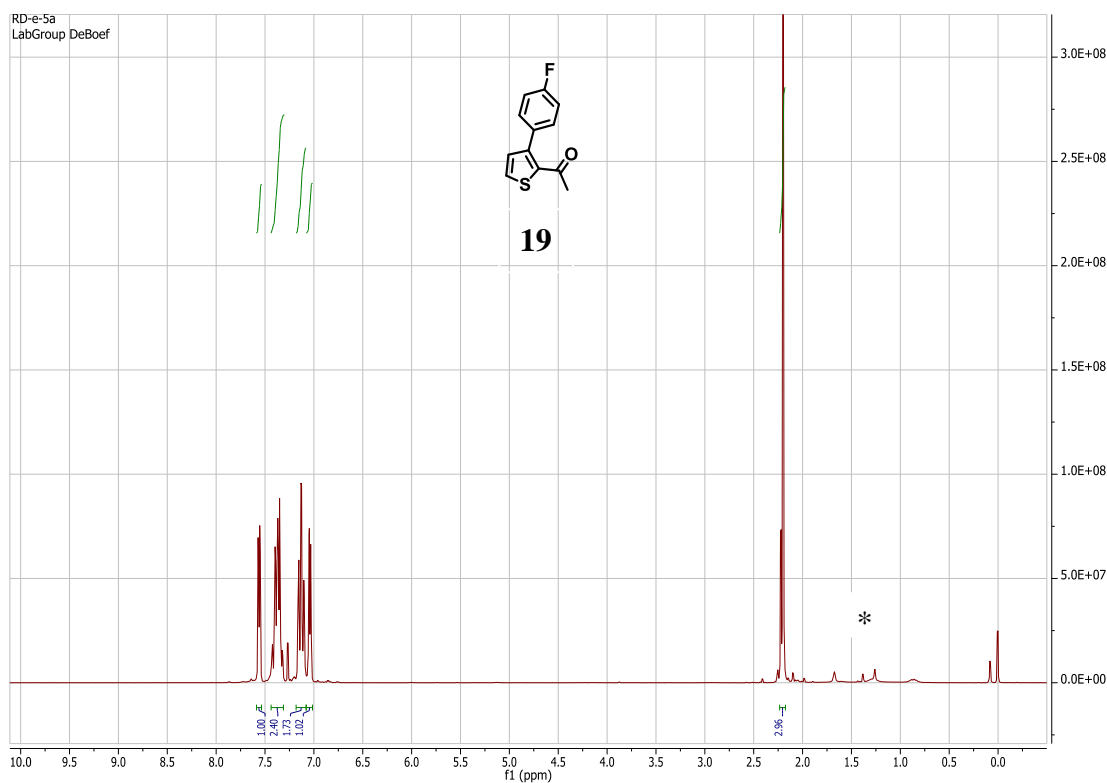


**Figure 4.23.** <sup>1</sup>H NMR of Compound 19

\* trace impurity, most likely from starting material.

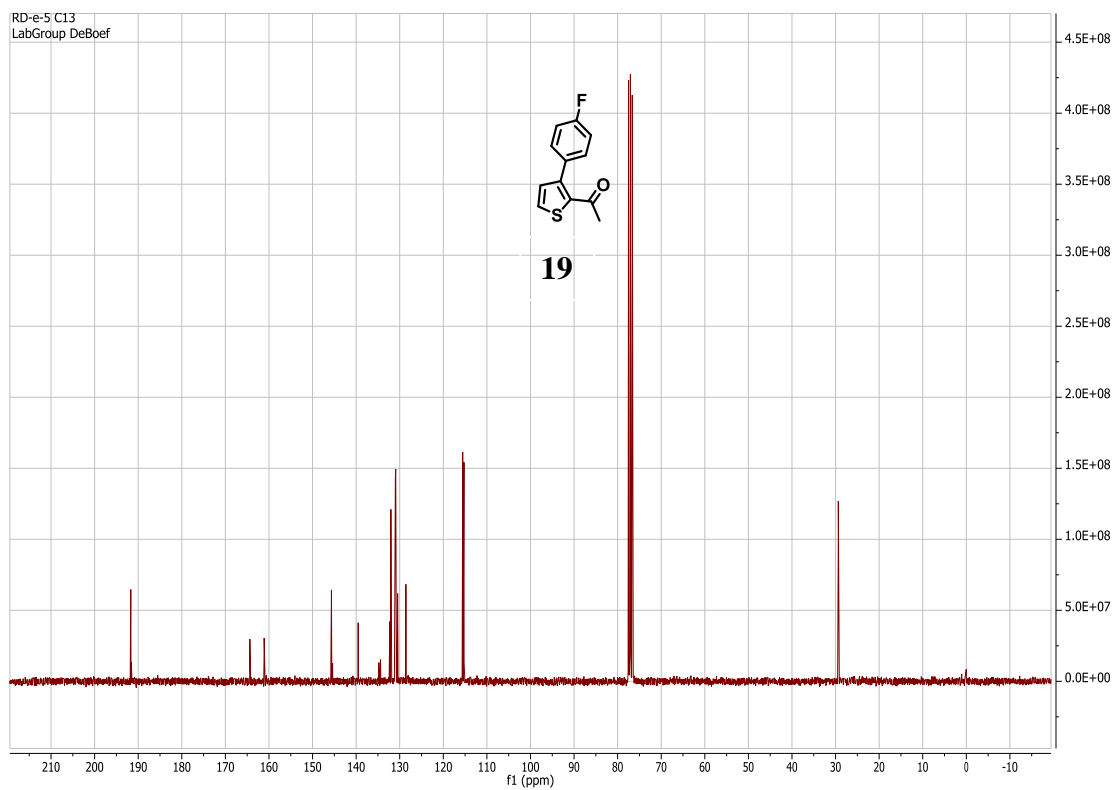


**Figure 4.24.**  $^{13}\text{C}$  NMR of Compound 19

Characterization of (20)

**$^1\text{H}$  NMR (300 MHz,  $\text{CDCl}_3$ ):**  $\delta$  7.56 (d,  $J=5.0$  Hz, 1 H), 7.35-7.20 (m, 4 H), 6.91-6.96 (d,  $J=5.0$  Hz, 1 H), 2.15 (s, 3 H)

**$^{13}\text{C}$  NMR (75 MHz,  $\text{CDCl}_3$ ):**  $\delta$  191.53, 145.39, 139.46, 134.79, 134.39, 131.90, 131.07, 130.49, 128.59, 29.45.

**IR:** 3100, 2998, 3033, 2957, 2922, 2360, 1671, 1649, 1595, 1566, 1479, 1373  $\text{cm}^{-1}$

**LRMS EI ( $m/z$ ):**  $[\text{M}^+]$  calc'd for  $\text{C}_{12}\text{H}_9\text{OSCl}$ : 236.01, observed 236.00 ( $m/z$ )

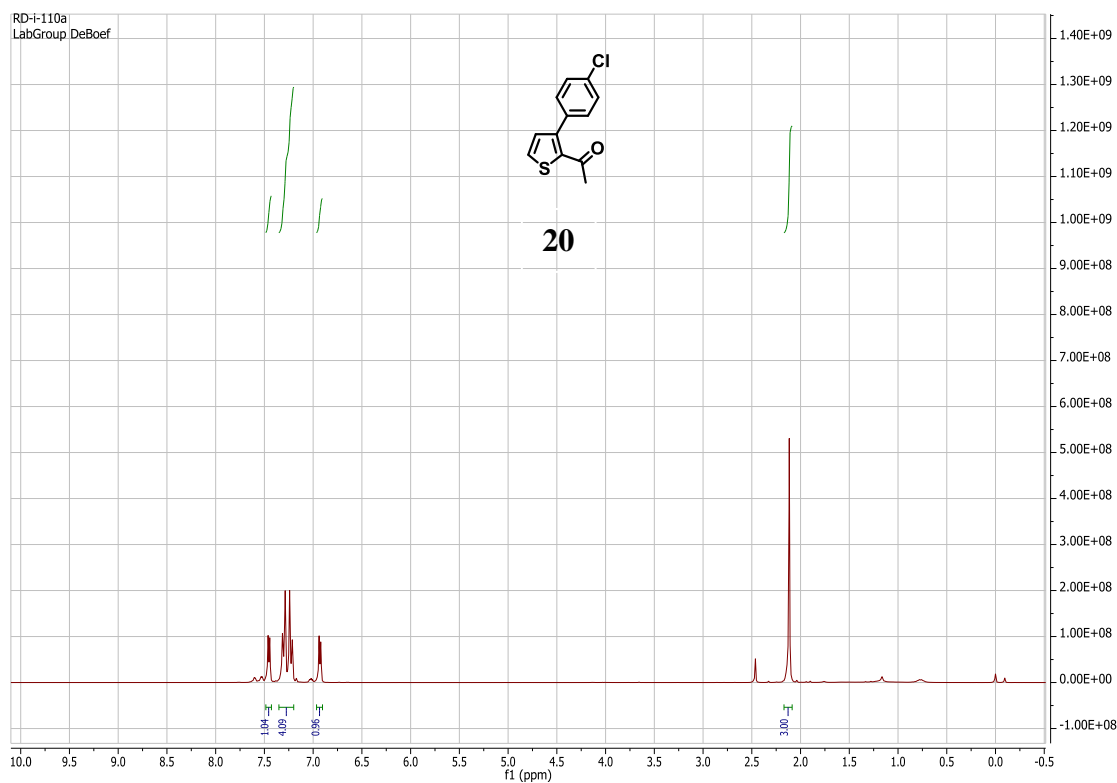


**Figure 4.25.**  $^1\text{H}$  NMR of Compound 20

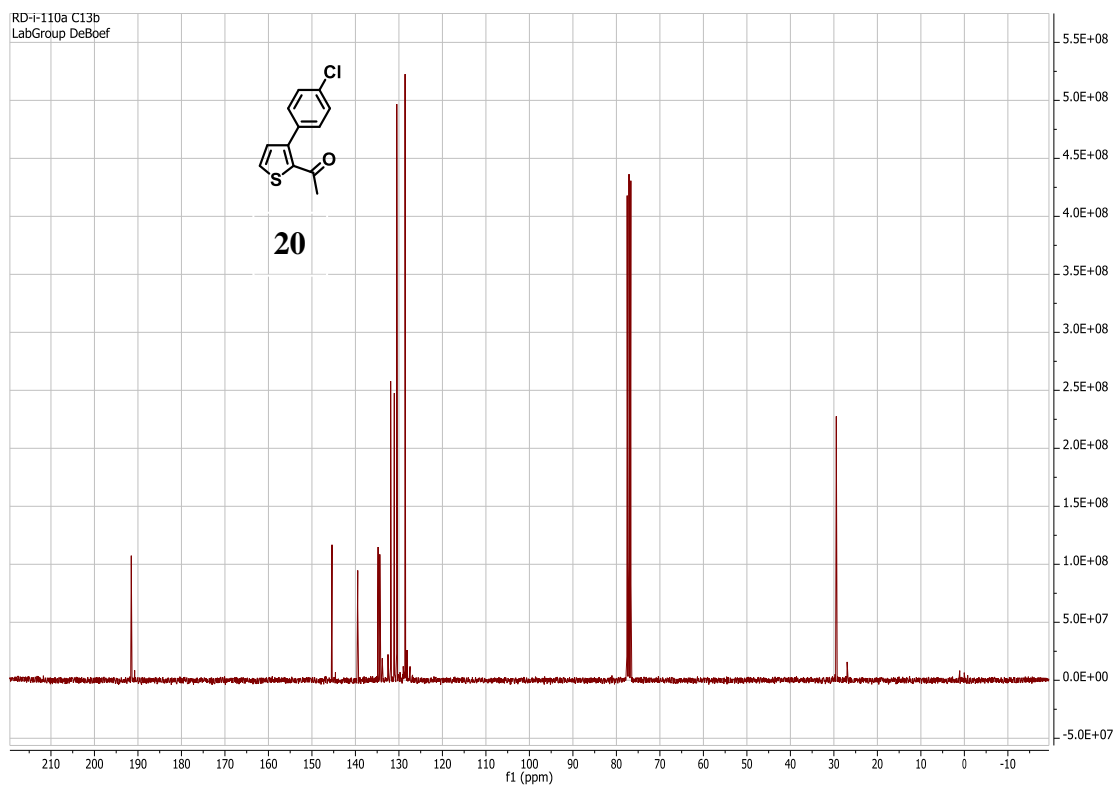


**Figure 4.26.**  $^{13}\text{C}$  NMR of Compound 20



Characterization of (21)<sup>11</sup>

**<sup>1</sup>H NMR (300 MHz, CDCl<sub>3</sub>):** δ 7.53 (d, *J*=5.10 Hz, 1H), 7.31 (d, *J*=8.82 Hz, 2H),  
7.03 (d, *J*=5.02 Hz, 1H), 6.99-6.93 (m, 2H), 3.86 (s, 3H), 2.17 (s, 3H)

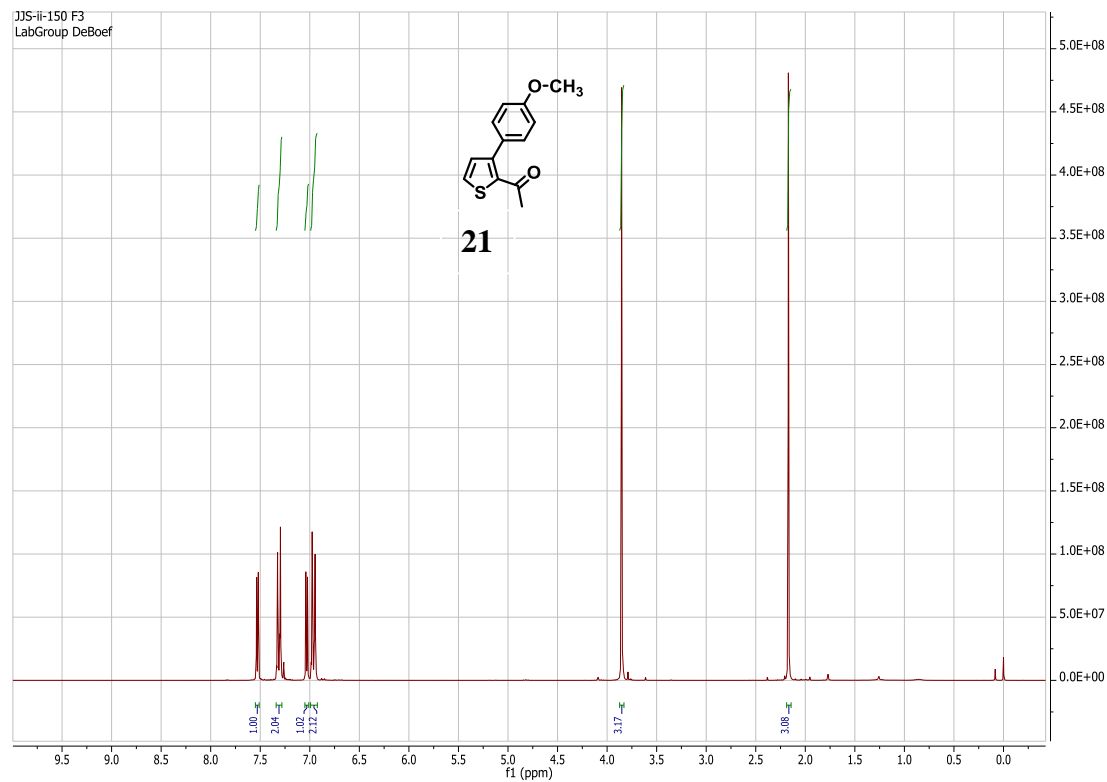


**Figure 4.27.** <sup>1</sup>H NMR of Compound 21

Characterization of (22)

**$^1\text{H}$  NMR (300 MHz,  $\text{CDCl}_3$ ):**  $\delta$  8.49 (d,  $J=5.43$  Hz, 1H), 7.86 (s, 1H), 7.74 (d,  $J=4.68$  Hz, 1H), 7.39 (t,  $J=7.69$  Hz, 2H), 7.14 (t,  $J=7.55$  Hz, 1H), 6.78 (d,  $J=7.90$  Hz, 2H), 2.23 (s, 3H)

**$^{13}\text{C}$  NMR (75 MHz,  $\text{CDCl}_3$ ):**  $\delta$  162.74, 152.39, 150.34, 150.13, 149.33, 129.15, 124.21, 122.09, 119.98, 118.97, 17.17

**LRMS EI ( $m/z$ ):**  $[M+]$  calc'd for 230.06, observed 230.00 ( $m/z$ )

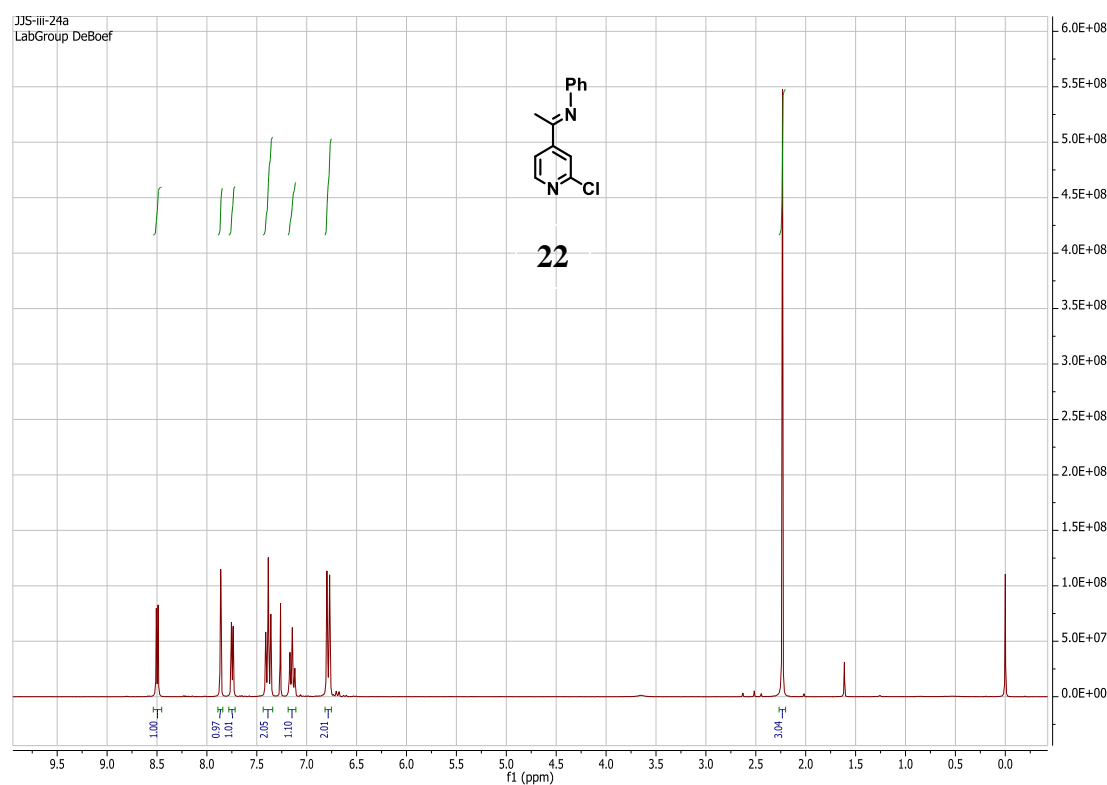


**Figure 4.28.**  $^1\text{H}$  NMR of Compound 22

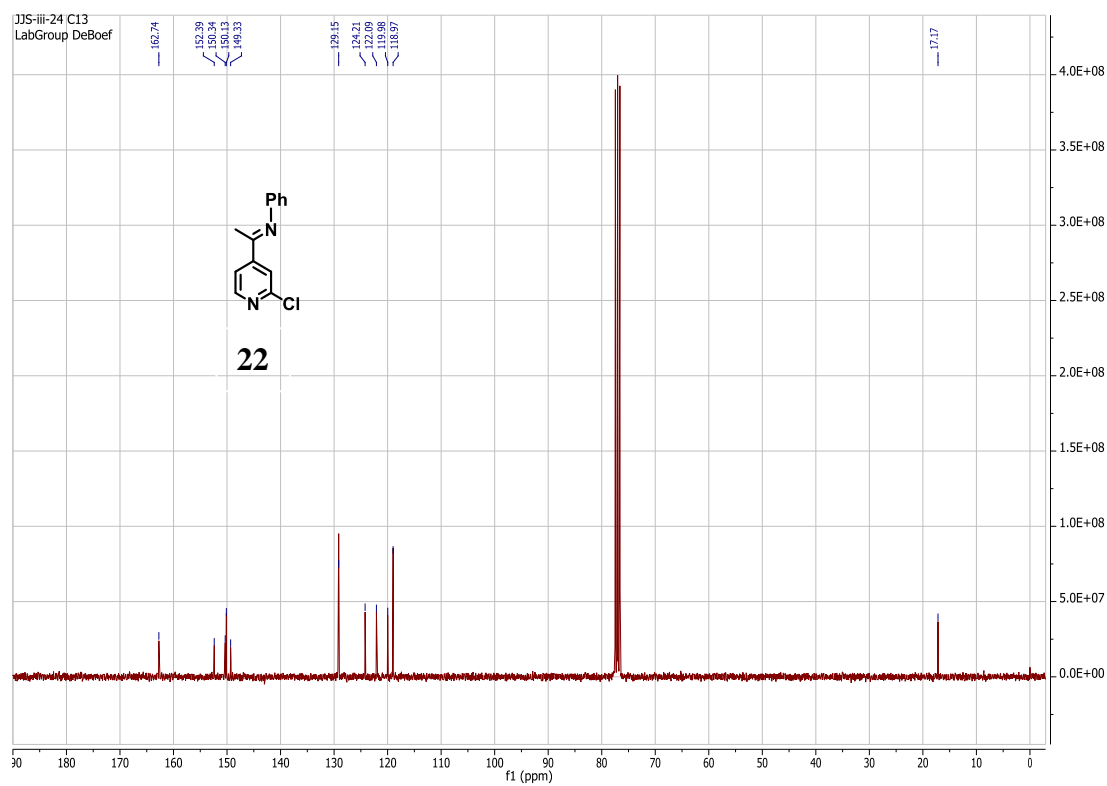


**Figure 4.29.**  $^{13}\text{C}$  NMR of Compound 22

Characterization of (23)<sup>12</sup>

**<sup>1</sup>H NMR (300 MHz, CDCl<sub>3</sub>):**  $\delta$  7.88-7.77 (m, 2H), 7.70 (s, 1H), 7.42-7.30 (m, 4H),

7.11 (t,  $J=7.29$  Hz, 1H), 6.85 (d,  $J=7.29$  Hz, 2H), 2.32 (s, 3H)

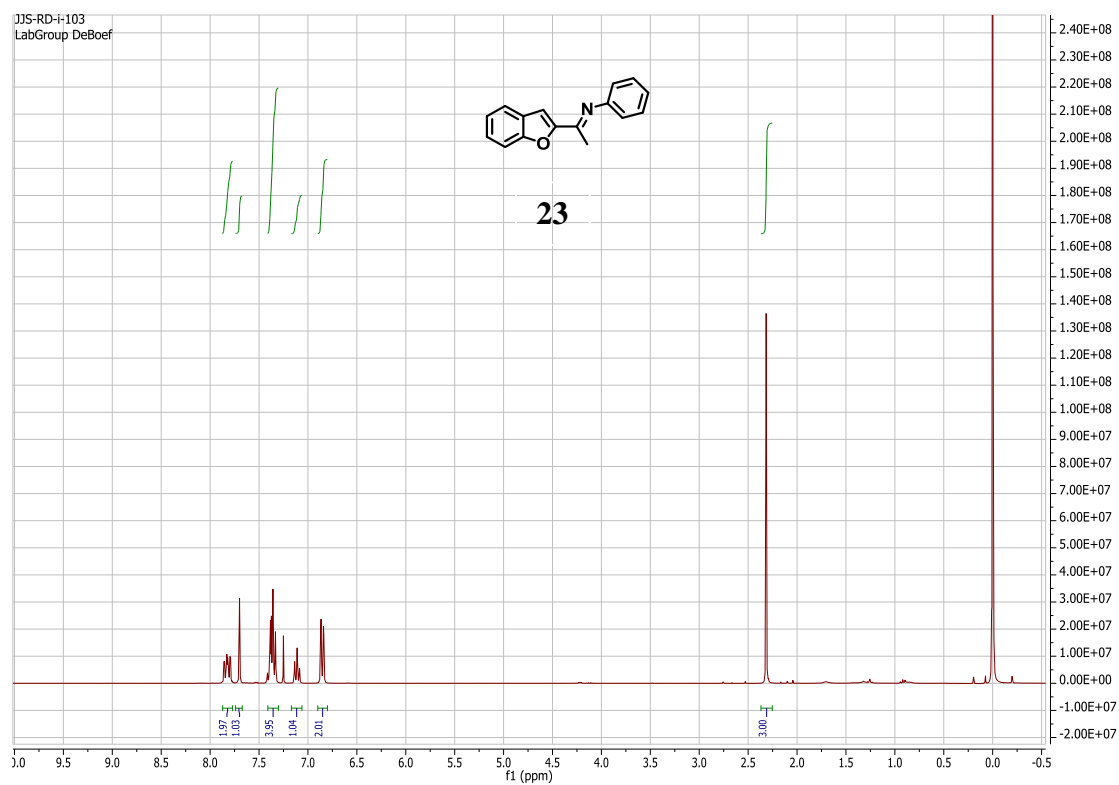


**Figure 4.30.** <sup>1</sup>H NMR of Compound 23

Characterization of (24)

**$^1\text{H}$  NMR (300 MHz,  $\text{CDCl}_3$ ):**  $\delta$  7.88-7.78 (m, 2H), 7.72 (s, 1H), 7.43-7.33 (m, 4H),

7.12 (t,  $J=7.40$  Hz, 1H), 6.86 (dd,  $J=8.22, 1.16$  Hz, 2H), 2.33 (s, 3H)

**$^{13}\text{C}$  NMR (75 MHz,  $\text{CDCl}_3$ ):**  $\delta$  160.98, 150.30, 146.58, 141.41, 139.74, 128.90,

126.06, 125.63, 124.63, 124.45, 123.82, 122.62, 119.92, 17.19

**LRMS EI ( $m/z$ ):**  $[M]^+$  calc'd for 251.08, observed 251.10 ( $m/z$ )

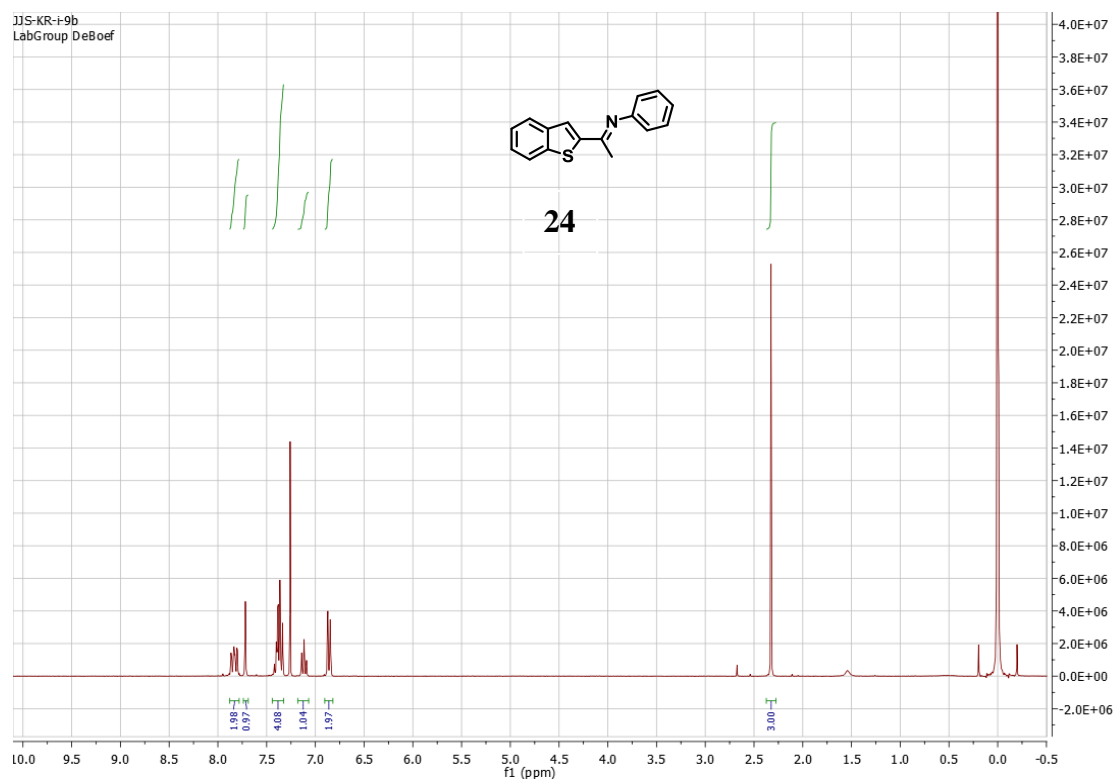


**Figure 4.31.**  $^1\text{H}$  NMR of Compound 24

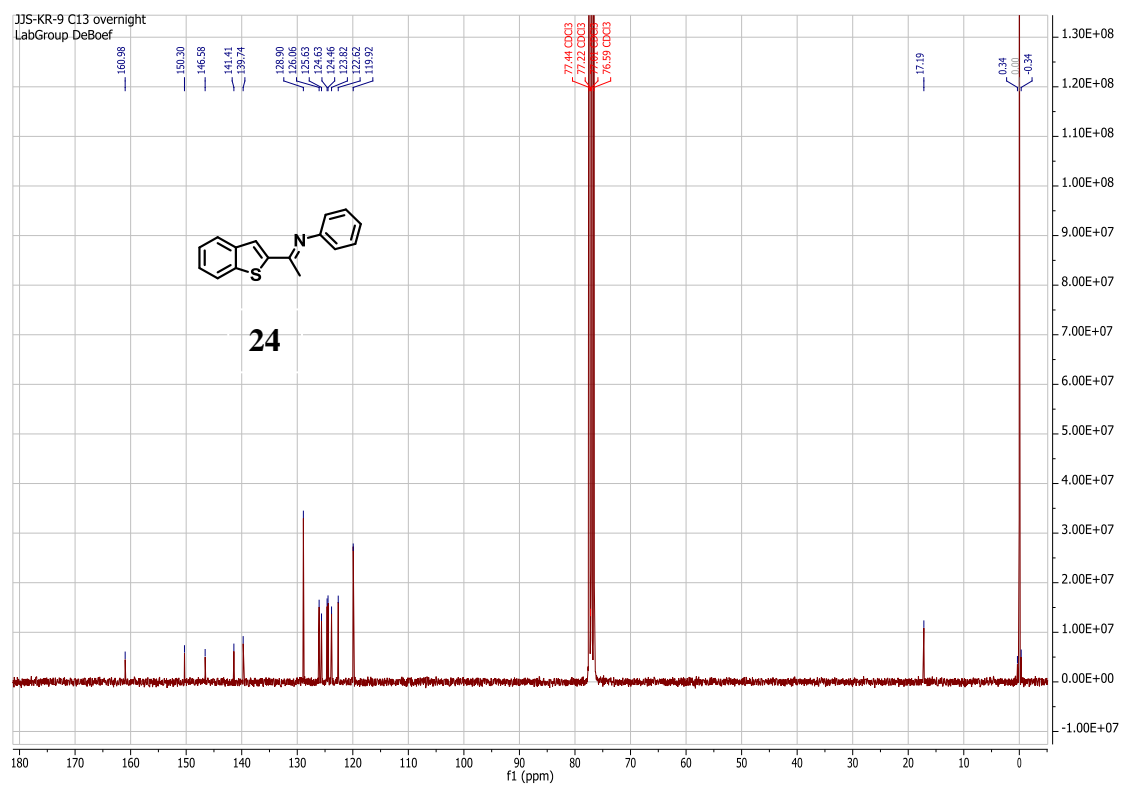


**Figure 4.32.**  $^{13}\text{C}$  NMR of Compound 24

Characterization of (25)

**<sup>1</sup>H NMR (300 MHz, CDCl<sub>3</sub>):** δ 9.49 (d, *J*=1.56 Hz, 1H), 8.64-8.59 (m, 2H), 7.39 (t, *J*=7.64 Hz, 2H), 7.17 (t, *J*=6.55 Hz, 1H), 6.84 (dd, *J*=8.54, 1.28 Hz, 2H), 2.34 (s, 3H)

**<sup>13</sup>C NMR (75 MHz, CDCl<sub>3</sub>):** δ 165.84, 151.44, 150.57, 145.14, 143.77, 142.89, 129.04, 124.04, 119.17, 16.05

**LRMS EI (m/z):** [M<sup>+</sup>] calc'd for 197.10, observed 197.10 (*m/z*)

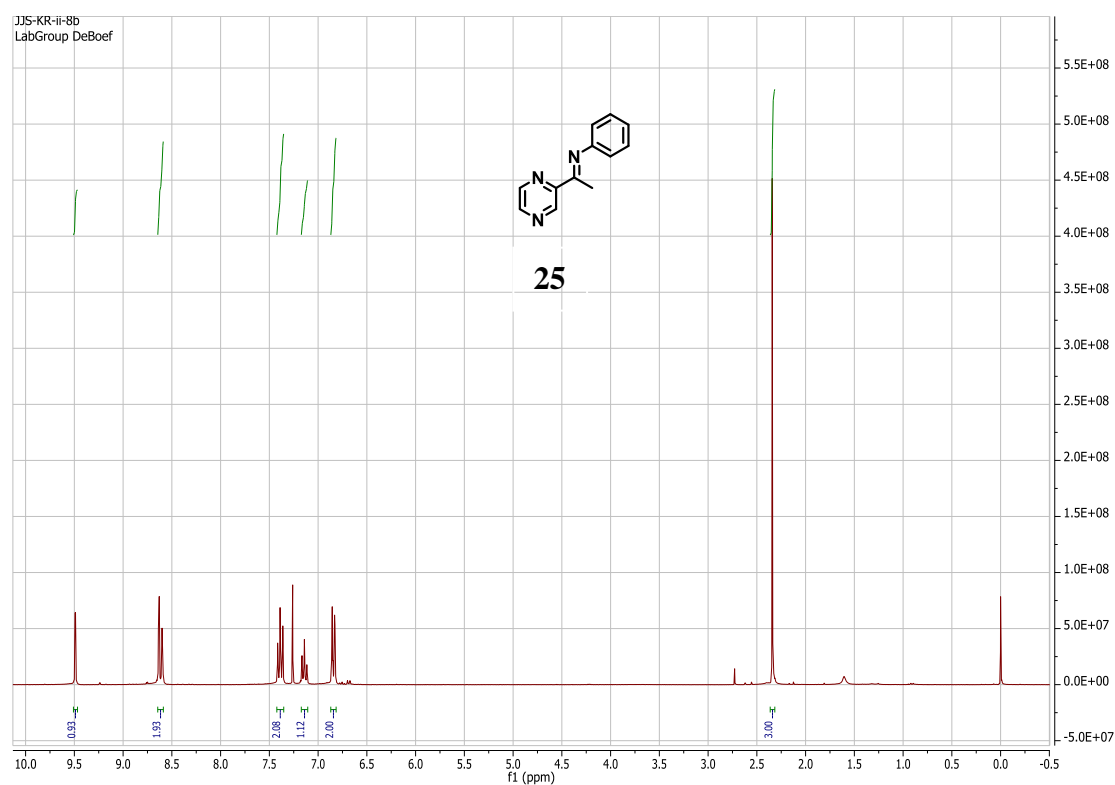


**Figure 4.33.** <sup>1</sup>H NMR of Compound 25

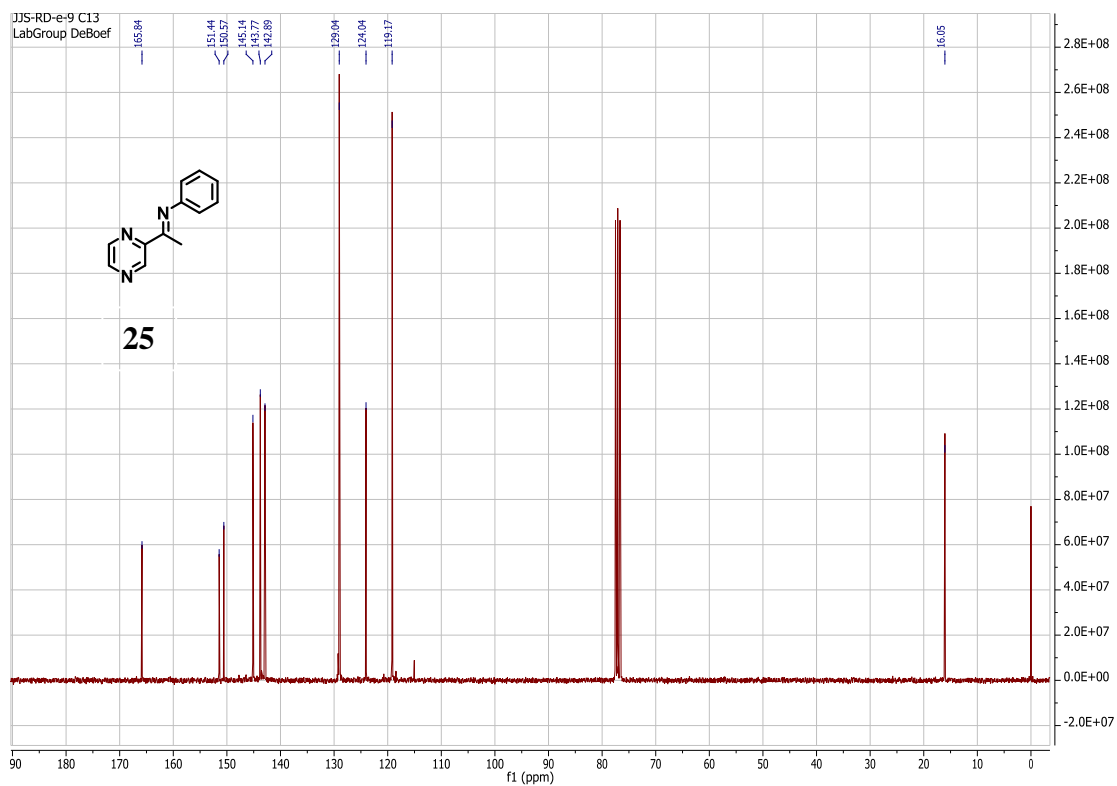


**Figure 4.34.**  $^{13}\text{C}$  NMR of Compound 25



Characterization of (26)

**$^1\text{H}$  NMR (300 MHz,  $\text{CDCl}_3$ ):**  $\delta$  7.31 (t,  $J=7.92$  Hz, 2H), 7.06 (t,  $J=7.47$ , 1H), 6.82

(dd,  $J=5.32, 1.63$  Hz, 3H), 6.11 (d,  $J=3.20$  Hz, 1H), 2.40 (s, 3H), 2.08 (s, 3H)

**$^{13}\text{C}$  NMR (75 MHz,  $\text{CDCl}_3$ ):**  $\delta$  156.10, 155.62, 152.01, 128.76, 123.30, 120.03,

115.04, 108.17, 16.35, 14.02

**LRMS EI ( $m/z$ ):**  $[M]^+$  calc'd for 199.10, observed 199.10 ( $m/z$ )

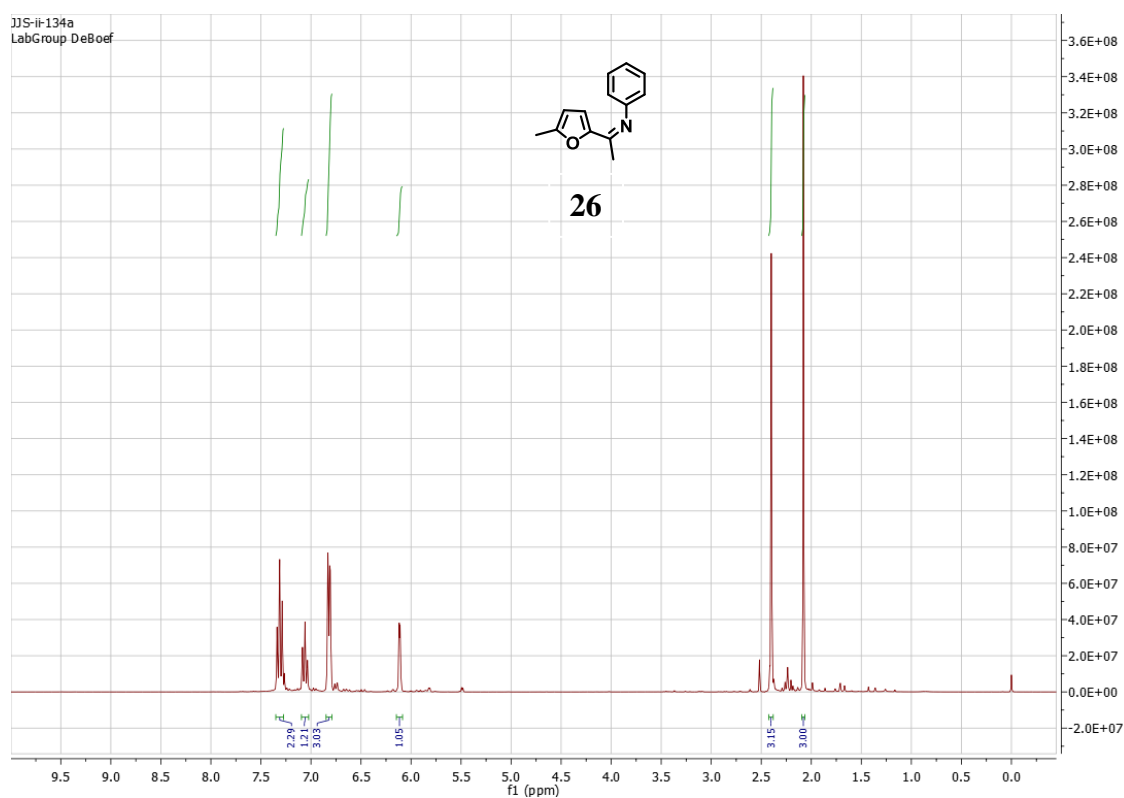


**Figure 4.35.**  $^1\text{H}$  NMR of Compound 26

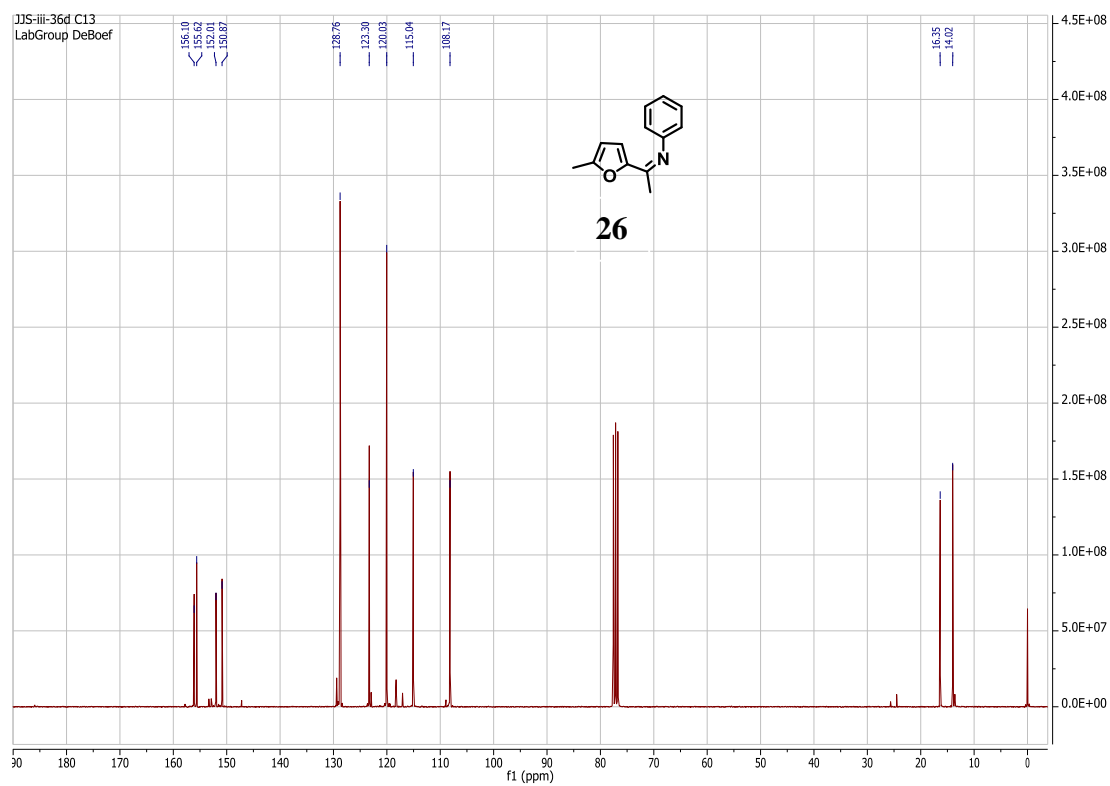


**Figure 4.36.**  $^{13}\text{C}$  NMR of Compound 26

Characterization of (27)<sup>13</sup>

**<sup>1</sup>H NMR (300 MHz, CDCl<sub>3</sub>):**  $\delta$  7.57 (d,  $J$ =1.29 Hz, 1H), 7.34 (t,  $J$ =7.38 Hz, 2H), 7.09 (t,  $J$ =7.28 Hz, 1H), 6.95 (d,  $J$ =3.85 Hz, 1H), 6.83 (d,  $J$ =7.38 Hz, 2H), 6.53 (dd,  $J$ =3.40, 1.77 Hz, 1H), 2.15 (s, 3H)

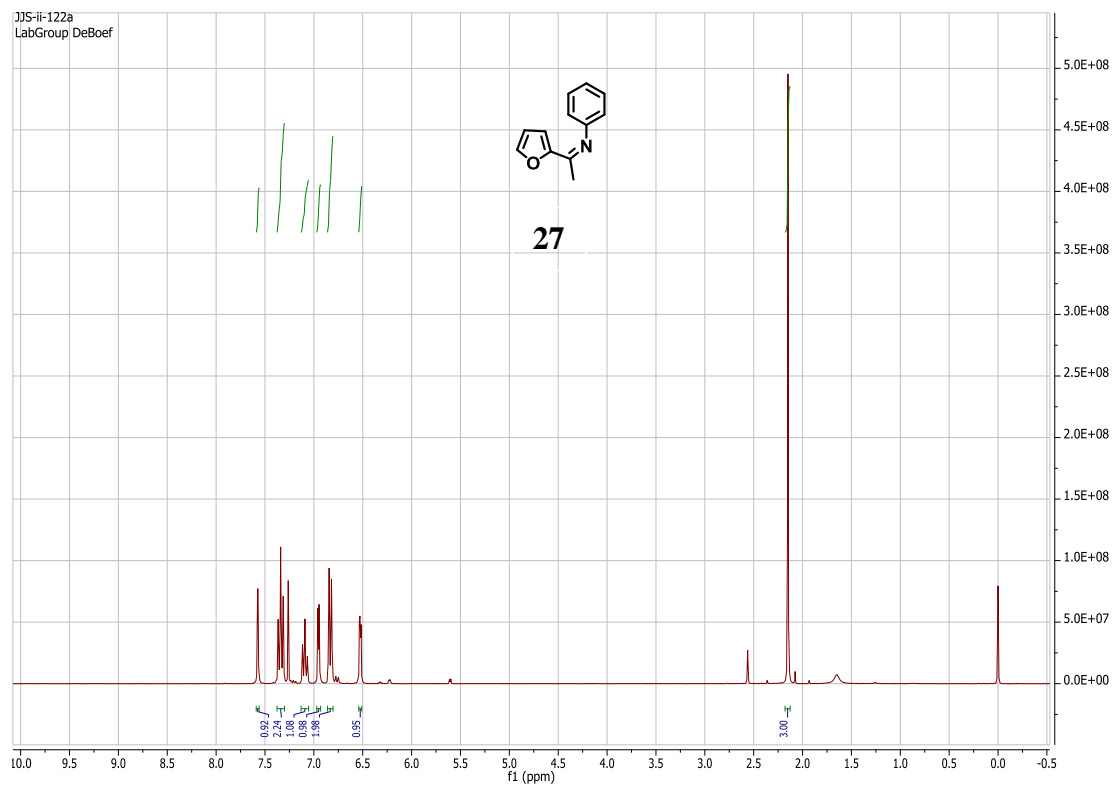


**Figure 4.37.** <sup>1</sup>H NMR of Compound 27

Characterization of (28)

**<sup>1</sup>H NMR (300 MHz, CDCl<sub>3</sub>):** δ 7.32 (t, *J*=7.41 Hz, 2H), 7.29 (d, *J*=1.0 Hz, 1H), 7.07 (t, *J*=7.49 Hz, 2H), 7.03 (s, 1H), 6.80 (d, *J*=7.29 Hz, 2H), 2.28 (s, 3H), 2.19 (s, 3H)

**<sup>13</sup>C NMR (75 MHz, CDCl<sub>3</sub>):** δ 160.31, 150.62, 145.94, 138.01, 130.78, 128.83, 125.38, 123.45, 120.02, 17.39, 15.79

**LRMS EI (m/z):** [M<sup>+</sup>] calc'd for 215.08, observed 215.00 (*m/z*)

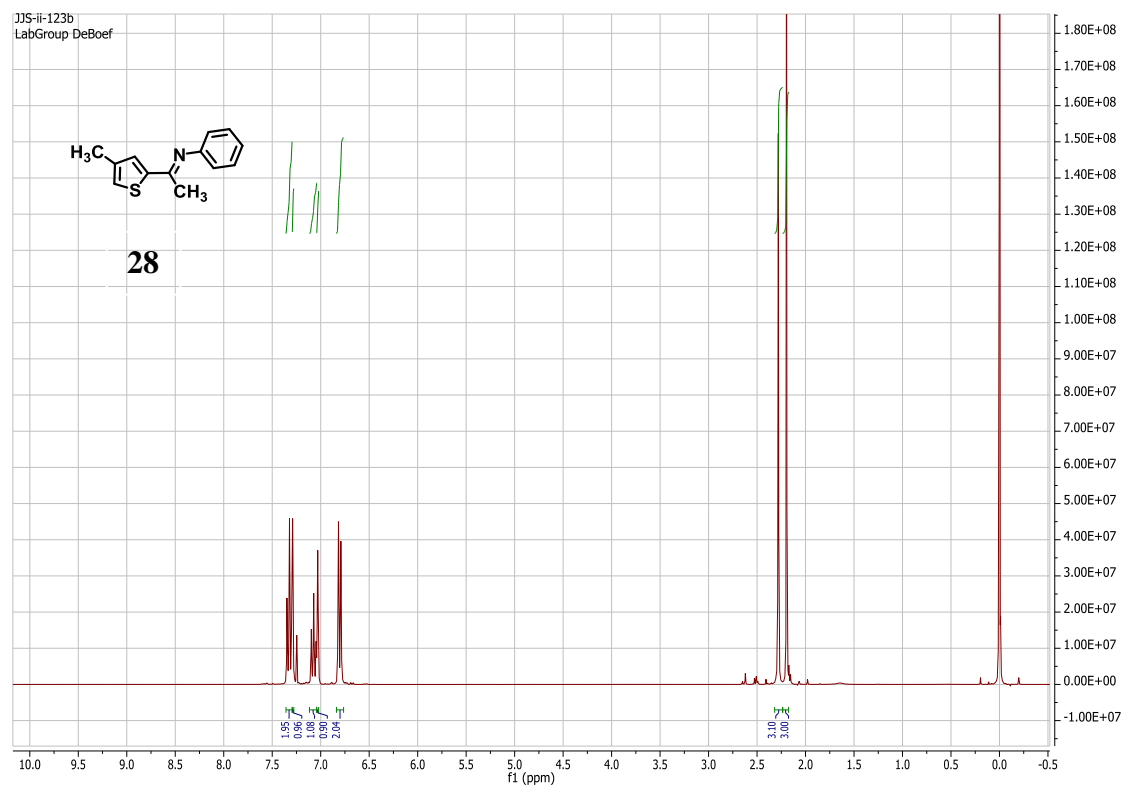


**Figure 4.38.** <sup>1</sup>H NMR of Compound 28

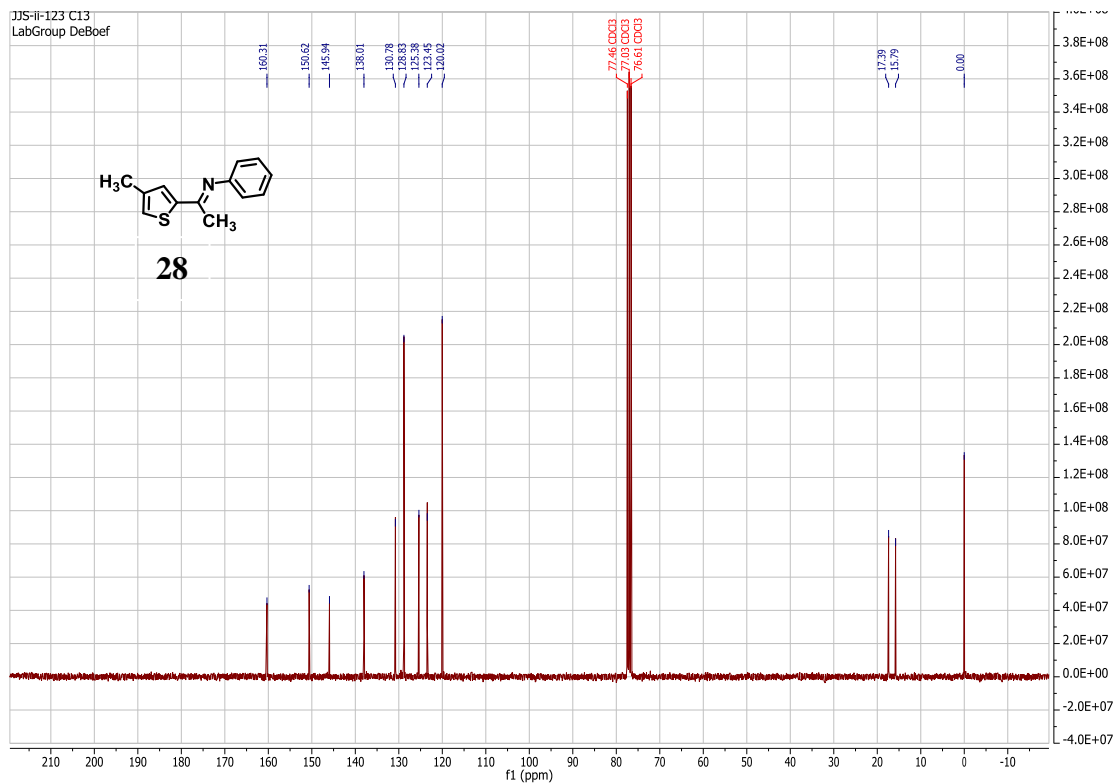


**Figure 4.39.**  $^{13}\text{C}$  NMR of Compound 28

Characterization of (29)<sup>14</sup>

**<sup>1</sup>H NMR (300 MHz, CDCl<sub>3</sub>):**  $\delta$  9.12 (s, 1H), 9.07 (d,  $J=4.55$  Hz, 1H), 8.87 (d,  $J=8.54$  Hz, 1H), 8.21 (d,  $J=8.74$  Hz, 1H), 7.94 (d,  $J=4.53$  Hz, 1H), 7.83-7.76 (ddd,  $J=8.38$ , 6.98, 1.49 Hz, 1H), 7.73-7.64 (ddd,  $J=8.40$ , 6.98, 1.45 Hz, 1H), 7.51-7.42 (t,  $J=7.88$  Hz, 2H), 7.36-7.29 (m, 3H)

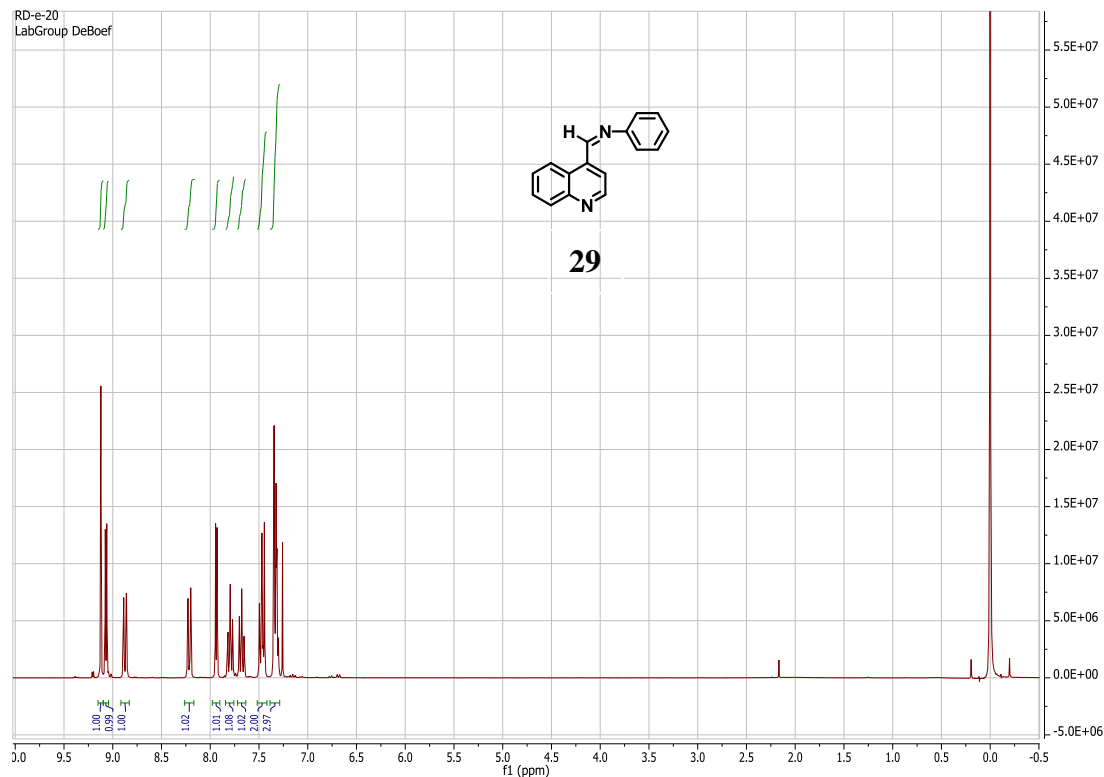


**Figure 4.40.** <sup>13</sup>C NMR of Compound 29

## REFERENCES

- 1.) Barluenga, J.; Jiménez-Aquino, A.; Aznar, F.; Valdés, C., *J. Am. Chem. Soc.*, **2009**, *131*, 4031
- 2.) Malkov, A. V.; Vranková, K.; Stončius, S.; Kočovský, P., *J. Org. Chem.*, **2009**, *74*, 5839
- 3.) Wong, W.-Y.; Wong, W.-K., *J. Organometallic Chem.*, **1999**, *584*, 48
- 4.) Sato, N.; Narita, N., *Synthesis* **2001**, *10*, 1551-1555
- 5.) Carrër, A.; Brinet, D.; Florent, J.-C.; Rousselle, P.; Bertounesque, E., *J. Org. Chem.* **2012**, *77*(3), 1316-1327
- 6.) Balaban, T. S.; Balaban, A. T.; Daia, D. E.; Turdybekov, K. M.; Lindeman, S. V.; Struchkov, Yu. T., *Struct. Chem.* **1992**, *3*(3), 191-4
- 7.) Redon, S.; Pannecoucke, X.; Franck, X.; Outurquin, F., *Organic & Biomolecular Chemistry*, **2008**, *6*(7), 1260-1267
- 8.) Yoshikai, N.; Matsumoto, A.; Norinder, J.; Nakamura, E., *Angew. Chem., Int. Ed.* **2009**, *48*(16), 2925-2928.
- 9.) Kirsch, G. and Deprets, S., *Euro. J. Org. Chem.* **2000**, *7*, 1353-1357
- 10.) Bourque, A. N.; Dufresne, S.; Skene, W. G., *J. Phys. Chem. C*, **2009**, *113*, 19677
- 11.) McBurney, R.T.; Slawin, A.M.Z.; Smart, L.A.; Yu, Y.; Walton, J.C., *Chem. Commun.*, **2011**, *47*, 7974-7976
- 12.) Aruna Kumar, D. B.; Prakash, G. K.; Kumaraswamy, M. N.; Nandeshwarappa, B. P.; Sherigara, B. S.; Mahadevan, K. M., *Ind. J. Chem.*, **2007**, *46B*, 336
- 13.) Schnell, B., *J. Heterocyclic Chem.*, **1999**, *36*, 541

- 14.) Fink, R.; Frenz, C.; Thelakkat, M.; Schmidt, H.W., *Macromolecules*, **1997**, 30, 8177



## CHAPTER 5: EXPERIMENTAL FOR MANUSCRIPT 2

**General Procedure for the synthesis of N-chloroamines:** To an oven dried 100 mL round bottom flask with a stir bar is added 5.00mL (1 eq.) of the amine and cooled to 0 °C followed by the addition of aqueous 4% NaOCl (2 eq.). The reaction is stirred for 5 minutes, then brought to room temperature and extraction with diethyl ether (3x) followed by a DI water wash (3x), and a brine wash (1x). The organic layer was dried over sodium sulfate, filtered, and concentrated *in vacuo*. The resulting oil is used as obtained after NMR characterization and purity analysis.

**General Procedure for the formation of C– N Bonds:** To an oven dried 50 mL round bottom flask is added the chloroamine (1.00 mmol) and 2.00 mL of 2-methyltetrahydrofuran. The system is sealed with a rubber septum, flushed with nitrogen, and cooled to the desired temperature. Grignard reagent (1.10 mmol) is added dropwise via syringe through the septum. The system is then brought to room temperature and purified by column chromatography.

Characterization of 4-chloromorpholine<sup>1</sup>

**<sup>1</sup>H NMR (300 MHz, CDCl<sub>3</sub>):** δ 3.67 (br s, 4H), 3.10 (br s, 4H)

**<sup>13</sup>C NMR( 75MHz, CDCl<sub>3</sub>):** δ 67.48, 62.81

**LRMS EI (m/z):** [M<sup>+</sup>] calc'd for 121.029, observed 121.00 (m/z)

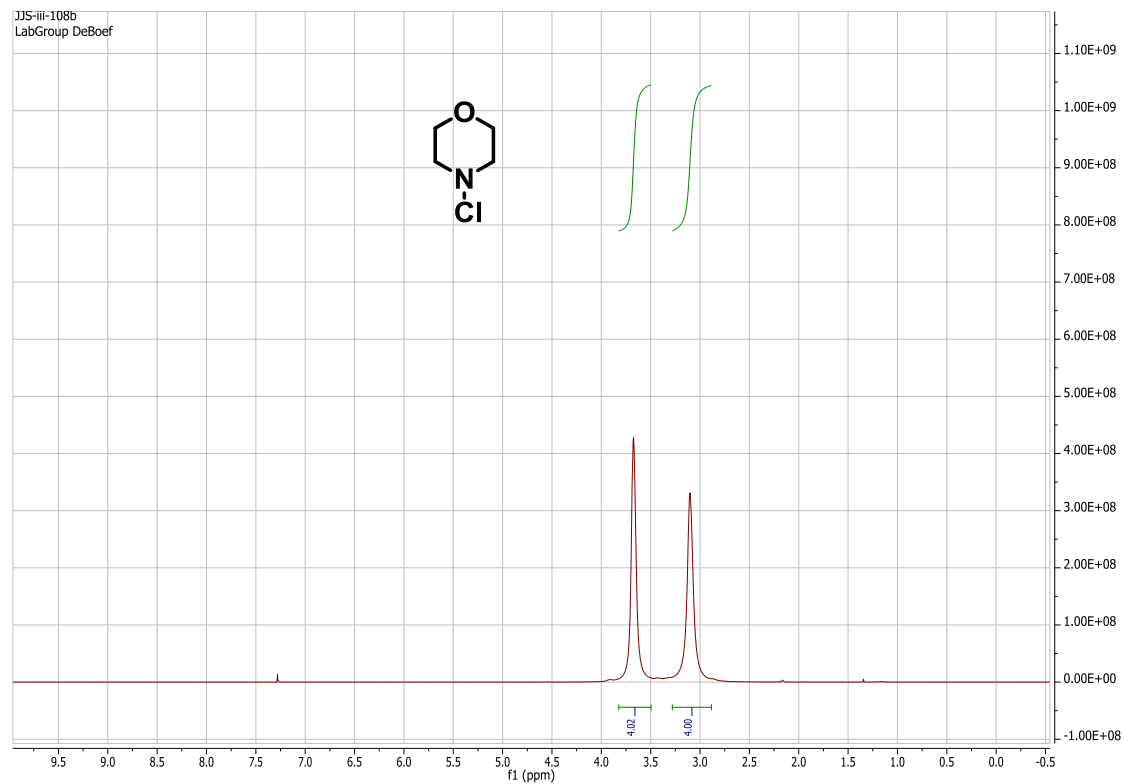


**Figure 5.1.** <sup>1</sup>H NMR of 4-chloromorpholine

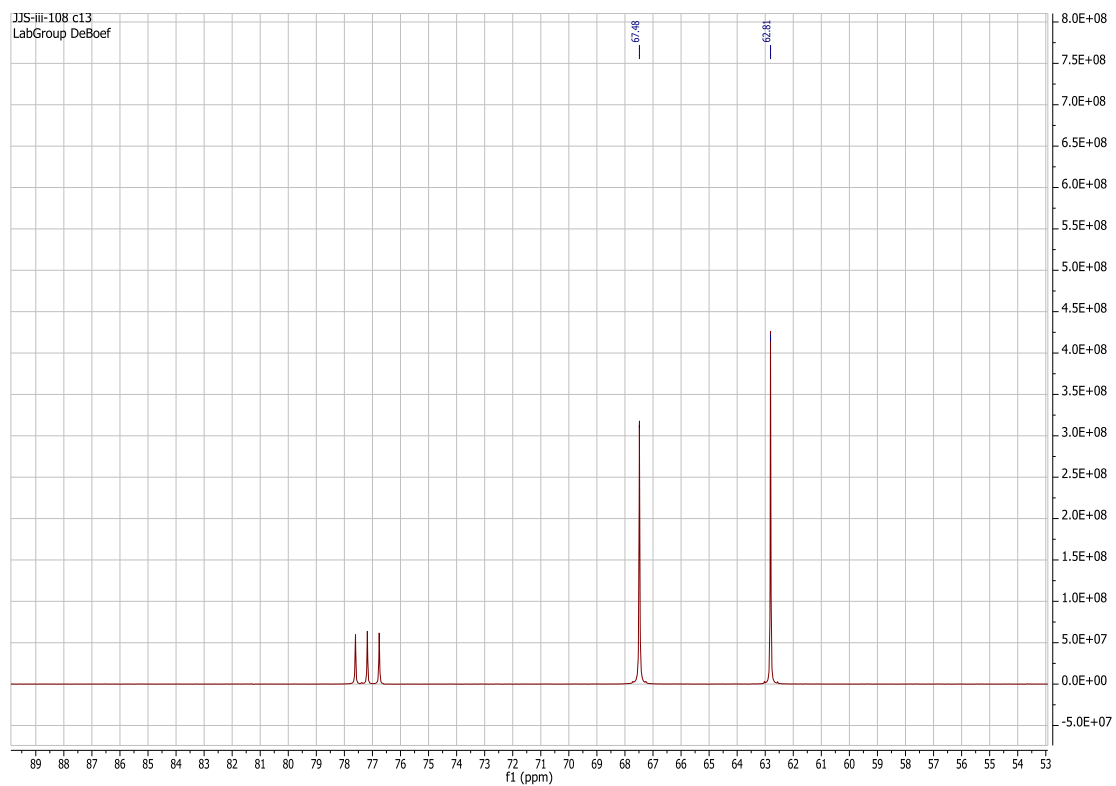


**Figure 5.2.**  $^{13}\text{C}$  NMR of 4-chloromorpholine

Characterization of 4-chloropiperidine<sup>1</sup>

**<sup>1</sup>H NMR (300 MHz, CDCl<sub>3</sub>):** δ 3.14 (br s, 4H), 1.80-1.60 (m, 4H) 1.47 (br s, 2H)

**<sup>13</sup>C NMR( 75MHz, CDCl<sub>3</sub>):** δ 63.90, 27.56, 22.93

**LRMS EI (m/z):** [M<sup>+</sup>] calc'd for 119.050, observed 119.100 (m/z)

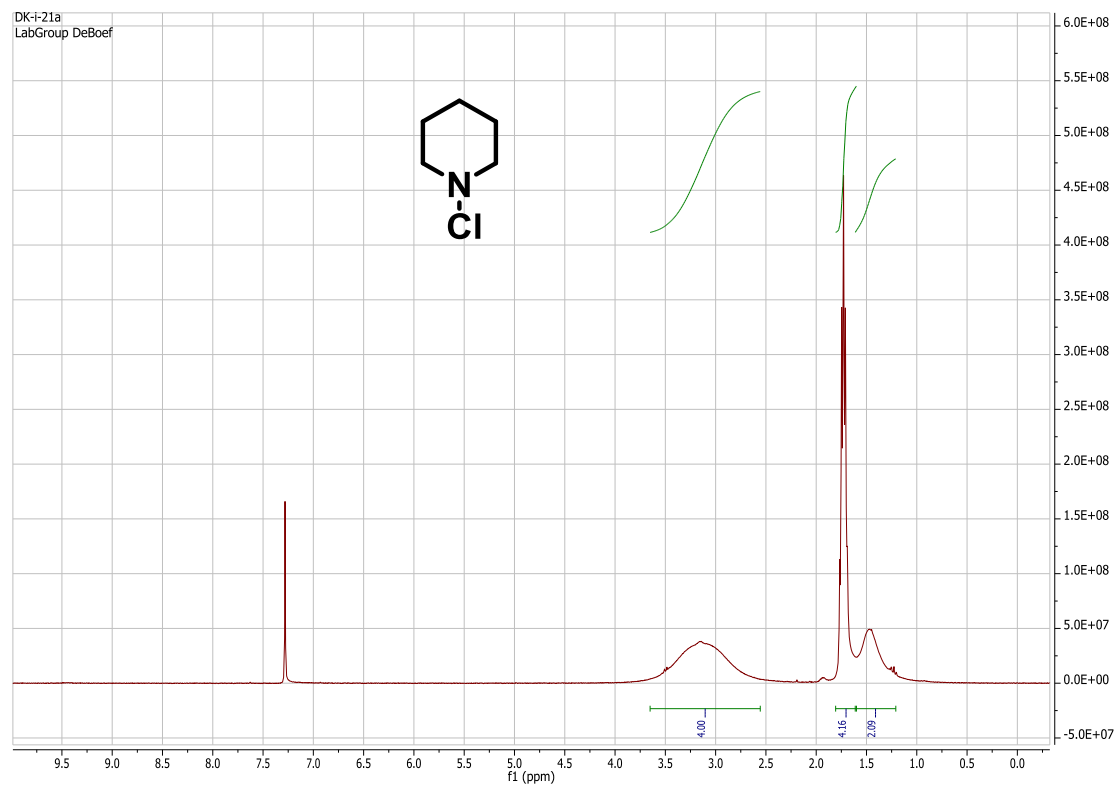


**Figure 5.3.** <sup>1</sup>H NMR of 4-chloropiperidine

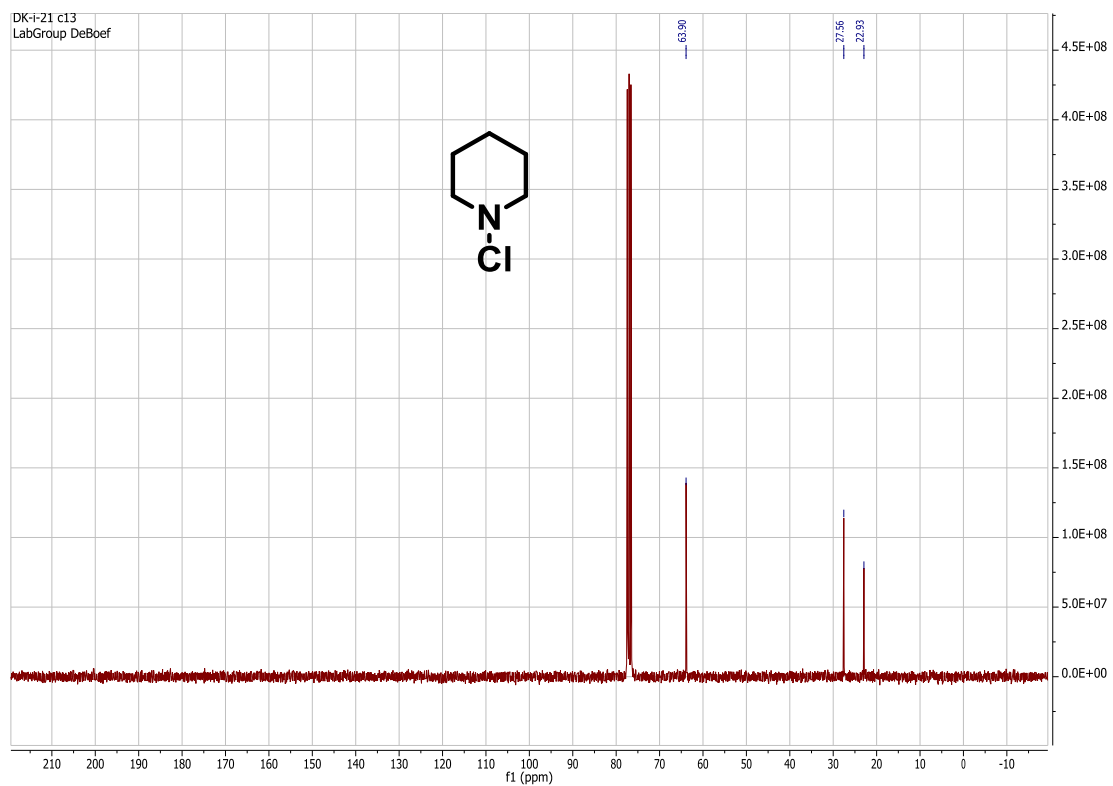


**Figure 5.4.**  $^{13}\text{C}$  NMR of 4-chloropiperidine

Characterization of 1,4-dichloropiperazine<sup>2</sup>

**<sup>1</sup>H NMR (300 MHz, CDCl<sub>3</sub>):** δ 3.22 (br s, 8H)

**LRMS EI (m/z):** [M<sup>+</sup>] calc'd for 154.006, observed 154.00 (m/z)

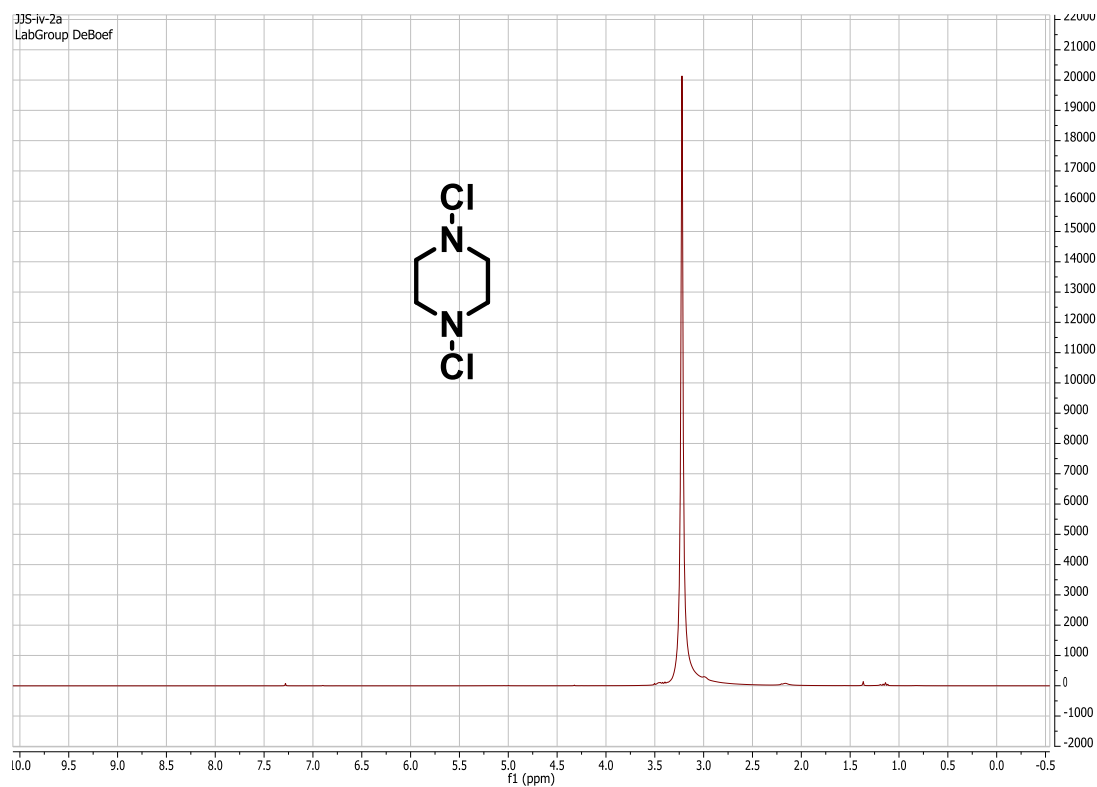


**Figure 5.5.** <sup>1</sup>H NMR of 1,4-dichloropiperazine

Characterization of 4-phenylmorpholine<sup>3</sup>

**<sup>1</sup>H NMR (300 MHz, CDCl<sub>3</sub>):** δ 7.26-7.16 (m, 2H), 6.91-6.77 (m, 3H), 3.79 (t, 4H, J=4.9), 3.09 (t, 4H, J=4.9)

**<sup>13</sup>C NMR (75MHz, CDCl<sub>3</sub>):** δ 151.23, 129.22, 120.15, 115.78, 66.94, 49.43

**LRMS EI (m/z):** [M<sup>+</sup>] calc'd for 163.100, observed 163.200 (m/z)

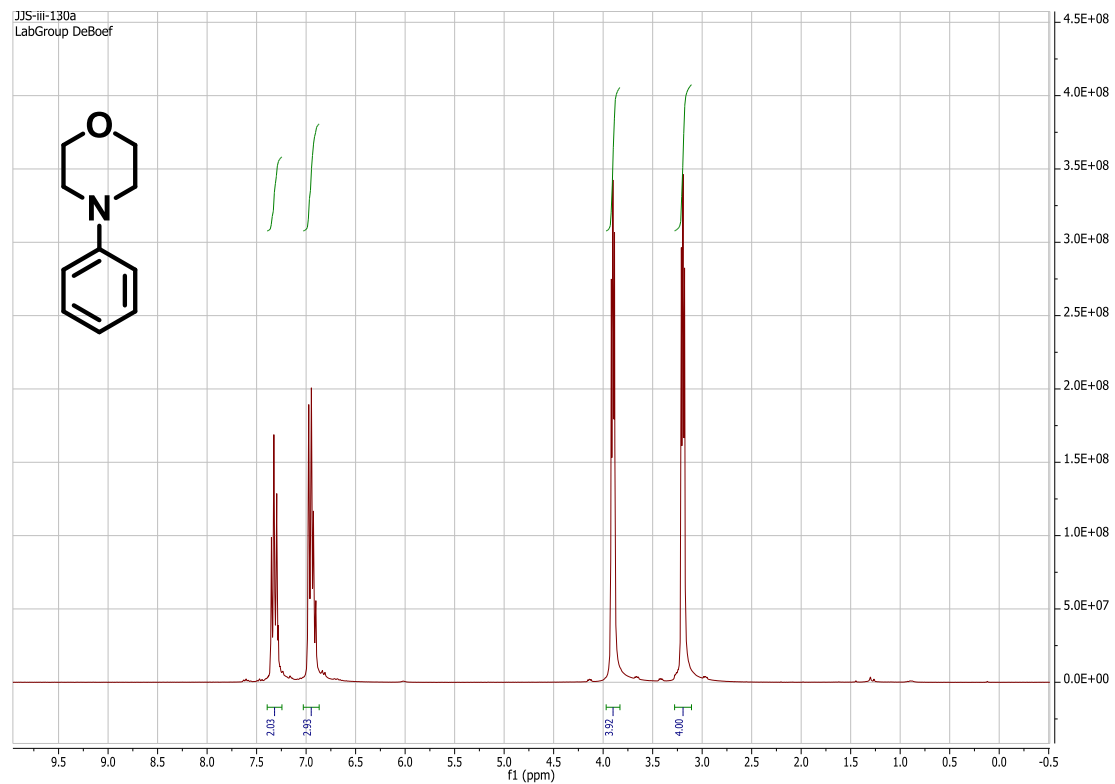


**Figure 5.6.** <sup>1</sup>H NMR of 4-phenylmorpholine

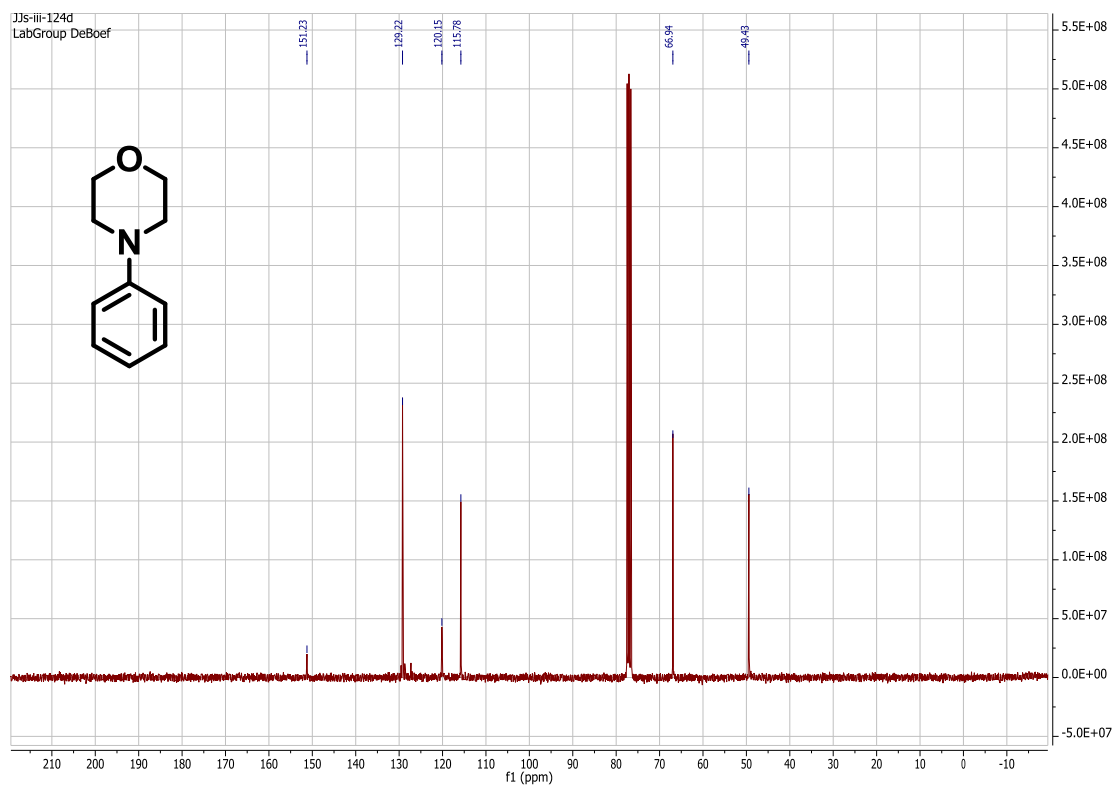


**Figure 5.7.**  $^{13}\text{C}$  NMR of 4-phenylmorpholine



Characterization of 4-(4-methylphenyl)-morpholine<sup>4</sup>

**<sup>1</sup>H NMR (300 MHz, CDCl<sub>3</sub>):** δ 7.02 (d, 2H, J = 8.5) 6.78 (d, 2H, J = 8.5) 3.78 (t, 4H, J = 4.67) 3.03 (t, 4H, J = 4.79) 2.20 (s, 3H)

**<sup>13</sup>C NMR( 75MHz, CDCl<sub>3</sub>):** δ 148.70, 129.79, 116.34, 115.17, 66.82, 50.25, 20.48

**LRMS EI (m/z):** [M<sup>+</sup>] calc'd for 177.115, observed 177.100 (m/z)

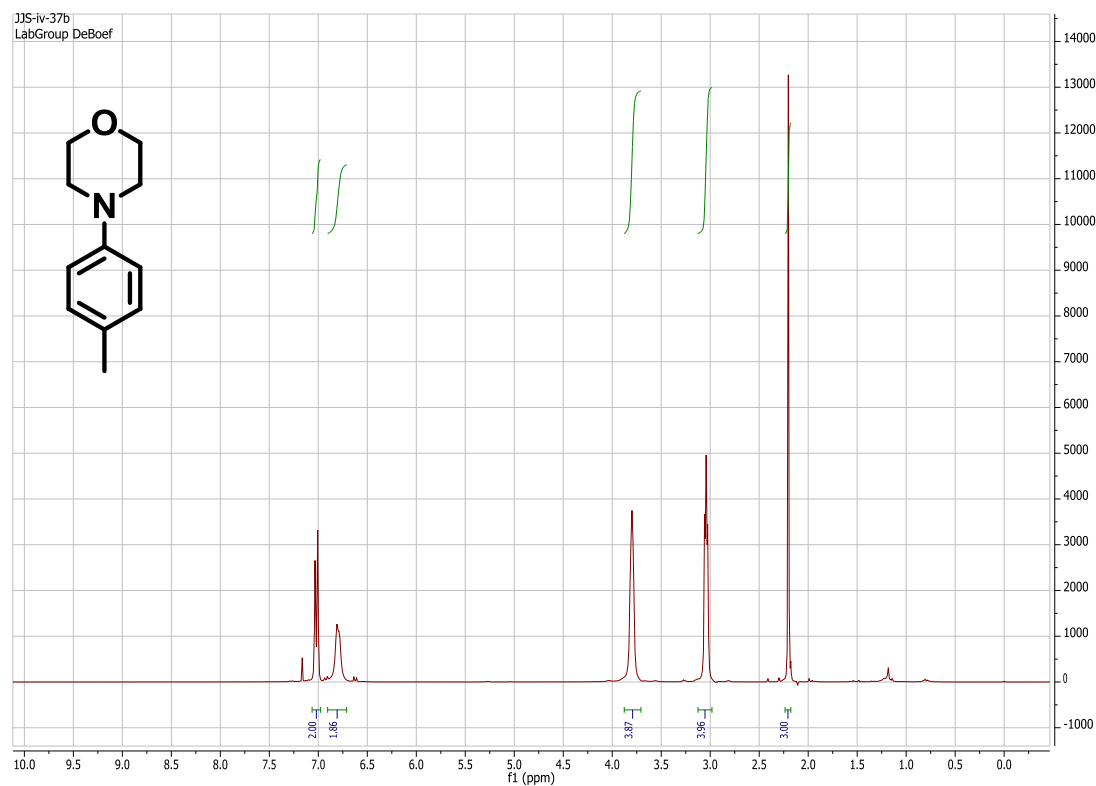


**Figure 5.8.** <sup>1</sup>H NMR of 4-(4-methylphenyl)-morpholine

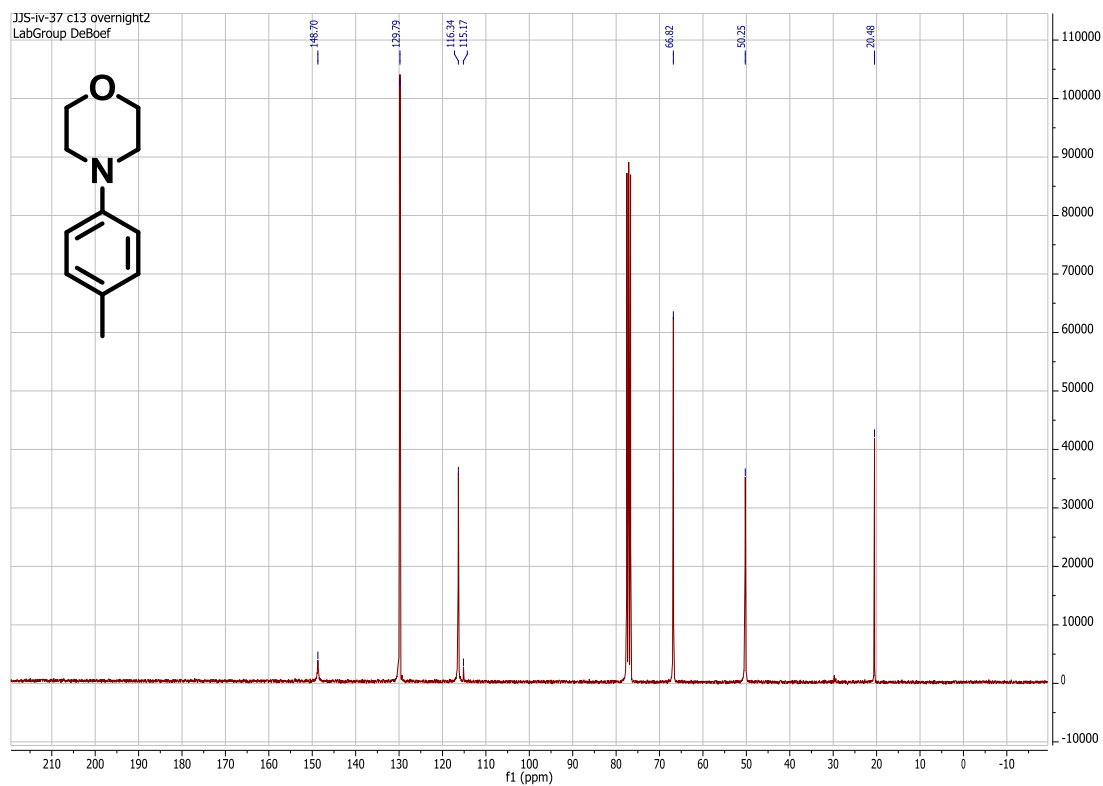


**Figure 5.9.**  $^{13}\text{C}$  NMR of 4-(4-methylphenyl)-morpholine

Characterization of 4-(4-methoxyphenyl)-morpholine<sup>5</sup>

**<sup>1</sup>H NMR (300 MHz, CDCl<sub>3</sub>):** δ 6.98-6.83 (m, 4H) 3.88 (t, 4H, J = 4.62), 3.79 (s, 3H), 3.08 (t, 4H, J = 4.88)

**<sup>13</sup>C NMR (75MHz, CDCl<sub>3</sub>):** δ 153.99, 145.65, 117.82, 114.53, 67.04, 55.58, 50.84

**LRMS EI (m/z):** [M<sup>+</sup>] calc'd for 193.110, observed 193.100 (m/z)

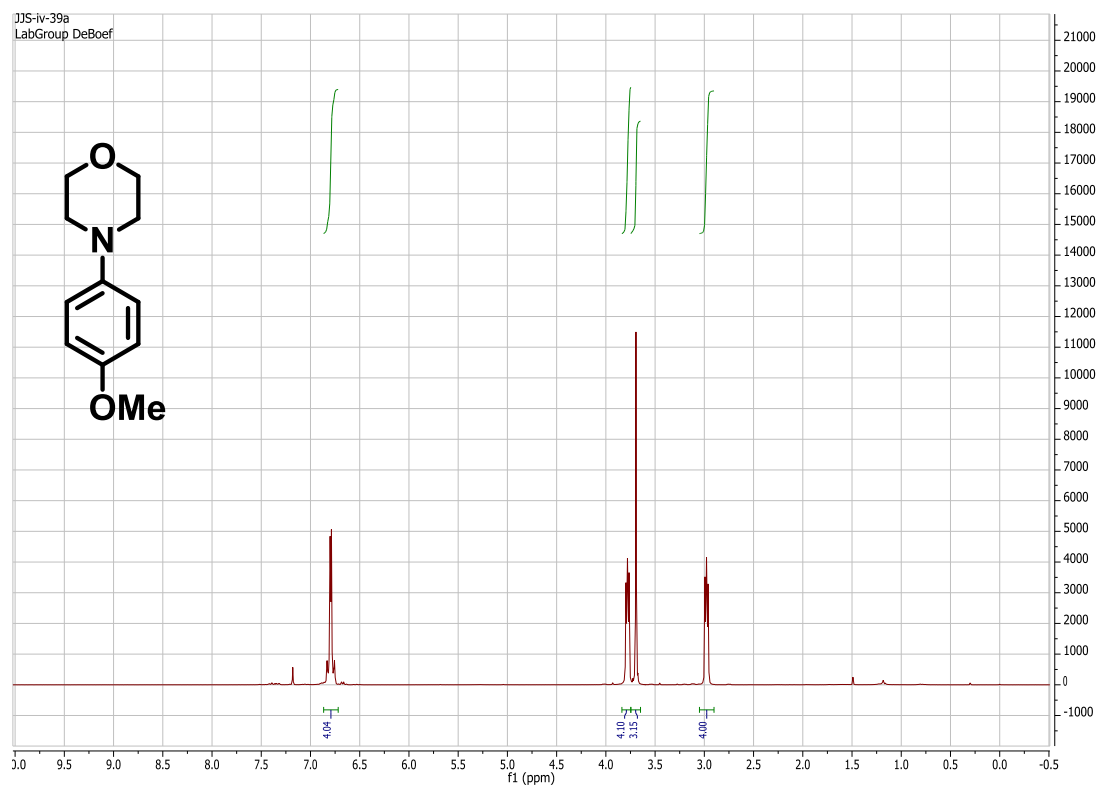


**Figure 5.10.** <sup>1</sup>H NMR of 4-(4-methoxyphenyl)-morpholine

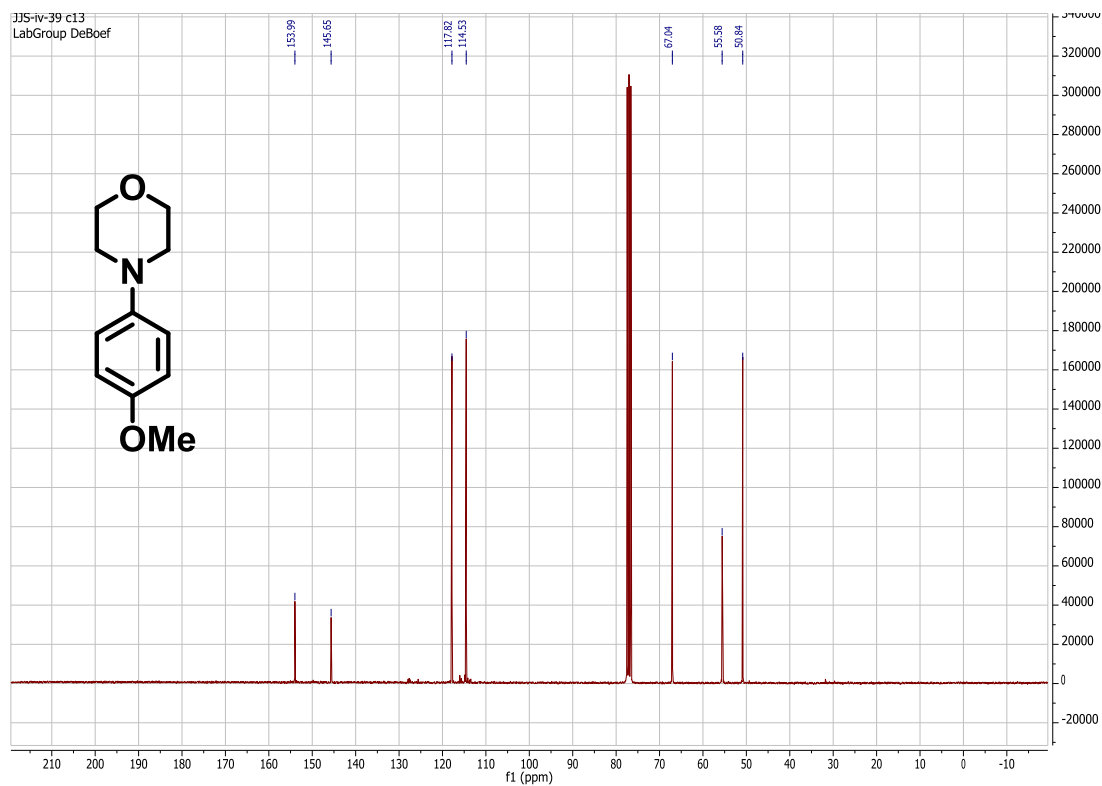


**Figure 5.11.**  $^{13}\text{C}$  NMR of 4-(4-methoxyphenyl)-morpholine

Characterization of 4-(4-methylphenyl)-piperidine<sup>6</sup>

**<sup>1</sup>H NMR (300 MHz, CDCl<sub>3</sub>):** δ 7.05 (d, 2H, J = 8.4) 6.85 (d, 2H, J = 8.4) 3.09 (t, 4H, J = 5.4) 2.26 (s, 3H) 1.75-1.65 (m, 4H), 1.59-1.49 (m, 2H)

**<sup>13</sup>C NMR (75MHz, CDCl<sub>3</sub>):** δ 150.27, 129.49, 128.70, 116.94, 51.31, 25.95, 24.29, 20.41

**LRMS EI (m/z):** [M<sup>+</sup>] calc'd for 175.136, observed 175.200 (m/z)

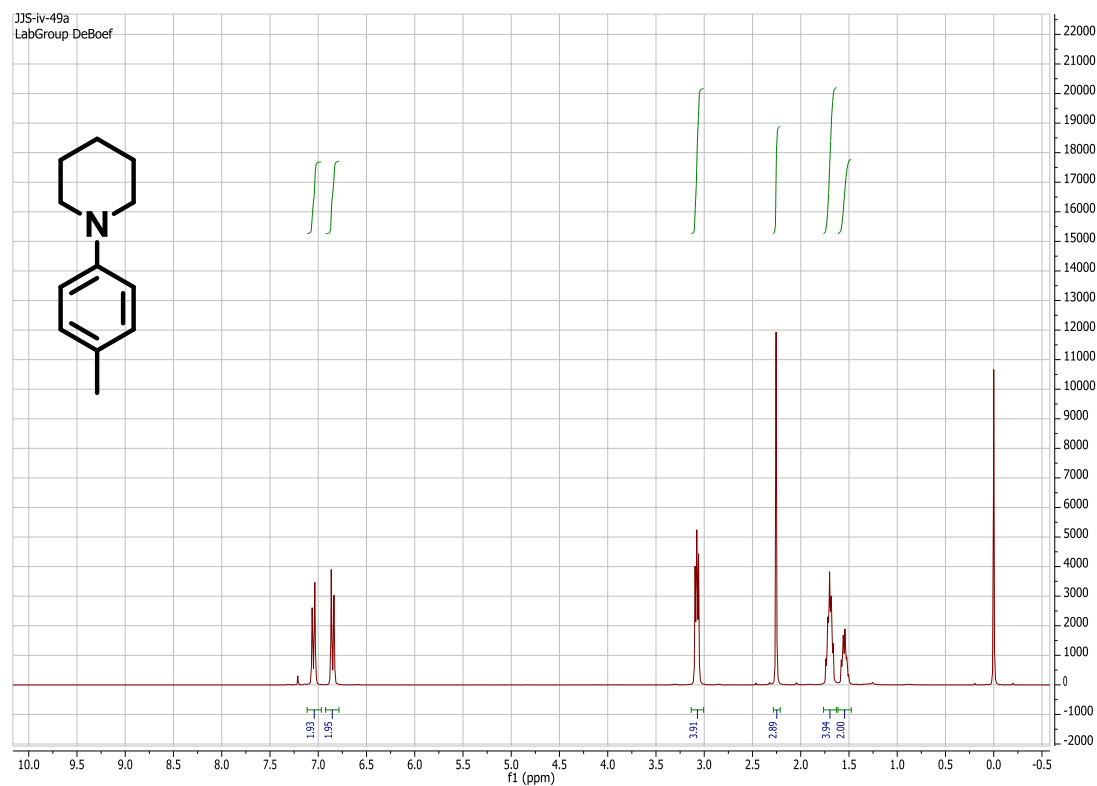


**Figure 5.12.** <sup>1</sup>H NMR of 4-(4-methylphenyl)-piperidine

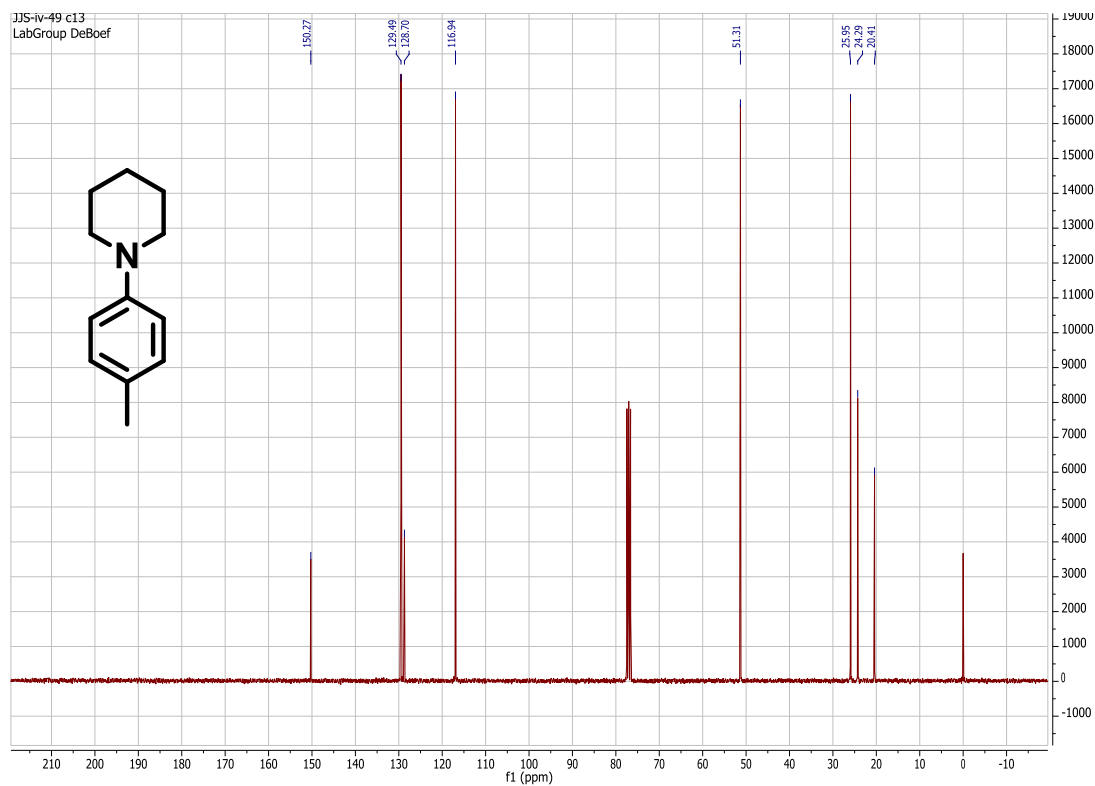


**Figure 5.13.**  $^{13}\text{C}$  NMR of 4-(4-methylphenyl)-piperidine

Characterization of 4-(4-methoxyphenyl)-piperidine<sup>7</sup>

**<sup>1</sup>H NMR (300 MHz, CDCl<sub>3</sub>):** δ 6.94-6.89 (m, 2H) 6.86-6.79 (m, 2H) 3.76 (s, 3H)

3.02 (t, 4H, J = 5.4) 1.77-1.67 (m, 4H), 1.59-1.48 (m, 4H)

**<sup>13</sup>C NMR (75MHz, CDCl<sub>3</sub>):** δ 153.53, 146.91, 118.75, 114.29, 55.55, 52.31, 26.13, 24.18

**LRMS EI (m/z):** [M<sup>+</sup>] calc'd for 191.31, observed 191.200 (m/z)

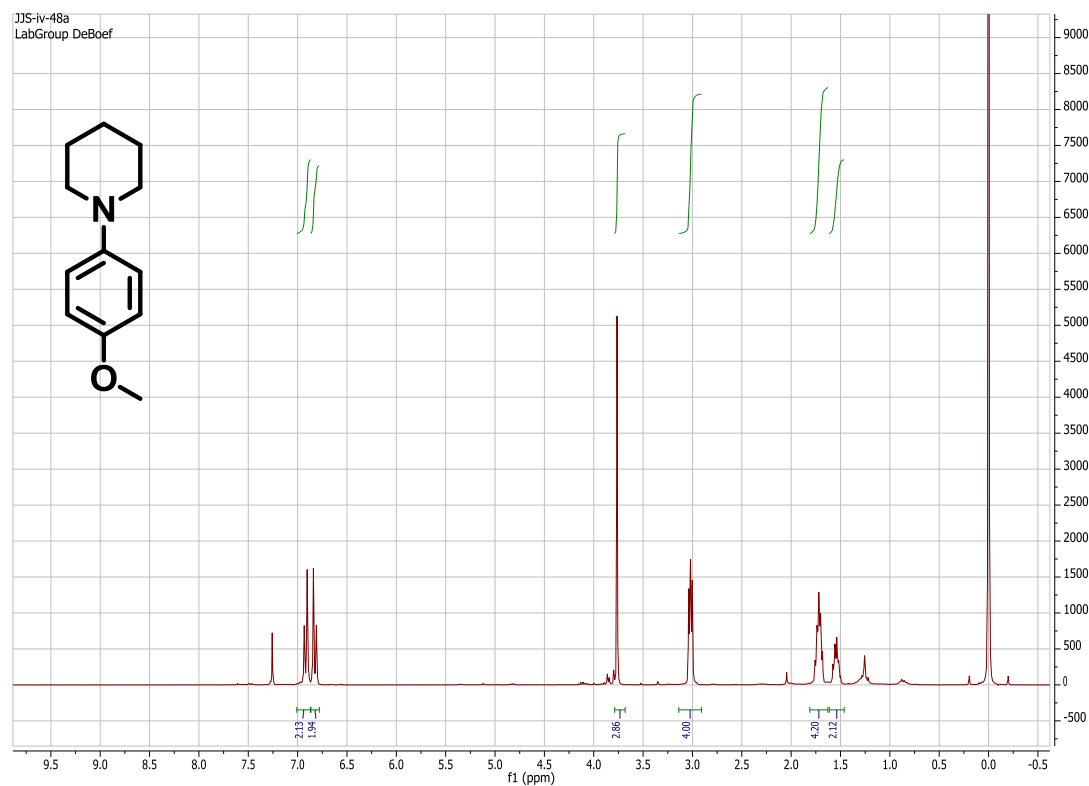


**Figure 5.14.** <sup>1</sup>H NMR of 4-(4-methoxyphenyl)-piperidine

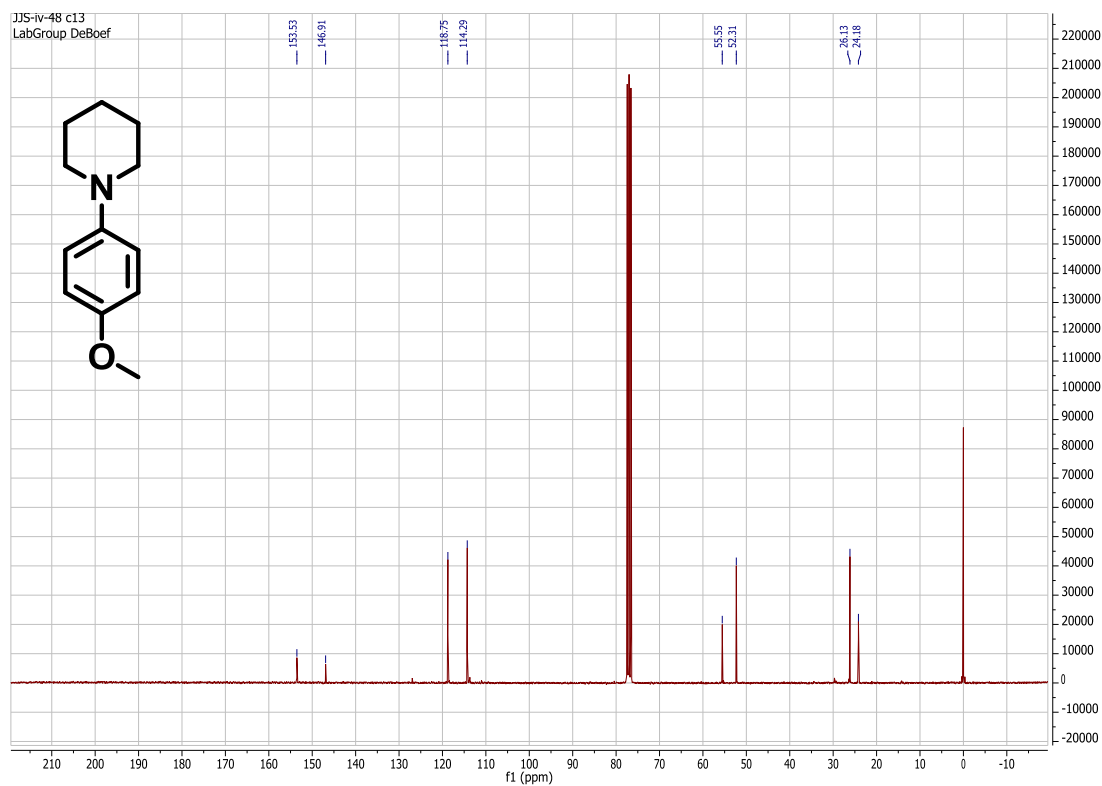


**Figure 5.15.**  $^{13}\text{C}$  NMR of 4-(4-methoxyphenyl)-piperidine



Characterization of 1,4-diphenylpiperazine<sup>2</sup>

**<sup>1</sup>H NMR (300 MHz, CDCl<sub>3</sub>):**  $\delta$  7.38 (t, 4H, J = 8.0), 7.07 (d, 4H, J = 8.2), 6.98 (t, 2H, J = 7.16), 3.42 (s, 8H)

**<sup>13</sup>C NMR (75MHz, CDCl<sub>3</sub>):**  $\delta$  151.32, 129.27, 129.19, 120.13, 116.42, 49.48

**LRMS EI (m/z):** [M<sup>+</sup>] calc'd for 238.147, observed 238.100 (m/z)

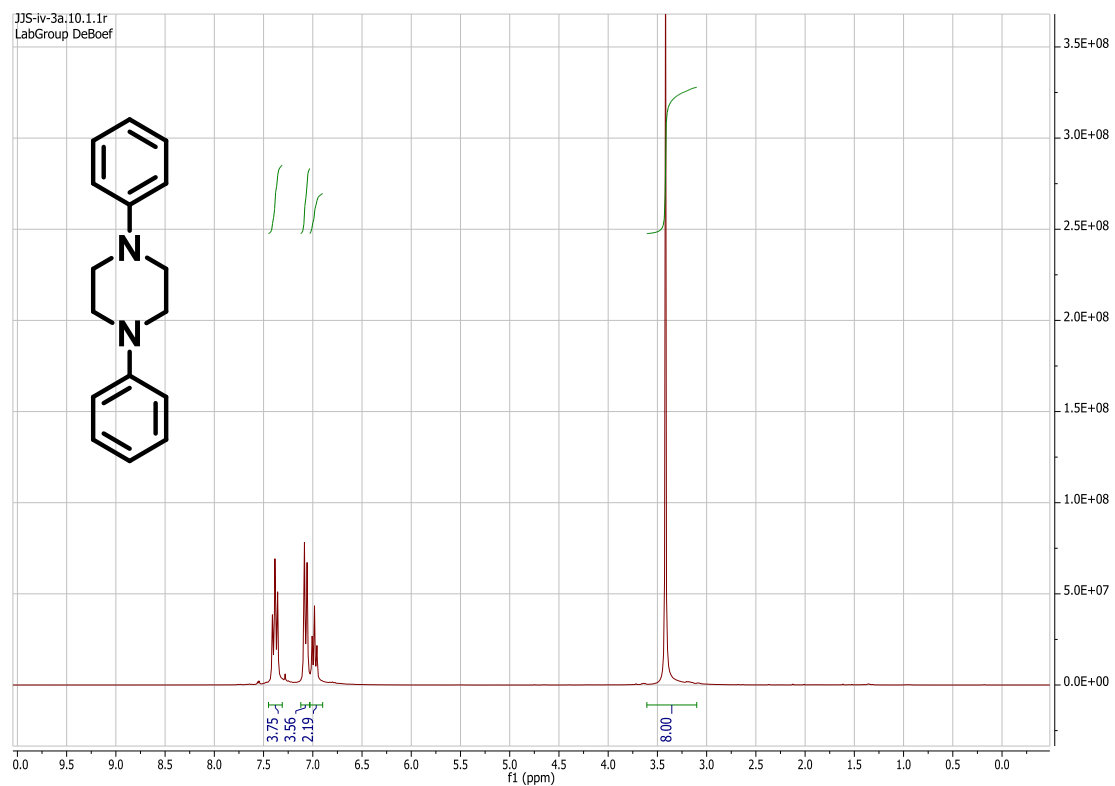


**Figure 5.16.** <sup>1</sup>H NMR of 1,4-diphenylpiperazine

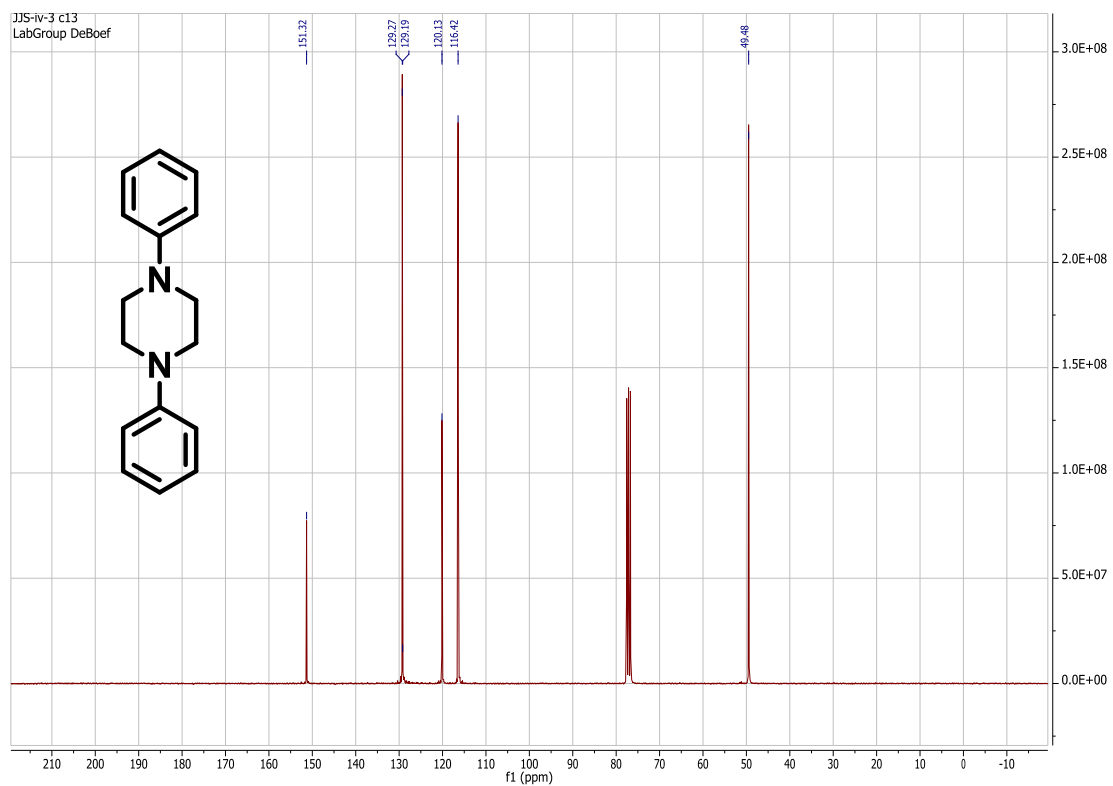
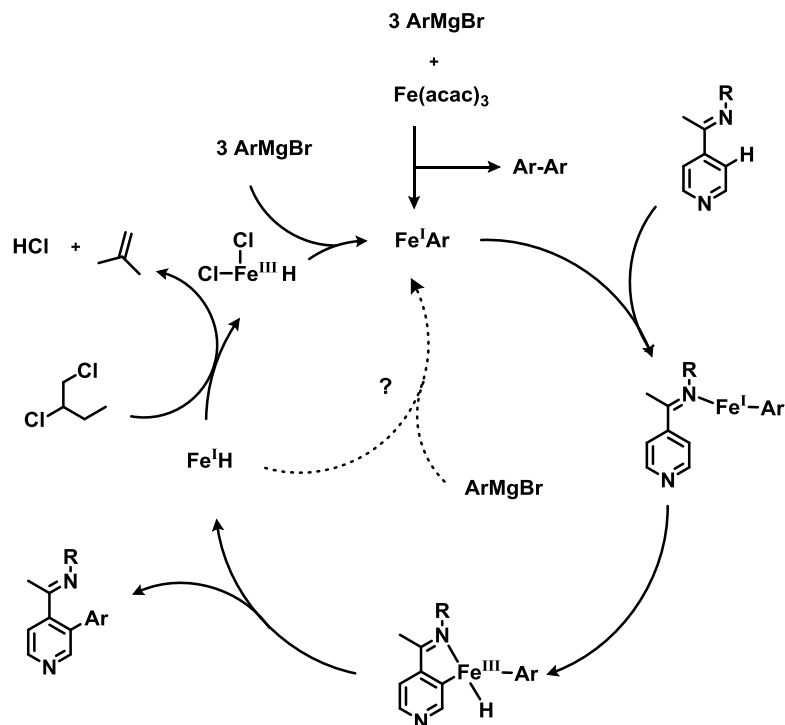


**Figure 5.17.**  $^{13}\text{C}$  NMR of 1,4-diphenylpiperazine

## REFERENCES

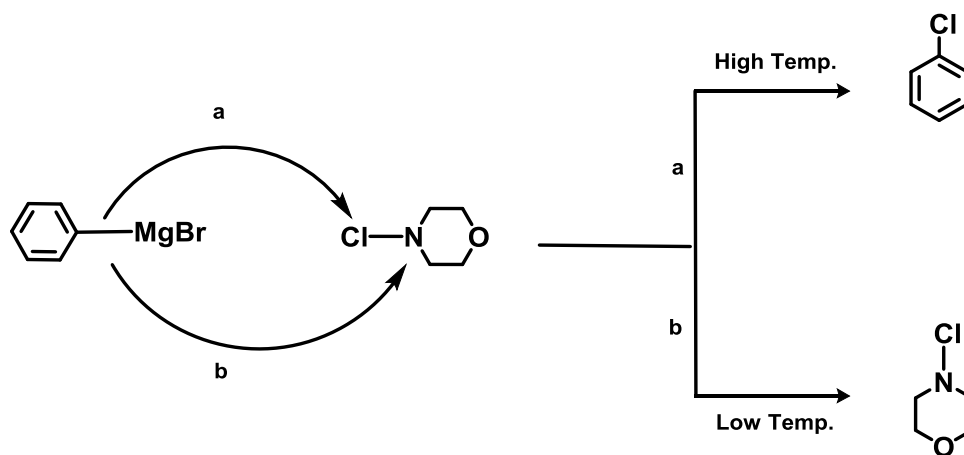
- 1.) Grohmann, C., Wang, H., Glorius, F.; *Org. Lett.* **2012**, *14* (2), 656-659
- 2.) Barker, T., Jarvo, E.; *J. Am. Chem. Soc.* **2009**, *131*, 15598-15599
- 3.) Brenner, E., Schneider, R., Fort, Y.; *Tetrahedron* **1999**, *55*, (44), 12829-12842
- 4.) Desmarets, C., Schneider, R., Fort, Y.; *J. Org. Chem.* **2002**, *67* (9), 3029–3036
- 5.) Wolfe, J.P., Buchwald, S.L.; *J. Org. Chem.* **1996**, *61*, 1133–1135
- 6.) Wolfe J.P., Buchwald, S.L.; *J. Org. Chem.* **1997**, *62*, 6066-6068
- 7.) Nguyen, M. H., Smith, III, A. B. *Org. Lett.* **2013**, *15* (18), 4872–4875

## APPENDIX A: Mechanism of Main Reaction in Manuscript 1



We propose the above mechanism to explain our iron-catalyzed reactions. The first step involves reduction of the  $\text{Fe}(\text{III})$  to  $\text{Fe}(\text{I})\text{-Ar}$  using three equivalents of Grignard reagent. This is followed by coordination between the lone pair on the imine nitrogen and the iron species. Oxidative addition and subsequent reductive elimination yields the desired product and a reactive iron hydride. We have experimentally determined trace amounts of a reduced imine byproduct that supports the generation of this iron hydride. This  $\text{Fe}(\text{I})$  species is then oxidized using 1,2-dichloroisobutane followed by a ligand exchange to regenerate the active  $\text{Fe}(\text{I})\text{-Ar}$ . This accounts for the observed biaryl formation and need for excess Grignard reagents. We envision another possible pathway going directly from the  $\text{Fe}(\text{I})$  hydride to the  $\text{Fe}(\text{I})\text{-Ar}$ . If this could be optimized the need for an oxidant and 3 equivalents of Grignard reagent can be eliminated.

## APPENDIX B: Possible Pathways for Main Reaction in Manuscript 2



The reaction of chloroamines and Grignard reagents can result in two different major products depending on the temperature of the reaction. At higher temperatures the chloramines act as an electrophilic source of chlorine; while at lower temperatures (pathway b) the same reagent acts as an electrophilic source of nitrogen. This can be explained by a Curtin-Hammett relationship, in which the reaction rates are temperature dependent, and one mechanism (pathway a) will slow down significantly more than the competing mechanism as a function of a temperature (pathway b). The results from the above experiments listed in Manuscript 2 support the proposed reaction pathways that proceed via both polung and umpolung reactivity.